



# Plutonium Futures —The Science

## Conference Transactions

Editors

K. K. S. Pillay

K. C. Kim

Topical Conference  
on Plutonium  
and Actinides

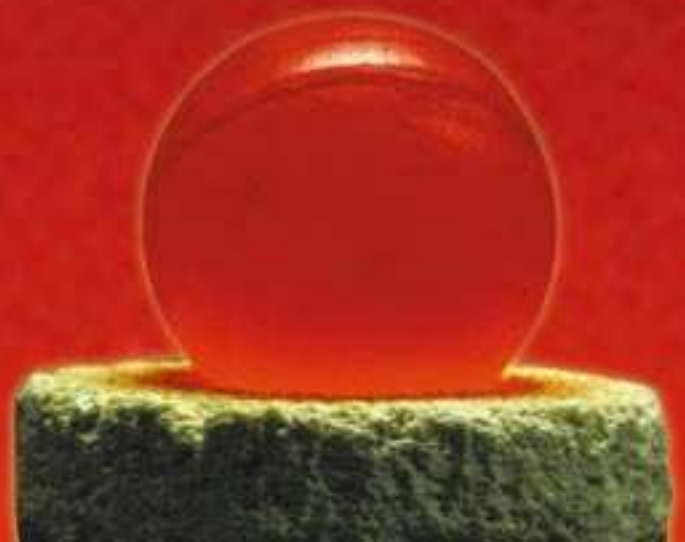
Santa Fe,  
New Mexico, USA  
July 10–13, 2000

Sponsored by  
Los Alamos National Laboratory  
in cooperation with the  
American Nuclear Society

**Los Alamos**  
NATIONAL LABORATORY  
Los Alamos, New Mexico 87545

**AMERICAN  
INSTITUTE  
OF PHYSICS**

Melville, New York  
AIP CONFERENCE  
PROCEEDINGS ■ 532



## Plutonium Futures—The Science Conference

### *General Chairs:*

*Sig Hecker, Los Alamos National Laboratory  
Bruce Matthews, Los Alamos National Laboratory*

### *Organizing Committee and Reviewers:*

*Kyu C. Kim, Los Alamos National Laboratory  
K. K. S. Pillay, Los Alamos National Laboratory  
Gerd M. Rosenblatt, Lawrence Berkeley National Laboratory  
David L. Clark, Los Alamos National Laboratory  
Paul T. Cunningham, Los Alamos National Laboratory  
Allen Hartford, Jr., Los Alamos National Laboratory  
Sandra L. Mecklenburg, Los Alamos National Laboratory  
David E. Hobart, Los Alamos National Laboratory  
Andria M. Liesse, Los Alamos National Laboratory*

### *Program Co-Chairs:*

*Kyu C. Kim, Los Alamos National Laboratory  
K. K. S. Pillay, Los Alamos National Laboratory*

### *Program Committee:*

*Richard A. Bartsch, Texas Tech University  
Gregory Choppin, Florida State University  
Rodney C. Ewing, University of Michigan  
Abdul Fattah, International Atomic Energy Agency, Vienna  
Darleane Hoffman, University of California, Berkeley  
Mal M. McKibben, Westinghouse Savannah River Company  
William J. Sutcliffe, Lawrence Livermore National Laboratory  
Gordon Brown, Stanford University  
Kenneth L. Peddicord, Texas A&M University/Amarillo Center  
Harold McFarlane, Argonne National Laboratory West  
Charles W. Forsberg, Oak Ridge National Laboratory  
Douglas Crawford, Argonne National Laboratory East*

*This transactions book was prepared by the Communications Arts and Services Group (CIC-1) of Los Alamos National Laboratory.*

*Coordinator: Andria M. Liesse*

*Editor: Ann Mauzy*

*Designer: Susan Carlson*

*Photocompositor: Joyce A. Martinez*

This conference was sponsored by Los Alamos National Laboratory in cooperation with the American Nuclear Society.



The Organizers of the Conference thank DOE Office of Basic Energy Sciences, Chemical Sciences Division and DOE Defense Programs for the generous support which makes this Conference possible.

# PLUTONIUM FUTURES— THE SCIENCE

## **Related Titles from the AIP Conference Proceedings**

**513** Nuclear and Condensed Matter Physics: VI Regional CRRNSM Conference  
Edited by Antonino Messina, April 2000, 1-56396-929-7

**495** Experimental Nuclear Physics in Europe: ENPE 99, Facing the Next Millennium  
Edited by Berta Rubio, Manuel Lozano, and William Gelletly, November 1999,  
1-56396-907-6

**481** Nuclear Structure 98  
Edited by C. Baktash, September 1999, 1-56396-858-4

**455** ENAM 98: Exotic Nuclei and Atomic Masses  
Edited by B. M. Sherrill, D. J. Morrissey, and C. N. Davids, December 1998,  
1-56396-804-5

**447** Nuclear Fission and Fission-Product Spectroscopy: Second International Workshop  
Edited by G. Fioni, H. Faust, S. Oberstedt, F.-J. Hambsch, October 1998,  
1-56396-823-1

**425** Tours Symposium on Nuclear Physics III  
Edited by M. Arnould, M. Lewitowicz, Yu. Ts. Oganessian, M. Ohta, H. Utsunomiya, and T. Wada, April 1998, 1-56396-749-9

**346** Accelerator-Driven Transmutation Technologies and Applications  
Edited by Edward D. Arthur, Anita Rodriguez, and Stan O. Schriber, 1995,  
1-56396-505-4

To learn more about these titles, or the AIP Conference Proceedings Series, please visit the webpage <http://www.aip.org/catalog/aboutconf.html>

# PLUTONIUM FUTURES— THE SCIENCE

Topical Conference on Plutonium and Actinides

*Santa Fe, New Mexico 10–13 July 2000*

*EDITORS*

**K. K. S. Pillay**

**K. C. Kim**

*Los Alamos National Laboratory,  
Los Alamos, New Mexico*

**AMERICAN  
INSTITUTE  
OF PHYSICS**

AIP CONFERENCE PROCEEDINGS ■ 532

Melville, New York

**Editors:**

K. K. S. Pillay  
K. C. Kim

Nuclear Materials Technology Division  
Los Alamos National Laboratory  
Mail Stop E-500  
Los Alamos, NM 87545  
USA

E-mail: s\_pillay@lanl.gov  
kck@lanl.gov

The articles on pp. 6–10, 13–14, 32, 38–44, 47–55, 63–68, 71–72, 86–92, 98–101, 104–121, 125–129, 141–147, 151–152, 155–156, 166–170, 173–174, 179, 202–204, 211–213, 221–222, 228–238, 243–251, 261–262, 267–273, 277–281, 284–287, 290–291, 299–311, 324–326, 329–335, 343–354, 364–382, 390–398, 406–409, 412–417, 420–423, and 426–432 were authored by U. S. Government employees and are not covered by the below mentioned copyright.

The articles on pp. 239 and 327–328 are © British Crown Copyright (2000) and are published by permission of the United Kingdom Ministry of Defence.

Authorization to photocopy items for internal or personal use, beyond the free copying permitted under the 1978 U.S. Copyright Law (see statement below), is granted by the American Institute of Physics for users registered with the Copyright Clearance Center (CCC) Transactional Reporting Service, provided that the base fee of \$17.00 per copy is paid directly to CCC, 222 Rosewood Drive, Danvers, MA 01923. For those organizations that have been granted a photocopy license by CCC, a separate system of payment has been arranged. The fee code for users of the Transactional Reporting Service is: 1-56396-948-3/00/\$17.00.

© 2000 American Institute of Physics

Individual readers of this volume and nonprofit libraries, acting for them, are permitted to make fair use of the material in it, such as copying an article for use in teaching or research. Permission is granted to quote from this volume in scientific work with the customary acknowledgment of the source. To reprint a figure, table, or other excerpt requires the consent of one of the original authors and notification to AIP. Republication or systematic or multiple reproduction of any material in this volume is permitted only under license from AIP. Address inquiries to Office of Rights and Permissions, Suite 1N01, 2 Huntington Quadrangle, Melville, NY 11747-4502; phone: 516-576-2268; fax: 516-576-2450; e-mail: rights@aip.org.

L.C. Catalog Card No. 00-104645  
ISSN 0094-243X  
ISBN 1-56396-948-3

Printed in the United States of America

# Contents

<b>Preface</b> .....	xvii
<b>How to Develop New Materials</b>	
Leo Brewer .....	3
<b>Status and Trends in Plutonium Recycling in Nuclear Power Reactors</b>	
Vladimir Onoufrieu .....	4
<b>Fundamentally, Why is Plutonium Such an Unusual Metal?</b>	
Siegfried S. Hecker .....	6
<b>Self-Irradiation of Pu, Its Alloys and Compounds</b>	
L. F. Timofeeva .....	11
<b>Modeling of Delta-Phase Stabilization and Compositional Homogenization in Pu-1 wt. % Ga Alloys</b>	
Jeremy N. Mitchell, Frank E. Gibbs, Thomas G. Zocco, Ramiro A. Pereyra .....	13
<b>Radiation Resistance of Gadolinium Zirconate Pyrochlore</b>	
S. X. Wang, L. M. Wang, R. C. Ewing, K. V. Govidan Kutty, W. J. Weber .....	15
<b>Plutonium Stabilization in Zircon: Effects of Self-Radiation</b>	
W. J. Weber, N. J. Hess, R. E. Williford, H. L. Heinisch, B. D. Begg, S. D. Conradson, R. C. Ewing .....	18
<b>Inert Matrix Fuels for Incineration of Plutonium and Transmutation of Americium</b>	
Hj. Matzke .....	20
<b>Capability of the MIMAS Process to Convert the Stockpiles of Separated Plutonium into MOX Fuel for Use in LWRs</b>	
Paul Deramaix, Yvon Vanderborck, Werner Couwenbergh .....	22
<b>Some Less Conventional Options for Plutonium Disposal</b>	
Wolfgang Stoll .....	24
<b>The Electronic Structure and Elastic Properties of the Actinide Chalcogenides (U,Np,Pu,Am): the Puzzle of AmTe</b>	
P. Wachter, M. Filzmoser, J. Rebizant .....	29
<b>Phase Transitions in Plutonium: New Insights from Diffraction</b>	
A. C. Lawson, B. Martinez, J. A. Roberts, R. B. Von Dreele, J. W. Richardson, Jr., A. Mehta, J. Arthur .....	32
<b>Magnetic Properties of Pu<sub>(1-x)</sub>Am<sub>x</sub> Solid Solutions</b>	
Marion Dorneval, Nathalie Baclet, Jean-Marc Fournier .....	33
<b>X-Ray Magnetic Scattering from Transuranium Systems</b>	
G. H. Lander, D. Mannix, F. Wastin and J. Rebizant, D. Mannix, E. Lidström, C. Vettier, R. Caciuffo, N. Bernhoeft, P. Normile, W. G. Stirling, A. Hiess, C. Vettier .....	35
<b>The Stabilization of fcc Plutonium: A Solid-State-Solution-Like Phase of Stable and Fluctuating Configuration Plutonium</b>	
Bernard R. Cooper .....	36
<b>Electronic Structure of <math>\alpha</math>- and <math>\delta</math>-Pu from PES Measurements</b>	
A. J. Arko, J. J. Joyce, L. Morales, J. Wills, J. Lashley .....	38
<b>Resonant Ultrasound Studies of Pu</b>	
A. Migliori, J.P. Baiardo, T.W. Darling, F. Freibert, B. Martinez, H. Roder, D.A. Dimitrov .....	40

## Presentations

Plenary  
Session

Materials  
Science/  
Nuclear Fuels

Condensed  
Matter Physics

Actinides in the Environment/ Separation and Analysis	<p><b>Aquatic Chemistry of Actinides: Is a Thermodynamic Approach Appropriate to Describe Natural Dynamic Systems?</b> J. I. Kim ..... 45</p> <p><b>Sorption of Plutonium onto Clinoptilolite (Zeolite) Colloids</b> Nadia L. Hakem, Axel Brachmann, Mavrik Zavarin, Annie B. Kersting ..... 47</p> <p><b>Actinide (Pu, U) Interactions with Aerobic Soil Microbes and Their Exudates: Fundamental Chemistry and Effects on Environmental Behavior</b> M. P. Neu, C. E. Ruggiero, M. T. Johnson, J. R. Fairlee, J. H. Matonic, L. A. Vanderberg, L. E. Hersman, L. He, M. M. Cox, D. J. Chitwood, P. D. Gladden, G. L. Wagner ..... 49</p> <p><b>The Interaction of Plutonium with Bacteria in the Repository Environment</b> J. B. Gillow, A. J. Francis, D.A. Lucero, H. W. Papenguth ..... 51</p> <p><b>Transuranium Removal from Hanford High Level Waste Simulants Using Sodium Permanganate and Calcium</b> W. R. Wilmarth, S. W. Rosencrance, C. A. Nash, F. F. Fonduer, D. P. DiPrete, C. C. DiPrete ..... 53</p> <p><b>Radiolysis of Hexavalent Plutonium in Solutions of Uranyl Nitrate Containing Fission Product Simulants</b> Peter J. W. Rance, B. Ya. Zilberman, G. A. Akopov ..... 56</p> <p><b>Contribution of the Surface Contamination of Uranium Materials on the Quantitative Analysis Results by Electron Probe Microbeam Analysis</b> Olivier Bonino, Cécile Fournier, Catherine Fucili, Olivier Dugne, Claude Merlet ..... 59</p>
Actinides/ Processing	<p><b>Oxidation/Reduction of Multivalent Actinides in the Subsurface</b> B. E. Rittmann, D. T. Reed, S. B. Aase, A. J. Kropf ..... 63</p> <p><b>Gas-Phase Plutonium Oxide Cluster Ions and Initial Actinide Ion Trapping Experiments</b> John K. Gibson, Richard G. Haire, Douglas C. Duckworth ..... 65</p> <p><b>Actinide Science with Soft X-Ray Synchrotron Radiation</b> David K. Shuh ..... 67</p> <p><b>Recent Achievements in the Development of Partitioning Processes of Minor Actinides from Nuclear Wastes Obtained in the Frame of the NEWPART European Programme (1996–1999)</b> C. Madic, M. J. Hudson, J. O. Liljenzin, J. P. Glatz, R. Nannicini, A. Fraccini, Z. Kolarik, R. Odoj ..... 69</p> <p><b>Actinide Chemistry: From Test Tube to Billion Dollar Plant – A BNFL Perspective</b> Peter Parkes ..... 70</p> <p><b>Robust Membrane Systems for Actinide Separations</b> Gordon D. Jarvinen, T. Mark McCleskey, Elizabeth A. Bluhm, Kent D. Abney, Deborah S. Ehler, Eve Bauer, Quyen T. Le, Jennifer S. Young, Doris K. Ford, David R. Pesiri, Robert C. Dye, Thomas W. Robison, Betty S. Jorgensen, Antonio Redondo, Lawrence R. Pratt, Susan L. Rempe ..... 71</p> <p><b>New Nuclear Safe Plutonium Ceramic Compositions with Neutron Poisons for Plutonium Storage</b> B. A. Nadykto, L. F. Timofeeva ..... 73</p>
Actinides/TRU Wastes	<p><b>Theoretical Predictions of Hydrolysis and Complex Formation of the Heaviest Elements</b> V. Pershina ..... 77</p> <p><b>New Field of Actinides Solution Chemistry: Electrochemical Study on Phase Transfer of Actinide Ions across Aqueous/Organic Solutions Interface</b> Yoshihiro Kitatsuji, Hisao Aoyagi, Zenko Yoshida, Sorin Kihara ..... 79</p>



<b>Extraction of Lanthanides and Actinides from H. A. Waste by Calix[4]arenes Bearing CMPO Units</b>	
J. F. Dozol, A. Garcia Carrera, H. Rouquette .....	82
<b>Two New Insoluble Polymer Composites For The Treatment of LLW: 1. Polypyrrole Doped By <math>UO_2^{2+}</math> Complexing Polyanions 2. <math>UO_2^{2+}</math> Complexing Sol-Gel Based Composites Stability Constants, Leaching Tests, Alpha and Gamma Irradiation</b>	
D. Leroy, L. Martinot, P. Mignonsin, F. Caprasse, C. Jérôme, R. Jérôme .....	84
<b>Waste Forms from the Electrometallurgical Treatment of DOE Spent Fuel: Production and General Characteristics</b>	
R. W. Benedict, S. G. Johnson, D. D. Keiser, T. P. O'Holleran, K. M. Goff S. McDeavitt, W. Ebert .....	86
<b>Plutonium and Uranium Disposition in a Sodalite/Glass Composite Waste Form via XAFS</b>	
Michael K. Richmann, Arthur J. Kropf, Donald T. Reed, Scot B. Aase, Mark C. Hash, Larry Putty, Dusan Lexa .....	89
<b>XANES and EXAFS Studies of Plutonium(III, VI) Sorbed on Thorium Oxide</b>	
R. Drot, E. Ordonez-Regil, E. Simoni, Ch. Den Auwer, Ph. Moisy .....	93
<b>Effects of Fission Product Accumulation in Cubic Zirconia</b>	
L. M. Wang, S. X. Wang, S. Zhu, R. C. Ewing .....	95
<b>Identification of a Physical Metallurgy Surrogate for the Plutonium—1 wt. % Gallium Alloy</b>	
Frank E. Gibbs, David L. Olson, William Hutchinson .....	98
<b>Innovative Concepts for the Plutonium Facilities at La Hague</b>	
B. Gillet, A. Gresle, F. Drain .....	102
<b>Anisotropic Expansion of Pu through the <math>\alpha</math>-<math>\beta</math>-<math>\gamma</math> Phase Transitions While Under Radial Compressive Stress</b>	
Dane R. Spearing, D. Kirk Veirs, F. Coyne Prenger .....	104
<b>Contribution of Water Vapor Pressure to Pressurization of Plutonium Dioxide Storage Containers</b>	
D. Kirk Veirs, John S. Morris, Dane R. Spearing .....	107
<b>Surveillance of Sealed Containers with Plutonium Oxide Materials</b>	
Laura Worl, John Berg, Doris Ford, Max Martinez, Jim McFarlan, John Morris, Dennis Padilla, Karen Rau, Coleman Smith, Kirk Veirs, Dallas Hill, Coyne Prenger .....	109
<b><math>PuO_2</math> Surface Catalyzed Reactions: Recombination of <math>H_2</math> and <math>O_2</math> and the Effects of Adsorbed Water on Surface Reactivity</b>	
Luis Morales .....	112
<b>Kinetics of the Reaction between Plutonium Dioxide and Water from 25°C to 350°C: Formation and Properties of the Phase <math>PuO_{2+x}</math></b>	
L. Morales, T. Allen, J. Haschke .....	114
<b>A Conceptual and Calculational Model for Gas Formation from Impure Calcined Plutonium Oxides</b>	
John L. Lyman, P. Gary Eller .....	117
<b>Status of the Pit Disassembly and Conversion Facility</b>	
Warren T. Wood, Lowell T. Christensen .....	120
<b>Plutonium Packaging and Long-Term Storage</b>	
Jane A. Lloyd, Douglas E. Wedman .....	121
<b>Phase Composition of Murataite Ceramics for Excess Weapons Plutonium Immobilization</b>	
I. A. Sobolev, S. V. Stefanovsky, B. F. Myasoedov, Y. M. Kuliako, S. V. Yudintsev .....	122

## Posters

## Materials Science

<b>Analysis of Strain Anisotropy in Delta Stabilized Pu-Ga Alloys</b> Luis Morales, Andrew Lawson, John Kennison .....	125
<b>Preparation of Actinide Boride Materials via Solid-State Metathesis Reactions and Actinide Dicarbolide Precursors</b> Anthony J. Lupinetti, Julie Fife, Eduardo Garcia, Kent D. Abney .....	127
<b>The Self-Irradiation Driven Enhancement of Diffusion Processes in Nuclear-Safe Ceramics</b> E. A. Smirnov, L. F. Timofeeva .....	130
<b>The Regularities of Diffusion Processes in the Low-Temperature Phases of Neptunium and Plutonium</b> E. A. Smirnov, A. A. Shmakov .....	132
<b>Interdiffusion in U–Pu–Zr and U–Zr–Ti Solid Solutions</b> O. A. Alexeev, A. A. Shmakov, E. A. Smirnov .....	135
<b>Research in the Patterns of Time-Related Change in the Structure and Properties of Plutonium Dioxide Produced with Different Process Streams</b> E. M. Glagovskiy, V. A. Zhmak, V. Ye. Klepatskiy, L. N. Konovalov, A. V. Laushkin, V. K. Orlov, Ya. N. Chebotarev, .....	138
<b>A Combinatorial Chemistry Approach to the Investigation of Cerium Oxide and Plutonium Oxide Reactions with Small Molecules</b> John T. Brady, Benjamin P. Warner, Jon S. Bridgewater, George J. Havrilla, David E. Morris, C. Thomas Buscher .....	141
<b>Destruction of Halogenated Organics with Hydrothermal Processing</b> Laura A. Worl, Steven J. Buelow, David M. Harradine, Dallas Hill, Rhonda McInroy, Dennis Padilla .....	145
<b>Preparation of Plutonium-Bearing Ceramics via Mechanically Activated Precursor</b> S. V. Chizhevskaya, S. V. Stefanovsky .....	148
<b>A Single Material Approach to Nuclear Waste Disposal</b> James V. Beitz, Clayton W. Williams .....	151
<b>Immobilization of Pu-Containing Solution Using a Porous Crystalline (Gubka) Matrix</b> A. S. Aloy, N. V. Sapozhnikova, A. V. Strelnikov, D. A. Knecht, A. G. Anshits, A. Tretyakov, T. J. Tranter, J. Macheret, L. J. Jardine .....	153
<b>Immobilization of Pu-Containing Wastes into Glass and Ceramics: Results of US-Russia Collaboration</b> E. B. Anderson, A. S. Aloy, B. E. Burakov, L. J. Jardine .....	155
<b>Performance Evaluation of Pyrochlore Ceramic Waste Forms by Single Pass Flow Through Testing</b> P. Zhao, W. L. Bourcier, B. K. Esser, H. F. Shaw .....	157
<b>Experience of V. G. Khlopin Radium Institute on Synthesis and Investigation of Pu-Doped Ceramics</b> B. E. Burakov, E. B. Anderson, V. G. Khlopin .....	159
<b>Absorption Spectra of Plutonium in Phosphate and Borosilicate Glasses</b> Yu .A. Barbanel', A. S. Aloy, V. V. Kolin, V.P. Kotlin, A. V. Trofimenko .....	161
<b>Microstructure and Thermodynamics of Zirconolite- and Pyrochlore-Dominated Synroc Samples: HRTEM and AEM Investigation</b> Huifang Xu, Yifeng Wang .....	164
<b>Electron Microscopy Study of a Radioactive Glass-Bonded Sodalite Ceramic Waste Form</b> Wharton Sinkler, Thomas P. O'Holleran, Tanya L. Moschetti .....	166
<b>Site Preferences of Actinide Cations in [NzP] Compounds</b> H. T. Hawkins, D. R. Spearing, D. M. Smith, F. G. Hampel, D. K. Veirs, B. E. Scheetz .....	168

<b>Actinide-Zirconia Based Materials for Nuclear Applications: Cubic Stabilized Zirconia Versus Pyrochlore Oxide</b>	
P. E. Raison, R. G. Haire .....	171
<b>Fundamental Aspects of Actinide-Zirconium Pyrochlore Oxides: Systematic Comparison of the Pu, Am, Cm, Bk and Cf Systems</b>	
R. G. Haire, P. E. Raison .....	173
<b>Identification of Source Term of Plutonium in the Environment Around WIPP Site</b>	
Balwan Hooda, Carl Ortiz .....	175
<b>Elimination or Reduction of Magnesium Oxide as the Engineered Barrier at the Waste Isolation Pilot Plant</b>	
Matthew K. Silva .....	176
<b>Immobilization of Plutonium-Containing Waste into Borobasalt, Piroxen and Andradite Mineral-Like Compositions</b>	
Yu. I. Matyunin, S. V. Yudintsev, L. J. Jardine .....	179
<b>Technology and Equipment Based on Induction Melters with “Cold” Crucible for Reprocessing Active Metal Waste</b>	
V. G. Pastushkov, A. V. Molchanov, V. P. Serebryakov, T. V. Smelova, I. N. Shestoporov .....	180
<b>Development of Technology for Ammonium Nitrate Dissociation Process</b>	
B. S. Zakharkin, V. P. Varykhanov, V. S. Kucherenko, L. N. Solov'yeva, V. V. Revyakin, .....	181
<b>The Myth of the “Proliferation-Resistant” Closed Nuclear Fuel Cycle</b>	
Edwin S. Lyman .....	187
<b>Advanced MOX Fabrication Methods for LWRs</b>	
D. Haas, J. Somers, C. Walker, S. Brémier .....	191
<b>Synthesis of the U.S. Specified Ceramics Using MOX Fuel Production Expertise</b>	
V. A. Astafiev, A. E. Glushenkov, M. Sidelnikov, G. B. Borisov, O. A. Mansourov, L. J. Jardine .....	193
<b>Research Program for the 660 MeV Proton Accelerator Driven MOX-Plutonium Subcritical Assembly</b>	
V. S. Barashenkov, V. S. Buttsev, G. L. Buttseva, S. Ju. Dudarev, A. Polanski, I. V. Puzynin, A. N. Sissakian .....	194
<b>Continuous Process of Powder Production for MOX Fuel Fabrication According to “GRANAT” Technology</b>	
V. E. Morkovnikov, L. S. Raginskiy, A. P. Pavlinov, V. A. Chernov, V. V. Revyakin, V. Varikhanov, V. N. Revnov .....	199
<b>Fabrication Technology and Characteristics of AmO<sub>2</sub>-MgO Cercer Materials for Transmutation</b>	
Y. Croixmarie, A. Mocellin, D. Warin .....	200
<b>Analysis Capabilities for Plutonium-238 Programs</b>	
A.S. Wong, G. H. Rinehart, M. H. Reimus, M. E. Pansoy-Hjelvik, P. F. Moniz, J. C. Brock, S. E. Ferrara, S. S. Ramsey .....	202
<b>Modeling of Fission Gas Release in MOX Fuel Considering the Distribution of Pu-Rich Particles</b>	
Yang-Hyun Koo, Byung-Ho Lee, Dong-Seong Sohn .....	205
<b>Comparative Analysis of Basic Process Arrangements for Converting Surplus Weapons Grade Plutonium to MOX Fuel</b>	
V. P. Varykhanov, E. M. Glagovskiy, B. S. Zakharkin, V. V. Revyakin, O. V. Khauystov .....	208

Nuclear Fuels/  
Isotopes

<b>Technical Challenges in Support of the Plutonium Materials Conversion Program in Russia</b>	
C. F. V. Mason, S. J. Zygmunt, W. K. Hahn, C. A. James, D. A. Costa, W. H. Smith, S. L. Yarbrow .....	211
<b>CHEMOX: An Integrated Facility for the Conversion of Russian Weapon-Grade Plutonium into Oxide for MOX Fuel Fabrication</b>	
E. Glagovski, Y. Kolotilov B. Sicard, F. Josso, G. Fraize N. Herlet, A. Villa, P. Brossard .....	214
<b>Radiation-Chemical Behaviour of Plutonium in Solutions DAMP and TOPO in n-dodecane</b>	
D. A. Fedoseev .....	215
<b>Dissolution of Phosphate Matrices Based on the Thorium Phosphate Diphosphate</b>	
N. Dacheux, A.C. Thomas, V. Brandel, M. Genet .....	216
<b>Modelling of Nitric Acid and U(VI) Co-Extraction in Annular Centrifugal Contactors</b>	
E. T. Gaubert, M. Jobson, J. E. Birket, I. S. Denniss, I. May .....	217
<b>The Measurement of U(VI) and Np(IV) Mass Transfer in a Single Stage Centrifugal Contactor</b>	
I. May, E. J. Birkett, I. S. Denniss, E. T. Gaubert, M. Jobson .....	219
<b>Actinide Chemistry in Room Temperature Ionic Liquids: Actinide Chemistry in RTIL Systems (Why?)</b>	
David A. Costa, Wayne H. Smith, Kent D. Abney, Warren J. Oldham .....	221
<b>Oxidation of Pu(IV) and Pu(V) with Sodium Hypochlorite</b>	
G. R. Choppin, A. Morgenstern .....	223
<b>Contribution of the "Simple Solutions" Concept to Estimate Density of Concentrated Solutions</b>	
Christian Sorel, Philippe Moisy, Binh Dinh, Pierre Blanc .....	225
<b>Structural Studies of f-Element Complexes with Soft Donor Extractants</b>	
Mark P. Jensen, Andrew H. Bond, Kenneth L. Nash .....	228
<b>Lewis Base Binding Affinities and Redox Properties of Plutonium Complexes</b>	
Susan M. Oldham, Ann R. Schake, Carol J. Burns, Arthur N. Morgan III, Richard C. Schnabel, Benjamin P. Warner, David A. Costa, Wayne H. Smith .....	230
<b>QSAR of Distribution Coefficients for Pu(NO<sub>3</sub>)<sub>6</sub><sup>2-</sup> Complexes Using Molecular Mechanics</b>	
Eddie Moody .....	232
<b>Materials Compatibility for <sup>238</sup>Pu-HNO<sub>3</sub>/HF Solution Containment: <sup>238</sup>Pu Aqueous Processing</b>	
M. A. Reimus, M. E. Pansoy-Hjelvik, G. Silver, J. Brock, J. Nixon, K. B. Ramsey, P. Moniz .....	234
<b>Process Parameters Optimization in Ion Exchange <sup>238</sup>Pu Aqueous Processing</b>	
M. E. Pansoy-Hjelvik, J. Nixon, J. Laurinat, J. Brock, G. Silver, M. Reimus, K. B. Ramsey .....	236
<b>Plutonium Pyrochemical Salts Oxidation and Distillation Processing: Residue Stabilization and Fundamental Studies</b>	
Donna M. Smith, Mary P. Neu, Eduardo Garcia, Vonda R. Dole .....	238
<b>Americium Extraction from Plutonium Metal</b>	
R. F. Watson .....	239
<b>Dry Process for Recovering Gallium from Weapons Plutonium Using a Rotary Furnace Equipped with a Copper Collector</b>	
C. V. Philip, Rayford G. Anthony, Chokkaram Shivraj, Elizabeth Philip, W. Wilson Pitt, Max Roundhill, Carl Beard .....	240
<b>Purification of Plutonium via Electromagnetic Levitation</b>	
J. C. Lashley, M.S. Blau, J. R. Quagliano .....	243

<b><sup>238</sup>Pu Recovery and Salt Disposition from the Molten Salt Oxidation Process</b>	
M. L. Remerowski, Jay J. Stimmel, Amy S. Wong, Kevin B. Ramsey .....	246
<b>Stabilization of <sup>238</sup>Pu-Contaminated Combustible Waste by Molten Salt Oxidation</b>	
Jay J. Stimmel, Mary Lynn Remerowski, Kevin B. Ramsey, J. Mark Heslop .....	248
<b>Low Temperature Reaction of Reillex<math>\phi</math> HPQ and Nitric Acid</b>	
William J. Crooks III, Edward A. Kyser III, Steven R. Walter .....	250
<b>Molten Salt Fuels for Treatment of Plutonium and Radwastes in ADS and Critical Systems</b>	
Victor V. Ignatiev .....	252
<b>High Level Waste Partitioning Studies at the Research Centre Jülich</b>	
Ulrich Wenzel .....	255
<b>Modeling Hollow Fiber Membrane Separations Using Voronoi Tessellations</b>	
Richard Long, Tsun-Teng Liang, John Rogers, Steve Yarbrow .....	257
<b>Identification of Oligomeric Uranyl Complexes under Highly Alkaline Conditions</b>	
Wayde V. Konze, David L. Clark, Steven D. Conradson, J. Donohoe, John C. Gordon, Pamela L. Gordon, D. Webster Keogh, David E. Morris, C. Drew Tait .....	261
<b>Process Support Conditions for Dissolving Metallic Plutonium in a Mixture of Nitric and Hydrofluoric Acids</b>	
B. S. Zakharkin, V. P. Varykhanov, V. S. Kucherenko, L. N. Solov'yeva .....	263
<b>Investigation of Radiation-Chemical Behaviour of Plutonium in the Groundwaters and Soils</b>	
D. A. Fedoseev, M. Yo. Dunaeva, M. V. Vladimirova .....	266
<b>Polymeric Species of Pu in Low Ionic Strength Media</b>	
V. V. Romanovski, C. E. Palmer, H. F. Shaw, W. L. Bourcier, L. J. Jardine .....	267
<b>Solubility and Speciation of Plutonium(VI) Carbonates and Hydroxides</b>	
Sean D. Reilly, Mary P. Neu, Wolfgang Runde .....	269
<b>Plutonium in the Environment: Speciation, Solubility, and the Relevance of Pu(VI)</b>	
W. Runde, D. Efurud, M. P. Neu, S. D. Reilly, C. VanPelt, S. D. Conradson .....	272
<b>Immobilizing U from Solution by Immobilized Sulfate-Reducing Bacteria of <i>Desulfovibrio desulfuricans</i></b>	
Huifang Xu, Larry L. Barton .....	274
<b>Interaction of Actinides with Aerobic Soil Bacteria</b>	
P. J. Panak, H. Nitsche .....	275
<b>Plutonium Uptake by Common Soil Aerobes</b>	
Seth John, Christy Ruggiero, Larry Hersman, Mary Neu .....	277
<b>XAS of Uranium(VI) Sorbed onto Silica, Alumina, and Montmorillonite</b>	
E. R. Sylwester, P. G. Allen, E. A. Hudson .....	279
<b>Interactions of Mixed Uranium Oxides with Synthetic Groundwater and Humic Acid Using Batch Methods: Solubility Determinations, Experimental and Calculated</b>	
David N. Kurk, Gregory R. Choppin, James D. Navratil .....	282
<b>Actinide Interactions with Aerobic Soil Microbes and Their Exudates: The Reduction of Plutonium with Desferrioxamine Siderophores</b>	
C. E. Ruggiero, J. H. Matonic, M. P. Neu, S. P. Reilly .....	284
<b>Interactions of Microbial Exopolymers with Actinides</b>	
Mitchell T. Johnson, Dawn J. Chitwood, Lee He, Mary P. Neu .....	286
<b>The Behaviour of Pu under Repository Conditions</b>	
Jordi Bruno, Esther Cera, Lara Duro, Mireia Grivé, Trygve Erikssen, Ulla-Britt Eklund, Kastriot Spahiu .....	288
<b>Interaction of Plutonium and Uranium with Apatite Mineral Surfaces</b>	
Craig E. Van Pelt, Mavis Lin, Donna M. Smith, Wolfgang H. Runde .....	290

Actinides in the Environment

<b>Equilibrium, Kinetic and Reactive Transport Models for Pu: Employing Numerical Methods to Uncover the Nature of the Intrinsic Colloid</b> Jon M. Schwantes, Bill Batchelor .....	292
<b>Uncertainty Reporting in Measurements of Plutonium Solution Speciation: How Can We Do Better?</b> John M. Berg, D. Kirk Veirs .....	299
<b>Production and Radiometric Measurements of the Large Particle Plutonium Oxide Non-Destructive Assay Standards</b> Denise L. Thronas, Amy S. Wong, Sandra L. Mecklenburg, Robert S. Marshall .....	301
<b>Analysis of Boron and Silicon in Plutonium Samples by Inductively Coupled Plasma Spectrometry</b> Billie A. Shepherd, Sandra L. Bonchin, Deborah J. Figg .....	303
<b>Laser Induced Breakdown Spectroscopy (LIBS) Applied to Plutonium Analysis</b> Coleman A. Smith, Max A. Martinez .....	305
<b>Emission from Neptunyl Ions in the Near IR</b> H. J. Dewey, T. A. Hopkins .....	307
<b>Spectroscopy of <math>\text{UO}_2\text{Cl}_4^{2-}</math> in Basic Aluminum Chloride: 1-Ethyl-3-methylimidazolium Chloride</b> Todd A. Hopkins, John M. Berg, David A. Costa, Wayne H. Smith, Harry J. Dewey .....	309
<b>ARIES Nondestructive Assay System Operation and Performance</b> Teresa L. Cremers, Walter J. Hansen, Gary D. Herrera, David C. Nelson, Thomas E. Sampson, Nancy L. Scheer .....	311
<b>Peak Asymmetry Understanding in <math>\alpha</math> Liquid Scintillation with <math>\beta/\gamma</math> Rejection</b> Jean Aupiais, Nicolas Dacheux .....	312
<b>A New Method of Alpha Spectrometry Based on Solid-State Nuclear Track Detection: Principles, Performance, Applicability</b> O. A. Bondarenko, Y. N. Onischuk, D. V. Melnichuk, S. Y. Medvedev, V. M. Petrishin .....	314
<b>Analysis of Aerosol Distribution inside the Object "Shelter"</b> O. A. Bondarenko, P. B. Aryasov, D. V. Melnichuk, S. Yu. Medvedev .....	315
<b>Ultratrace Analysis of Plutonium in Environmental Samples by Resonance Ionization Mass Spectrometry (RIMS)</b> N. Trautmann, N. Erdmann, C. Grüning, J.V. Kratz, A. Waldek, G. Huber, M. Nunnemann, G. Passler .....	322
<b>Rad Calc III: Radioanalysis Calculation Program for Plutonium and Americium Determination</b> J. M. Blackadar, A. S. Wong, N. D. Stalnaker, J. R. Willerton .....	324
<b>A New Glovebox—Surface Science Facility for the Study of Plutonium Surface Chemistry at AWE</b> T. J. Piper, D. S. Shaw, P. Roussel, D. A. Geeson* .....	327
<b>Detection of Leaking Actinide Hexafluoride Storage Cylinders</b> James V. Beitz and Clayton W. Williams .....	329
<b>Plutonium Process Monitoring (PPM) System</b> A. S. Wong, T. E. Ricketts, M. E. Pansoy-Hejvik, K. B. Ramsey, K. M. Hansel, M. K. Romero .....	331
<b>Determining Analyte Concentrations in Plutonium Metal by X-Ray Fluorescence Using a Dried Residue Method</b> Christopher G. Worley, George J. Havrilla .....	334



<b>Comparison of Different Surface Quantitative Analysis Methods: Application to Corium</b> Nathalie Guilbaud, Delphine Blin, Philippe Pérodeaud, Olivier Dugne Christine Guéneau .....	336
<b>Qualification of the Bubble Detector as Neutron Dosimeter at the MOX Plant of BELGONUCLEAIRE</b> P. Kockerols, F. De Smet, A. Vandergheynst .....	338
<b>Microscopic Determination of the Size Distribution of PuO<sub>2</sub>-Rich Zones and Pores in MOX Pellets with an Image Analysis System</b> J. Vandezande, H. Pauwels, A. Vandergheynst .....	340
<b>Plasmon Resonance Spectroscopy of Plutonium Metal</b> Roland K. Schulze, J. Doug Farr, Jeffrey C. Archuleta .....	343
<b>Atomic H(D) Adsorption on Polycrystalline UO<sub>2</sub> and UO<sub>2</sub>(111) Surfaces</b> M. R. Voss, M.T. Paffett .....	346
<b>Accelerator Mass Spectrometry Measurements of Actinide Concentrations and Isotope Ratios</b> Jeffrey E. McAninch, Terry F. Hamilton .....	348
<b>Determination of Mercury in Radioactive Samples by Cold Vapor Atomic Fluorescence Spectrometry</b> Michael N. Jaspersen, Lawrence R. Drake .....	350
<b>Single Crystal Growth of (U<sub>1-x</sub>Pu<sub>x</sub>)O<sub>2</sub> Mixed Oxides</b> J. Rebizant, E. Bednarczyk, P. Boulet, C. Fuchs, F. Wastin .....	355
<b>Metallofullerenes Encapsulating Actinide Atoms</b> H. Nakahara, K. Sueki, K. Akiyama, Y. L. Zhao, Y. Nagame, K. Tuskada .....	357
<b>Kinetics of the Oxidation of Pu(IV) by Manganese Dioxide</b> A. Morgenstern, G. R. Choppin .....	358
<b>Calculation of Structural and Thermodynamic Properties of Pu-Doped Thorium Phosphate Diphosphate Th<sub>4-x</sub>Pu<sub>x</sub>(PO<sub>4</sub>)<sub>2</sub>P<sub>2</sub>O<sub>7</sub></b> C. Meis .....	360
<b>Prediction of Thermodynamic Property of Pu-zircon and Pu-pyrochlore</b> Huifang Xu, Yifeng Wang .....	363
<b>Utilization of Principal Component Analysis on Plutonium EXAFS Data from the Advanced Photon Source</b> Jeff Terry, Roland K. Schulze, Thomas G. Zocco, J. Doug Farr, Jeff Archuleta, Mike Ramos, Ray Martinez, Barbara Martinez, Ramiro Pereyra, Jason Lashley, Steve Wasserman, Mark Antonio, Suntharalingam Skanthakumar, Lynne Soderholm .....	364
<b>Surface Analysis of Pu Oxide Powders: Thermal Dehydration/Water Vapor Rehydration Studies</b> J. Douglas Farr, Roland K. Schulze, Mary P. Neu, Luis A. Morales .....	367
<b>Important New Insights into f-Electron Behavior via Ultra-High Pressure Studies of Transplutonium Elements</b> R. G. Haire, S. Heathman, A. Lindbaum, K. Litfin, Y. Meressé, T. LeBihan .....	369
<b>Steric vs. Electronic Effects in Binary Uranyl Alkoxides: A Spectroscopic Perspective</b> David E. Morris, Marianne P. Wilkerson, Carol J. Burns, Brian L. Scott, Marianne P. Wilkerson, Robert T. Paine .....	371

Pu & Pu  
Compounds

Actinide  
Compounds &  
Complexes

<b>Structural Preferences and Reactivity of Uranyl Alkoxide Complexes Prepared in Non-Protic Media</b>	
Carol J. Burns, Marianne P. Wilkerson, David E. Morris, Brian L. Scott, Robert T. Paine .....	377
<b>Synthesis and Structural Studies of Plutonium Complexes Containing Nitrogen and Sulfur Donor Ligands</b>	
John H. Matonic, Mary P. Neu, Brian Scott, Marinella Mazzanti .....	379
<b>Structures of Plutonium Coordination Compounds: A Review of Past Work, Recent Single Crystal X-Ray Diffraction Results, and What We're Learning about Plutonium Coordination Chemistry</b>	
M. P. Neu, J. H. Matonic, D. M. Smith, B. L. Scott .....	381
<b>Characterisation of Uranium Compounds after a Fire Ignition</b>	
D. Labroche, D. Pisson, P. Ramel, O. Dugne .....	383
<b>Solid State Chalcophosphate Compounds of Actinide Elements</b>	
Paula M. Briggs Piccoli, Ryan F. Hess, Kent D. Abney, Jon R. Schoonover, Peter K. Dorhout .....	384
<b>Thermodynamic and Structural Characterisation of the UFe<sub>4</sub> Compound</b>	
D. Labroche, J. Rogez, O. Dugne, J. P. Laval .....	387
<b>Thermodynamic Properties of Pu<sup>3+</sup> and Pu<sup>4+</sup> Aquo Ions</b>	
F. David, B. Fourest, S. Hubert, J. Purans, V. Vokhmin, C. Madic .....	388
<b>Modeling the Thermodynamic Properties of Plutonium</b>	
Marius Stan .....	390
<b>Theoretical Studies of Actinyl Crown Ether Inclusion Complexes</b>	
Richard L. Martin, P. Jeffrey Hay, Georg Schreckenbach .....	392
<b>Non-Aqueous Chemistry of Uranyl Complexes with Tripodal Ligands</b>	
Carol J. Burns, David L. Clark, Paul B. Duval, Brian L. Scott .....	397
<b>Organoactinides—New Type of Catalysts for Carbon-Carbon, Carbon-Nitrogen, and Carbon-Silicon Bond Formations</b>	
Moris S. Eisen .....	399
<b>A Novel Equation for Predicting Stability Constants of Aqueous Metal Complexes and Actinide Binding to Protein</b>	
Huifang Xu, Yifeng Wang .....	402
<b>Radiation Effects in Uranium-Niobium Titanates</b>	
J. Lian, S. X. Wang, L. M. Wang, R. C. Ewing .....	403
<b>Electronic and Geometric Structure of Pu Metal: A High-Resolution Photoelectron Spectromicroscopy Study</b>	
J. Terry, R. K. Schulze, T. Zocco, Jason Lashley, J. D. Farr, K. Heinzelman, E. Rotenberg, D. K. Shuh, M. Blau, J. Tobin .....	406
<b>Preliminary Study of (Pu<sub>1-x</sub>Am<sub>x</sub>) Solid Solutions</b>	
F. Wastin, E. Gomez-Marin, D. Bouëxière, J.C. Spirlet, J.M. Fournier .....	410
<b>Actinide Electronic Structure and Atomic Forces</b>	
R. C. Albers, Sven P. Rudin, Dallas R. Trinkle, M. D. Jones .....	412
<b>Determination of Mechanical Properties of Aged Plutonium from ARIES Pits by Instrumented Sharp Indentation</b>	
Tonya Huntley, Kaye Johnson, David Olivas, Robi Mulford, Wendel Brown, Kevin Walter, Mike Stout .....	414
<b>Density of Plutonium Metal as a Function of Age</b>	
R. N. Mulford, M. Valdez .....	416
<b>Electronic Structure of Elements and Compounds and Electronic Phases of Solids</b>	
B. A. Nadykto .....	418

Condensed  
Matter Physics



<b>5f Band Dispersion in the Highly Correlated Electronic Structure of Uranium Compounds</b>	
D. P. Moore, J. J. Joyce, A. J. Arko, L. Morales, J. Sarrao .....	420
<b>All-Electron Density Functional Theory Calculations of the Zero-Pressure Properties of Plutonium Dioxide</b>	
Jonathan C. Boettger, Asok K. Ray .....	422
<b>Predictions of Plutonium Alloy Phase Stability Using Electronic Properties</b>	
D. L. Olson, G. R. Edwards, D. E. Dooley .....	424
<b>Structural Stability in High Temperature Pu and Pu Alloys</b>	
John Wills, Heinrich Roder, Olof R. Eriksson .....	426
<b>Diffusion of Helium in Plutonium Alloys</b>	
D. Dooley, B. Martinez, D. Olson, D. Olivas, R. Ronquillo, T. Rising .....	428
<b>Effects of Self-Irradiated Damage on Physical Properties of Stabilized Pu Alloys</b>	
F. Freibert, B. Martinez, J. P. Baiardo, J. Olivas, R. Ronquillo .....	431
<b>Author Index</b> .....	433



# Plutonium Futures—The Science

## Preface

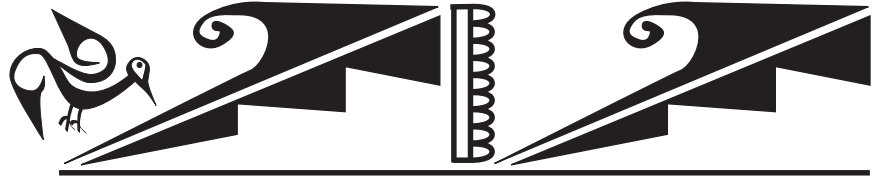
R. Bruce Matthews  
*Conference Co-Chair*

The scientific papers presented at the second “Plutonium Futures-The Science” conference held in Santa Fe, New Mexico, in July 2000 are contained in these proceedings. The first “Plutonium Futures-The Science” conference, held in August of 1997, attracted more than 300 scientists and engineers from fourteen countries. Participants representing more than 60 institutions, universities, and research laboratories presented more than 125 papers. That conference helped increase awareness of the importance of the scientific underpinnings of plutonium research and its global nature. The breadth and technical content of this year’s conference exceeds the previous one. More than 180 papers cover activities in materials science, actinide process chemistry, nuclear fuels, transuranic waste forms, actinides in the environment, actinide separation and analysis, and condensed matter physics of actinides. In addition, a tutorial session on nuclear and radiochemistry, the chemistry and physics of plutonium, and recent advances in plutonium oxide and surface science precedes the conference.

Why the interest in plutonium? Scientists are attracted to the most scientifically fascinating and technically challenging element in the periodic chart. At the same time, plutonium and its uses represent one of the most politically charged international issues on the planet. Science is the focus of this conference, but because of the importance of plutonium in the balance of world power, the focus on its science is dictated to a large degree by international policies and issues of grave political importance. The world is more concerned than ever with nuclear proliferation in many of the traditionally non-nuclear weapon states. Safe management of nuclear materials still looms as an important issue worldwide. A great deal of work still needs to be done under the Russian/U.S. agreement to dispose of up to fifty metric tons each of weapons plutonium. At the same time there has been a renewed interest in the U.S. and Russia to develop plutonium/uranium mixed oxide fuels as a means of disposing of the excess plutonium.

Advances in the understanding of plutonium sciences underpin many of these issues, and an amazing amount of new plutonium science has emerged worldwide since the last conference. For example, detailed Russian studies on the Pu-Ga phase diagram raised questions on thermodynamic-versus-kinetic stability. Applications of synchrotron radiation revealed local structure changes about the Pu or Ga atom using x-ray absorption fine structure (XAFS), and the electronic structure of  $\alpha$  and  $\delta$  Pu was refined using soft x-ray resonant photoemission spectroscopy. Detailed studies of plutonium oxides revealed the existence of a higher oxide thereby advancing the understanding of corrosion mechanisms. Resonant ultrasound spectroscopy and neutron diffraction studies have given additional insights into the phonon modes of pure and alloyed plutonium. New ceramic compositions are being developed for plutonium storage. Finally, sophisticated studies on the migration behavior of plutonium in the environment have underscored the importance of colloid-facilitated transport of plutonium in ground water. Clearly, the scientific advances of the twenty-first century are continuing to unlock the importance of the many mysteries surrounding plutonium. A significant portion of the scientific advances mentioned above and much more will be presented at the “Plutonium Futures-The Science” conference.

Plutonium science provides exciting opportunities for scientists and engineers to apply their talents to technical issues of international importance. One of the goals of this conference is to acquaint students with the world of plutonium and the opportunities to pursue careers in actinide sciences. Plutonium is a global science issue and requires the participation of scientific institutions, universities and students. The Plutonium Futures conference creates a forum where researchers in diverse fields may come together to present the latest scientific advances in a wide range of technical areas with the common thread of plutonium science. Los Alamos National Laboratory, in cooperation with the American Nuclear Society and the plutonium research community, is pleased and proud to sponsor this conference.



## **Plenary Session**



## How to Develop New Materials

The Manhattan Project required a large amount of innovative work to develop new techniques and new materials. A review of such activities could be useful for future developments of the actinides. It is important to work out techniques for handling radioactive waste. I will review the activities dealing with the development of plutonium containment that could serve as a guide for future needs.

Processes will have to be developed for safe storage and applications of the actinides if adequate agreement is reached on reduction of nuclear weapons. One of the key problems facing us in the near future is the production of adequate electrical power, and it may be essential to expand the use of plutonium and uranium for the fuels of nuclear reactors. It is particularly important that the design of the nuclear reactors anticipate possible accidents, so that procedures need to be developed to minimize health problems. We must have nuclear designs that are less risky than power plants using coal, oil and other combustible materials to convince the public that nuclear reactors can be safe.

To deal with the many problems that will have to be resolved in the future, we have to consider novel materials that would have properties of unique value for the processes. One source of materials with a wide range of properties is the intermetallics of transition metals or mixtures of transition metals with ordinary metals. Considering the multicomponent mixtures that can be used, there are millions of novel materials that can be developed. It is possible to predict the thermodynamic stabilities and other properties of these materials. The predictions have been illustrated for aluminides of the transition metals using a modified Born-Haber cycle to take into account both covalent and ionic interactions. This treatment is being expanded to predict the properties of transition metals with gallium and other non-transition metals, as well as dealing with multicomponent mixtures of just transition metals, including the lanthanides and actinides as part of the transition metal group.

To deal with so many materials and to consider their applications will require a large amount of time, and it will be very important to recruit more scientists to carry out these predictions.

**Leo Brewer**  
*University of  
California, Berkeley,  
CA 74720, USA*

## Status and Trends in Plutonium Recycling in Nuclear Power Reactors

Vladimir Onoufrieu  
International Atomic  
Energy Agency,  
Vienna, Austria

The controlled use of plutonium in power reactors has become an important factor in considering the ongoing development of nuclear power. On one hand a continuing accumulation of unused plutonium presents a future challenge to the world community because of an increasing risk of its use for nonpeaceful purposes. On the other hand only with plutonium use may one utilize practically unlimited resources of fertile uranium-238 in energy generation. Initially plutonium was sought to be used primarily in fast breeder reactors (FBRs), where its recycling increases the energy available 50 fold or more, making fission energy by far the largest energy resource available, indeed, a virtually inexhaustible one. In the beginning, the use of plutonium in the form of mixed-oxide (MOX) fuel in thermal reactors was taken only as an alternative back-end policy option. Plutonium use in thermal reactors also increases uranium efficiency, but only about twice. Nevertheless, today the plutonium recycling in light-water reactors (LWRs) has evolved to an industrial level in some countries engaged in the recycling policy. This happened mainly because of the delays in the development of FBRs and the need to realize at least a partial return on investments made in reprocessing facilities.

Already during the well-known IAEA International Fuel Cycle Evaluation Study of 1976-80,<sup>[1]</sup> the different aspects of plutonium utilization in the form of MOX fuel were discussed and followed up in the many international meetings during the last two decades. An International Symposium on MOX Fuel Cycle Technologies for Medium and Long Term Deployment, organized by the IAEA in co-operation with OECD/NEA and held in Vienna in May 1999, was a milestone which reviewed the past, present and future of Pu recycling in nuclear power reactors.<sup>[2]</sup> This paper presents major results of the Symposium in the context of present conditions of deregulated electricity market and in the future and its role in the reduction of stockpiles of separated civil and surplus ex-weapons plutonium. In addition to current and projected MOX production and requirement capacities, the paper presents the IAEA evaluation of this data and data on separated civil Pu inventories worldwide up to 2020 made using the VISTA Code.<sup>[3]</sup> The IAEA estimations are done for different scenarios of nuclear power and fuel cycle strategies.

More than 30 years of reactor experience using MOX fuel as well as the fabrication of 2000 LWR MOX assemblies, with the use of 85 t of Pu separated from spent fuel from power reactors, indicates that the recycling of Pu as MOX fuel in LWRs has become a mature industry. The technology for reprocessing, fabrication, transportation, and safeguarding is well progressed, and the facilities, institutions and procedures are in place (with capacity extensions being planned). This is to meet the anticipated increase in amounts of separated plutonium from the production of nuclear power. The number of countries engaged in plutonium recycling (at present-6) could be increasing in the near future, aiming at the reduction of stockpiles of separated plutonium from earlier and existing reprocessing contracts. Economic and in some cases strategic considerations were the main factors on which such decisions on MOX use were based.



MOX fuel is designed to meet the same key safety parameters as uranium fuel for all normal and off-normal events, and it is demonstrated at each core loading that there is no challenge to the design basis. The IAEA symposium of 1999 reconfirmed the good and almost defect-free performance of MOX fuel at increasingly high burnup levels. Design codes to accommodate the special characteristics of MOX have been developed. To reach burnup levels equivalent to uranium fuels up to 70 MWd/kg, work is still ongoing to confirm required MOX fuel behaviour under extreme transient and accident conditions and to confirm models of fission gas release whereby this release may be mitigated by changing the fuel microstructures. The paper presents a review of major MOX fuel performance and design data.

The reactor-based weapons-grade (WG) plutonium disposition approach proposed by the USA and Russian Federation in part builds upon proven commercial MOX fuel technologies supplemented by other R&D that provides some optimism on implementation of WG MOX disposition. The goal of the U.S. and Russian plutonium disposition programmes is to render the surplus plutonium as inaccessible and unattractive for retrieval and weapons use as the residual plutonium in spent fuel from power reactors. Progress in these and some other activities on WG Pu disposition is presented in the paper.

The paper ends with an analysis of different scenarios on the long-term future of Pu recycling and MOX fuels. The first phase, with the full introduction of MOX recycling on a large scale in several countries and with build-up of approximately 190 t of separated civil Pu is coming to an end. The second phase is now beginning. After a further expansion of MOX recycling to include other countries and additional nuclear plants being licensed for MOX fuel, it can be expected that the separated Pu stockpiles (both, civil and WG) would begin to diminish and move to significantly lower levels. Apart from extending the number of power reactors able to use MOX fuel, the technology also needs to be developed for advanced and more environmentally friendly reprocessing methods and also new fuel technologies such as inert matrix fuels and advanced plutonium "incinerators." Such new technologies will be needed in a third stage of development to cover the case where nuclear power may for a time diminish in some countries even perhaps on a wide scale. The need would be to handle the remaining plutonium inventories or, more probably, to match a new revival of nuclear power to allow a positive and effective management of plutonium recycling keeping stockpiles at a minimum and permitting fuel and waste repositories to be "plutonium free." Such scenarios might be better managed and be more transparent under an international regime still to be evolved. Eventually this third phase of MOX recycling might be one in which MOX fuels become one of the standard nuclear fuels for plants specifically designed for the use of MOX fuels. This phase could only start when MOX recycling becomes commercially viable to the utilities.

### References

1. International Atomic Energy Agency, International Nuclear Fuel Cycle Evaluation, INFCE Summary Volume, IAEA, Vienna (1980).
2. International Atomic Energy Agency, International Symposium on MOX Fuel Cycle Technologies for Medium and Long Term Deployment, IAEA, Vienna (2000), in press.
3. Shan, R., Using VISTA to evaluate MOX fuel trends, Nuclear Engineering International, September 1999 (33-35).

## Fundamentally, Why is Plutonium Such an Unusual Metal?

Siegfried S. Hecker  
Los Alamos National  
Laboratory, Los  
Alamos, NM 87545,  
USA

Plutonium is an element at odds with itself—with little provocation it can change its density by as much as 25 percent; it can be as brittle as glass or as malleable as aluminum; it expands when it solidifies; and its silvery, freshly machined surface will tarnish in minutes, producing nearly every color in the rainbow. In addition, plutonium's continuous radioactive decay causes self-irradiation damage that can fundamentally change its properties over time. Plutonium appears to be truly unique with no analogues in the periodic table. What are the fundamental reasons for its unusual behaviors?

Plutonium fits near the middle of the actinide series. It is of practical interest principally because the  $^{239}$  isotope has attractive nuclear properties for energy production and nuclear explosives. Its structural properties are particularly unusual. The thermal instability of plutonium—that is, the large length (or volume) changes during heating or cooling—is the most important consequence of the unusual properties of plutonium. The huge volume changes in the solid state result primarily from structural transformations among an unprecedented six solid allotropes. The ambient-temperature phase of plutonium is a low-symmetry monoclinic crystal lattice, more typical of minerals than of metals. The high-symmetry, close-packed face-centered cubic phase exhibits the lowest density. The liquid is denser than the high-temperature solid phases resulting in contraction upon melting.

For a fundamental understanding we must turn to electronic structure because it determines all of these properties. In solids, the valence electrons of the isolated atomic states occupy the conduction band. In actinides, the 7s, 6d, and 5f electrons, all of nearly equivalent energies, form overlapping (hybridized) bands. The dominant band controls the bonding and resulting properties. The 5f electron wave functions are closely confined to the atomic cores and possess a very narrow energy band with a high density of states at the Fermi level. The key question for the actinides and plutonium is to determine what exactly the 5f electrons are doing. I believe the peculiarities of plutonium can be summarized by three features of its electronic structure.

(1) The spatial extent of the 5f electrons in plutonium is just enough to bond. The f electron wave functions are closely constrained to their atomic cores. In fact, the 4f electrons in the lanthanides are sufficiently constrained to be localized—that is, they do not form bonds and are, therefore, chemically inert. However, in the light actinides, the 4f electrons partially screen the nuclear charge allowing the 5f wave functions to extend somewhat more. Likewise, additional relativistic forces in the actinides allow the 5f wave functions to extend as well, resulting in just enough extension for the 5f electrons in the light actinides to form bands and participate in chemical bonding. The narrow band, high density of states at the Fermi level exhibited by the 5f electrons energetically favors a distorted crystal lattice over that of the high-symmetry structures typically observed in metals.

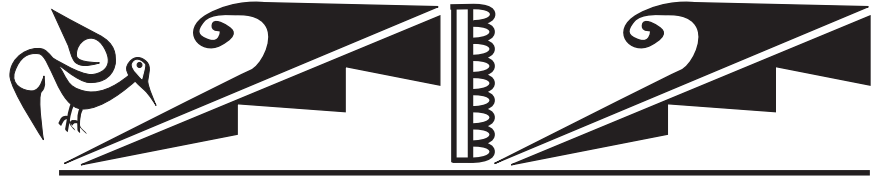
(2) Multiple electronic configurations of nearly equal energy levels. The 7s, 6d, and 5f atomic orbitals in isolated atoms possess nearly identical energy levels, and they form overlapping bands in the solid. With internal energy (at absolute

zero temperature) levels so close, it is relatively easy to lower the total free energy of the system externally by changing temperature, pressure, or chemistry. Particularly, at elevated temperatures, entropy contributions to the total free energy become more important, and crystal structures such as the relatively open body-centered cubic lattice with its high vibrational entropy are favored.

(3) Sitting on the knife-edge between bonding and localized behavior. As the nuclear charge increases across the actinide series, atomic radii contract, and the 5f wave functions gradually pull in more closely to the atomic cores. Since the 5f wave functions in the actinides just barely overlap to bond in the first place, this slight contraction finally pulls the 5f wave functions into the core at americium—that is the 5f electrons become localized and do not participate in chemical bonding. The consequences are dramatic—the s and d-electron bands dominate, atomic volumes increase enormously, and high-symmetry crystal structures are favored. This transition from bonding to localized behavior appears to occur right at plutonium. In the  $\alpha$  phase all 5f electrons bond, but the higher-temperature phases can best be characterized by having some of their 5f electrons localized.

I will present examples of how these three features strongly affect resulting crystal structures, melting points, and phase stability of plutonium and the actinides.





## **Materials Science/ Nuclear Fuels**



## Self-Irradiation of Pu, Its Alloys and Compounds

Self-irradiation of Pu, its alloys and compounds by products of known  $\alpha$ - decomposition is a continuous complicated process, which includes numerous different phenomena. The accumulation of Pu decomposition products causes material structure and properties change. This problem is the subject of many works, most of them concerned with the behavior of Pu and its alloys at low (liquid He and N) temperatures.

The survey is given of the results of our experiments connected with radiogenic helium behavior, crystal structure and properties of Pu metallic compounds and Pu oxide ceramics in a self-irradiation process at room temperature under isochronal heat treatments.

1. Radiogenic helium behavior in  $\delta$ -phase alloys of Pu with Ga at room temperature and under heating to melting has been studied. It was established that not more 10% of whole helium accumulated is released under heating of alloy with 0.08% He in solid state by the method of thermal degassing in a vacuum with continuous stepped annealing. There is one pick at 250°C–300°C in the spectrum of degassing due to different mechanisms of He migration to the sample surface and the change of helium form. Helium migration proceeds by the interstitial mechanism with activation energy  $E=0.2$  eV within 20°C–120°C, while in the range of 120°C–250°C it proceeds by a vacancy mechanism. It was shown by the method of positron annihilation that practically whole radiogenic helium is contained in pores of two sizes 0.4–0.8 nm and 17–23 nm<sup>[1]</sup>. The pores were absent from the initial alloy structure. There is only 37% He in pores at 575°C, the remaining amount apparently is contained inside bubbles, the appearance of which is observed in microstructure beginning from 425°C–450°C. The quantity of micro pores and their sizes are growing with temperature. As a result of isothermal annealing at 600°C during 1000 hours the porous structure is formed where pores apparently filled by helium take about 8% volume. From the thermodynamic point of view they present second phases in two phase region ( $\delta$ -Pu+Ga) of a Pu-Ga-He system by section (Pu,Ga)-He<sub>x</sub>. Taking into account the change of He form in alloy  $\delta$ -Pu+Ga, the fragment of such a hypothetical diagram was considered.
2. The influence of self-irradiation on Pu<sub>3</sub>Ga and two phase ( $\delta$ -Pu + Pu<sub>3</sub>Ga) alloys structure and properties has also been studied. As it was shown earlier, the compound Pu<sub>3</sub>Ga, which had tetragonal or ordered cubic structure in the initial state, acquired a disordered cubic structure due to the self-irradiation at room temperature. The change of Pu<sub>3</sub>Ga crystal structure in the two phase alloys ( $\delta$ -Pu+ Pu<sub>3</sub>Ga) has the same character, but the transition from the tetragonal to the cubic phase occurs for a longer time. During subsequent isochronal annealing the tetragonal structure has been recovered at 300°C; the lattice parameter  $\delta$ -phase of alloys has been recovered at temperature higher than 150°C.

The measurements of residual electrical resistance of Pu<sub>3</sub>Ga and two phase ( $\delta$ -Pu+ Pu<sub>3</sub>Ga) alloys stored during 900 days at room temperature have shown that the electrical resistance of Pu<sub>3</sub>Ga and all alloys has been increased in the process of storage independently of their structure. The growth of electrical

**L. F. Timofeeva**  
GNC RF  
A.A.Bochvar's VNIINM  
(All-Russia Scientific  
Research Institute of  
Inorganic Materials),  
Moscow, Russia

resistance occurs in several stages, and in every stage it follows the exponential law, except in the initial one. The character of electrical resistance change, the quantity of stages, the value and the direction of changes in the process of self irradiation depend on Pu<sub>3</sub>Ga modification and the composition of the alloy and its structure and are defined by structure changes of Pu<sub>3</sub>Ga in the process of storage. Subsequent annealing of samples occurs in several stages and does not lead to recovering of initial values of electrical resistance that gives an evidence about the preservation of defects and more deep changes of metal fine structure occurring during the process of self-irradiation.

3. Behavior of Pu contained ceramics in the process of self-irradiation was also studied. The behavior of ceramic compositions of homogenized and heterogeneous types contained Pu oxides and neutron absorbers (Hf, Gd) in an amount supplied by the existence of the system without critical mass have been studied at room temperature during 300-400 days by x-ray diffraction and positron annihilation methods.<sup>[2,3]</sup> Some interesting results have been obtained of samples studied with the structure of monoclinic HfO<sub>2</sub> and two cubic solid solutions of Pu and Hf oxides. These samples permit us to observe the behavior of three phases simultaneously on one sample. The  $\alpha$ -radiation influence on nonradioactive HfO<sub>2</sub> lattice on these and heterogenic type samples were shown. It was also shown that as Pu contained phases are changed, so are phases without Pu crystal lattice parameters in the process of self-irradiation. As a whole the increase of the oxide elementary cell volume occurred. Based on the positron lifetime spectra analysis of Hf/Pu ceramic, the presence of several types of defects was defined, and the influence of crystal lattice type on defect characteristics was shown. Long duration measurements of Pu-Hf ceramic positron lifetime have revealed the integral spectra characteristics change (width of spectrum on half of high) depending on self irradiation time. The increase of the average positron lifetime duration in the process of sample storage pointed to an accumulation of radioactive defects in the samples.

### Conclusion

The variety of self-irradiation changes in the structure and properties of Pu, alloys and compounds is illustrated by given data and shows the difference in the behavior of Pu radioactive decomposition products depending on the nature of the material.

### References

1. V. M. Filin, V. I. Bulkin, L. F. Timofeeva, M. Yu. Poliakov // Radiochimy, 1988 No.6, s.721-726.
2. Nadykto B. A., Timofeeva L. F. // Proceedings KONTEC'99, 4th International Symposium, "Conditioning of Radioactive Operational & Decommissioning Wastes" 15 - 17 March 1999, Hamburg, p.p. 932-939.
3. L. F. Timofeeva, V. M. Filin, V. I. Bulkin // Intern. Confer. / Ageing Studies and Lifetime Extension Materials, Oxford, 12-14 July 1999.



## Modeling of Delta-Phase Stabilization and Compositional Homogenization in Pu-1 wt. % Ga Alloys

One of the key issues in understanding the phase stability of Pu-1 wt. % Ga is the solid-state microsegregation that occurs in cast alloys. This process, referred to as coring, results in a microstructure consisting of  $\delta$ -phase Pu grains with Ga-rich (~1.6 wt. %) cores and Ga-poor (~0.1 wt. % Ga) edges (Figure 1). Coring is preserved due to the comparatively slow (4-7 orders of magnitude) interdiffusion of Ga in  $\delta$  Pu as compared to that in the  $\epsilon$  phase. The Ga-poor,  $\delta$ -phase edges of as-cast grains are metastable and can transform to a phase during cold working, metallographic sample preparation, or storage. Delta Pu can be stabilized throughout a cored sample by annealing at elevated temperatures (i.e., >300 °C) for relatively short times (i.e., minutes). Cored grains can be compositionally homogenized at moderately high temperatures (i.e., >400°C) for longer times (i.e., minutes to hours). However, the times required to achieve  $\delta$ -phase structural stability and chemical homogeneity are not well constrained. Homogenization is a function of the interdiffusion coefficient for Ga in  $\delta$  Pu ( $\tilde{D}_{\delta Pu}^{Ga}$ ), and tracking the extent of homogenization is important in predicting the behavior of the alloy. Although  $\tilde{D}_{\delta Pu}^{Ga}$  has been measured in several careful diffusion-couple experiments [1,2], there has been minimal application of these data toward predicting the homogenization of Pu-Ga alloys.

In this study, we present the results of analytical models that have been used to determine the homogenization characteristics of Pu-Ga alloys. Modeling methods include modified thin film, residual segregation index, and several separation-of-variables solutions to Fick's Second Law. The latter technique includes (1) the sinusoidal model, (2) the equilibrium-profile model, which uses an initial solute profile developed from the equilibrium phase diagram, and (3) the experimental-

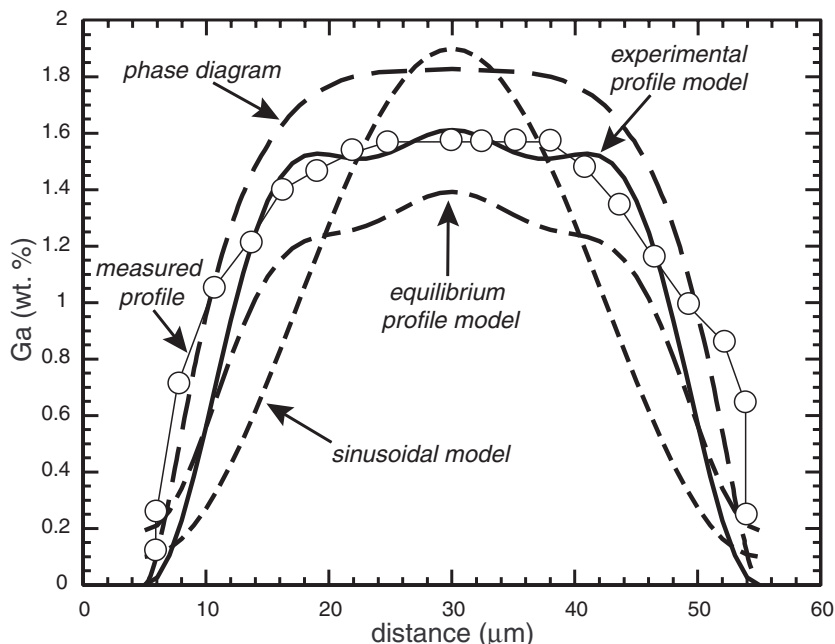


Figure 1. Measured<sup>[3]</sup> and simulated Ga coring profiles for an as-cast 50- $\mu$ m grain of Pu-1 wt. % Ga. Undulations in the profile model results are a product of the polynomial curve fits to the data used in these models and disappear rapidly after simulated annealing.

profile model, which uses electron microprobe profiles from grains of as-cast alloys (Figure 1). We also review the experimental investigations that have used analytical tools such as x-ray diffraction, density, dilatometry, and electron microprobe analysis to characterize Pu-Ga alloy homogenization. Data from these studies are used as a basis of comparison with modeling results for a range of grain sizes (10-80  $\mu\text{m}$ ) and temperatures (420°C–480°C).

There is a surprising paucity of published data on the homogenization of Pu alloys, and the data sets that do exist are not systematic or internally consistent. However, of the five simulation techniques used in this study, the equilibrium- and experimental-profile models compare most favorably with measured experimental results and are the most useful for predicting alloy homogenization. The value of the experimental-profile model will be greatly enhanced with the development of a systematic and comprehensive data set for  $\delta$ -phase stabilization and chemical homogenization.

### References

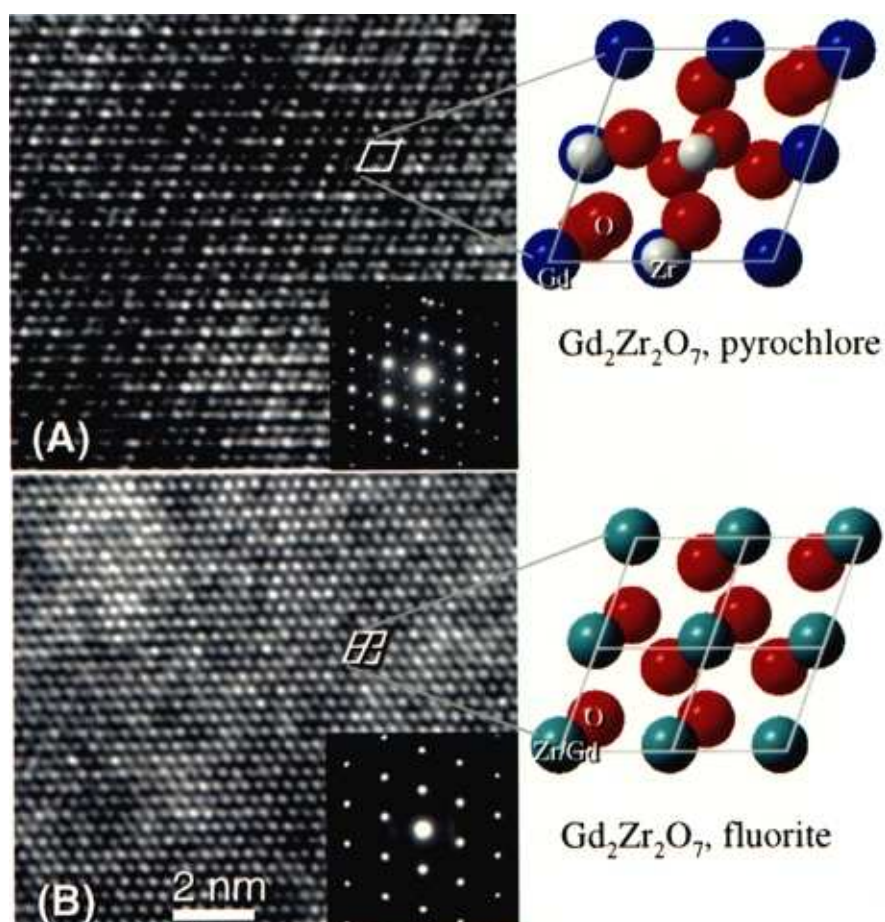
1. A. L. Rafalski, M. R. Harvey, and D. H. Riefenberg: *Am. Soc. Metals Trans. Q.*, 1967, vol. 60, pp. 721-723.
2. G. R. Edwards, R. E. Tate, and E. A. Hakkila: *J. Nucl. Mat.*, 1968, vol. 25, pp. 304-309.
3. R. J. Erfurdt: Ph.D., Colorado School of Mines, 1979, 218 p.

## Radiation Resistance of Gadolinium Zirconate Pyrochlore

The pyrochlore structure-type is a proposed host phase for the immobilization of plutonium. Previous studies have shown that a wide variety of actinide pyrochlores can be synthesized. Gadolinium zirconate with the pyrochlore structure has been shown to be remarkably radiation resistant. We report additional results of ion-beam irradiation studies.

Samples of  $Gd_2Zr_2O_7$  and three variations from the ideal composition ( $Gd_{2.0}Zr_{1.8}Mg_{0.2}O_{6.8}$ ,  $Gd_{1.9}Sr_{0.1}Zr_{1.9}Mg_{0.1}O_{6.85}$ , and  $Gd_{1.9}Sr_{0.1}Zr_{1.8}Mg_{0.2}O_{6.75}$ ) were prepared by solution combustion synthesis. All samples were confirmed to have the pyrochlore structure by electron diffraction. Irradiation experiments with 1.5 MeV  $Xe^+$  and 1 MeV  $Kr^+$  were performed using the HVEM-Tandem Facility at the Argonne National Laboratory.

All samples, irradiated to a dose of  $8.9 \times 10^{15}$  ions/cm<sup>2</sup> (or 16 dpa, assuming  $E_d = 50$  eV) with 1.5 MeV  $Xe^+$  at room temperature, showed no evidence of amorphization. A similar irradiation series with 1.5 MeV  $Xe^+$  on the four samples was repeated at a temperature of 20 K, and no amorphization was observed after a dose of 5 dpa. Clearly, compositions in this regime will be extremely stable and resistant to amorphization under repository conditions, even after reaching high radiation doses. All the samples experienced an irradiation-induced pyrochlore-to-fluorite structural transformation, shown by HREM and SAED (Fig. 1).



S. X. Wang,  
L. M. Wang,  
R. C. Ewing  
University of  
Michigan, Ann Arbor,  
MI 48109-2104, USA

K. V. Govidan Kutty  
Indira Gandhi Centre  
for Atomic Research,  
Kalpakkam 60312,  
India

W. J. Weber  
Pacific Northwest  
National Laboratory,  
Richland, WA 99352,  
USA

Figure 1. HREM image and electron diffraction patterns of  $Gd_2Zr_2O_7$ , showing the transformation from pyrochlore (A) to fluorite (B) structure due to 1.0 MeV  $Kr^+$  irradiation. The order-disorder transformation is illustrated in the schematic crystal structures.

Diffuse maxima (Fig. 2) were observed in the electron diffraction patterns of all samples. The Fourier transformation (Fig. 3B) of the HREM image (Fig. 3A) showed similar diffuse patterns, as in the real electron diffraction patterns (Fig. 3D). Inverse Fourier transformation (Fig. 3C) of Fig. 3B using only the Bragg diffraction maxima and the diffuse maxima revealed nano-sized domains bordered by Moiré fringes, which are the source of the diffuse maxima in the diffraction patterns. The Moiré fringes can be attributed to overlap of nano-domains. Because of the strong tendency for simultaneous recovery, rather than amorphization, in the  $Gd_2Zr_2O_7$  and the heterogeneous nature of the damage by heavy ions, slightly rotated nano-domains with the fluorite structure form during irradiation.

**Figure 2.** Electron diffraction patterns of ion-irradiated  $Gd_2Zr_2O_7$  showing the diffuse maxima in addition to the basic diffraction patterns of fluorite structure. The indices are according to the fluorite structure.

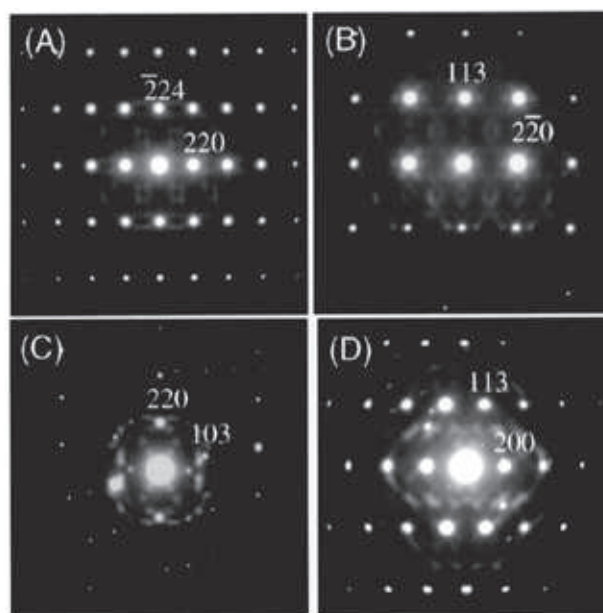
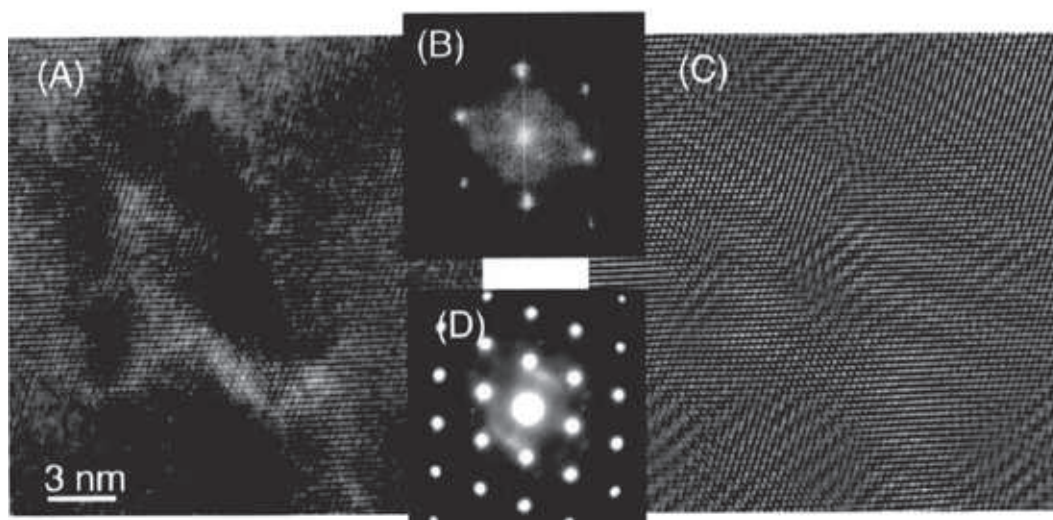


**Figure 3.** (A) HREM image of irradiated  $Gd_2Zr_2O_7$ . (B) Fourier transformation of the HREM reveals the diffuse patterns. (C) Inverse Fourier transformation of (B) using only the regular Bragg spots and the diffuse maxima. (D) The real diffraction of [110] zone showing the same diffuse patterns as in (B).



The pyrochlore-fluorite structure can incorporate a wide variety of different elements. Zirconate pyrochlore also has a superior chemical stability when in contact with water. The rare earths, particularly Gd, in zirconates are effective neutron absorbers. The combination of all of these properties with its remarkable radiation resistance makes  $Gd_2Zr_2O_7$ -based material an exceptionally promising host for the immobilization of plutonium.

### **Acknowledgments**

This work was supported by the Office of Basic Energy Sciences, U.S. Department of Energy (DE-FG02-97ER45656).



## Plutonium Stabilization in Zircon: Effects of Self-Radiation

**W. J. Weber,**  
**N. J. Hess,**  
**R. E. Williford,**  
**H. L. Heinisch,**  
*Pacific Northwest  
National Laboratory,  
Richland, Washington  
99352, USA*

**B. D. Begg,**  
*Australian Nuclear  
Science and  
Technology  
Organisation, Menai,  
NSW 2234, Australia*

**S. D. Conradson**  
*Los Alamos National  
Laboratory, Los  
Alamos, New Mexico  
89545, USA*

**R. C. Ewing**  
*University of  
Michigan, Ann Arbor,  
Michigan 48109, USA*

Zircon ( $\text{ZrSiO}_4$ ) is the most thoroughly studied of all candidate ceramic phases for the stabilization of plutonium.<sup>1-2</sup> Self-radiation damage from  $\alpha$ -decay of the  $^{239}\text{Pu}$ , which releases a 5.16 MeV  $\alpha$ -particle and a 0.086 MeV  $^{235}\text{U}$  recoil nucleus, can significantly affect the structure and properties of zircon (e.g., up to 18% volume expansion). Two types of synthetic Pu-containing zircons, prepared in 1981, have provided an opportunity to characterize in detail the effects of Pu decay on the structure and properties of zircon and to make unique comparisons to observations of radiation effects in natural zircons.<sup>3-4</sup> One set of zircon samples contained a mixture of 8.85 wt. %  $^{238}\text{Pu}$  and 1.15 wt. %  $^{239}\text{Pu}$ , while the other set of samples contained 10 wt. %  $^{239}\text{Pu}$ . In both instances, the Pu was substituted directly for Zr, giving a  $\text{Zr}_{0.92}\text{Pu}_{0.08}\text{SiO}_4$  stoichiometry. Initial characterization by XR, found both samples to be single-phase zircons. The zircons containing 8.85 wt. %  $^{238}\text{Pu}$ , with its 87.7 year half-life, provided a means of accelerating the  $\alpha$ -decay rate (i.e., damage rate) by a factor of  $\sim 250$  when compared to the zircons containing 10 wt. %  $^{239}\text{Pu}$ . Self-heating in the  $^{238}\text{Pu}$ -substituted zircon specimens during storage has been minimal, and specimen temperatures have been estimated to be less than 50°C. The accumulated doses in these samples are  $2.8 \times 10^{19}$  and  $1.2 \times 10^{17}$   $\alpha$ -decays/g for the  $^{238}\text{Pu}$ - and  $^{239}\text{Pu}$ -substituted zircons, respectively.

Self-radiation from Pu decay in zircon results in the simultaneous accumulation of point defects and amorphous domains that eventually lead to a completely amorphous state.<sup>3</sup> The swelling in zircon increases sigmoidally with dose and is well saturated at the highest dose. The saturation swelling increases with decreasing porosity of the synthesized zircon pellets, from 16.6% swelling for synthetic zircons with 5.5% porosity to 18.4% for natural zircons (0% porosity). In all cases, the swelling can be accurately modeled based on the contributions from crystalline and amorphous components. The XAS results at the highest doses confirmed that self-radiation damage had transformed the  $^{238}\text{Pu}$ -substituted zircon into a fully amorphous state lacking long-range order.<sup>5</sup> Surprisingly, the Pu  $L_{\text{III}}$ -edge XANES indicated that the Pu in both zircon samples is trivalent. This was an unexpected result of originally preparing the Pu-substituted zircons under a reducing atmosphere (oxygen-purged flowing argon). Recent computer simulations using energy minimization techniques indicate that the lowest energy configuration occurs for a defect cluster composed of two near-neighbor  $\text{Pu}^{3+}$  substitutions on  $\text{Zr}^{4+}$  sites and a neighboring charge-compensating oxygen vacancy.<sup>6</sup>

Detailed X-ray absorption spectroscopy and X-ray diffraction methods have characterized the short-range and long-range structures of each zircon type.<sup>7</sup> The amorphous state of the  $^{238}\text{Pu}$ -substituted zircon is consistent with the loss of long-range order and edge-sharing relationships between  $\text{SiO}_4$  and  $\text{ZrO}_8$  polyhedra. Despite this, a distorted zircon structure and stoichiometry, which consists of  $\text{SiO}_4$  and  $\text{ZrO}_8$  polyhedra that have rotated relative to each other, are retained over length scales up to 0.5 nm. The recrystallization of the amorphous  $^{238}\text{Pu}$ -substituted zircon could be achieved directly at temperatures as low as 1200°C if heated rapidly through the intermediate temperature regime where decomposition to oxides is preferred. The decomposition of amorphous zircon to constituent oxides observed at intermediate temperatures is probably kinetically limited by Zr diffusion, which has a lower energy barrier than the polyhedral rotation required

for recrystallization of the zircon structure from the amorphous state. The oxidation of  $\text{Pu}^{3+}$  to  $\text{Pu}^{4+}$  in the crystalline  $^{239}\text{Pu}$ -substituted zircon during annealing in air results in a decrease in lattice distortion due to the decrease in ionic radius of  $\text{Pu}^{3+}$  to  $\text{Pu}^{4+}$  on the  $\text{Zr}^{4+}$  site.

Atomic-scale computer simulations have also been used to study defect accumulation and amorphization in zircon containing  $^{238}\text{Pu}$ .<sup>8</sup> A kinetic Monte Carlo simulation has been used that includes the stochastic production of defects in displacement cascades, the subsequent diffusion of defects, and the identification of amorphous regions. The displacement cascades in zircon from  $^{234}\text{U}$  recoils are generated using a crystalline binary collision model, and the diffusion of the defects is followed as they hop stochastically through the crystal lattice. The simulation results for the amorphous fraction as a function of alpha-decay dose are in excellent agreement with the experimental results. Furthermore, the simulation results indicate that cascade overlap may be the dominant process for amorphization of zircon at 300 K; however, the results also suggest that there is a minor contribution from direct impact amorphization.

### References

1. R. C. Ewing, W. Lutze, and W. J. Weber, *J. Materials Research* 10, 243-246 (1995).
2. E. B. Anderson, B. E. Burakov, and E. M. Pazukhin, *Radiochimica Acta* 60, 149-151 (1993).
3. W. J. Weber, *J. Materials Research* 5, 2687-2697 (1990).
4. T. Murakami, B. C. Chakoumakos, R. C. Ewing, G. R. Lumpkin, and W. J. Weber, *Am. Mineralogist* 76, 1510-1532 (1991).
5. N. J. Hess, W. J. Weber, and S. D. Conradson, *J. Nuclear Materials* 254, 175-184 (1998).
6. R. E. Williford, B. D. Begg, W. J. Weber, and N. J. Hess, *J. Nuclear Materials* (2000), in press.
7. B. D. Begg, N. J. Hess, W. J. Weber, S. D. Conradson, M. J. Schweiger, and R. C. Ewing, *J. Nuclear Materials* (2000), in press.
8. H.L. Heinisch and W.J. Weber, *J. Nuclear Materials* (2000), in press.

## Inert Matrix Fuels for Incineration of Plutonium and Transmutation of Americium

Hj. Matzke  
European  
Commission, Joint  
Research Centre,  
Institute for  
Transuranium  
Elements, 76125  
Karlsruhe, Germany

In conventional U-based nuclear fuels, both Pu and higher actinides (mainly Am, but also Np and Cm) are formed by neutron capture reactions and  $\alpha$ - or  $\beta$ -decay. If a strategy of reprocessing is adopted as in some European nations and in Japan, the separated Pu can be recycled as (U,Pu)O<sub>2</sub> (or mixed-oxide—MOX) fuel. The high-level liquid waste of reprocessing is presently vitrified. However, the alternative of separating the minor actinides from the fission products (partitioning) and subsequent transmutation in existing reactors or in new dedicated actinide burners is widely studied as a possible means to reduce the radiotoxicity of the waste. The separated actinides are incorporated into a U-free fuel, the support for the actinides being “inert” to actinide formation, i.e., an “inert matrix” with atomic numbers lower than that of U. Inert matrices can also be used to burn excess Pu much more effectively than in MOX fuel (“burn” scenario). Furthermore, inert matrices can be used for safe long-time storage or final disposal of excess Pu (“bury” scenario).<sup>1</sup>

Requested material properties of candidate matrices are: low neutron capture cross-sections, large-scale availability at acceptable costs, good thermal properties (heat capacity, thermal conductivity) and high melting points, good compatibility against cladding (Zircaloy or stainless steel) and coolant (H<sub>2</sub>O or Na), good mechanical properties, good radiation stability and either suitability for currently used reprocessing methods or good stability in a deep geological repository, i.e., high leach resistance for the “bury” scenario. A particular problem needing extensive research is radiation stability because of the very different physical and chemical effects of the different radiation sources: neutrons and fission fragments during reactor operation, hence at elevated temperatures, and  $\alpha$ -,  $\beta$ - and  $\gamma$ -decay events also during storage, hence at low temperatures. Finally, reliable thermodynamic data (oxygen potential, solubilities, phase diagrams, etc.) must exist to reliably predict the in-pile behavior under normal and off-normal conditions.

Based on the above criteria, a number of inert matrix candidates were selected, both ceramics (e.g., (Y,Zr)O<sub>2</sub>, MgO, MgAl<sub>2</sub>O<sub>4</sub>, CeO<sub>2</sub>, SiC, ZrN etc. for the “burn” scenario and e.g., (Y,Zr)O<sub>2</sub>, ZrSiO<sub>4</sub>, CePO<sub>4</sub> etc. for the “bury” scenario) and metals (e.g., Zircaloy, stainless steel, W etc.). At present, a hybrid ceramic fuel is tested in Europe, i.e., a fuel containing the actinide in small ZrO<sub>2</sub> beads incorporated in a spinel or MgO matrix, called “cercer” (ceramic-ceramic) fuel. In this way, the (relatively) good radiation stability against fission damage of ZrO<sub>2</sub> and the good thermal conductivity of the MgAl<sub>2</sub>O<sub>4</sub> or MgO are used. This concept will be discussed in detail, together with possible solutions to solve the problem of He-accumulation due to  $\alpha$ -decay.

The existing knowledge (and the gaps in the knowledge) in the relevant thermodynamic, physical and chemical properties of these inert matrices are discussed.<sup>2</sup> Emphasis is put on radiation damage since some of the materials show very different responses to the above-mentioned different damage sources. For instance, the spinel MgAl<sub>2</sub>O<sub>4</sub> is shown to be very stable against neutrons and  $\alpha$ -particles whereas it amorphizes and shows significant swelling under the impact of fission products of fission energy.<sup>3</sup> The physical reasons for this behavior will be explained.



Finally, the questions of reduction of radiotoxicity and of proliferation-resistance for different “bury” scenarios will be mentioned and the potential of ThO<sub>2</sub>-based actinide fuels as “quasi-inert matrix fuels” will be discussed.

### References

1. Hj. Matzke and J. van Geel, “The Pu-Issue: Going MOX or Alternative Solutions? Materials Science Aspects,” *Radwaste Magazine* **3** (1996) 71.
2. Hj. Matzke, V. V. Rondinella and T. Wiss, “Materials Research on Inert Matrices in ITU,” *J. Nucl. Mater.* **274** (1999) 47.
3. S. J. Zinkle, Hj. Matzke and V. A. Skuratov, “Microstructure of Swift Heavy Ion Irradiated MgAl<sub>2</sub>O<sub>4</sub> Spinel”, *Mat. Res. Soc., Warrendale, PA 1999, MRS Symp. Proc.* **540** (1999) 299.

# Capability of the MIMAS Process to Convert the Stockpiles of Separated Plutonium into MOX fuel for Use in LWRs

Paul Deramaix,  
Yvon Vanderborck,  
Werner Couwenbergh  
BELGONUCLEAIRE  
S.A., Brussels,  
Belgium

## Introduction

Long-term storage of plutonium separated from fission products is not a good solution according to the current non-proliferation criteria as well as from an economic point of view. This material has thus to be converted to the equivalent of the "spent fuel standard." Only one technique has so far reached the industrial maturity necessary to convert the important existing plutonium stockpiles: it is the use of plutonium to manufacture and irradiate mixed-oxide (MOX) fuel.

After the establishment of peaceful relationships between US and the former Soviet Union in the early 1990s, US and Russia's Governments have realized that it is no longer necessary to maintain a significant stockpile of weapons plutonium. They have called for this surplus of plutonium to be converted more or less simultaneously into a nonproliferant status, that is resistant to reuse in nuclear weapons. It is the intention of Russia to convert weapons plutonium into MOX fuel to be irradiated in power reactors.

On March 22, 1999, the US Department of Energy (DOE) moved ahead with at least a first phase of the US disposition effort to convert about 33 t Pu of the excess US weapons plutonium into MOX and to burn it in commercial US reactors.

## Description of the Actual Work

The paper reviews first the existing information over the existing separated plutonium stockpiles, including the material declared today as excess as a result of the dismantling of the nuclear arsenals. The transformation into MOX of these large stockpiles is of an international nature, not only because of the limited MOX fabrication capacities but also owing to the need of reactors licensed for the use of MOX fuel. The second part of the paper focuses on the technical potential of the BELGONUCLEAIRE MIMAS fabrication process for the dry conversion into MOX fuel of various forms of separated plutonium: investigated parameters include physical form of the feed material ( $\text{PuO}_2$  or  $\text{UO}_2\text{-PuO}_2$ , powder or pellets), age or americium content, impurities, and the plutonium content of MOX. Preproduction runs confirm the potential of the MIMAS route for the dry processing of a significant part of the stockpiles.

The present MIMAS process invented by BELGONUCLEAIRE in the early 1980s was implemented in 1985. It is the result of the evolution of successive fabrication techniques developed by BELGONUCLEAIRE to produce pelletized MOX fuel. The previous processes were used for fuel fabrication for various light water reactors (LWRs) (i.e., BWR and PWR) and also fast breeders. The MOX fuel produced according to this route was of adequate quality. However, for use in LWRs the interdiffusion of Pu and U during sintering was not preventing the presence of large size high Pu content agglomerates, raising concern for RIA behavior experience, and with regard to the reprocessing capability in commercial reprocessing plants currently in operation. It is the reason why MIMAS was developed.

The third part of the paper describes the continuous R&D associated with the supply of MOX fuel in commercial reactors. This R&D work is made through international programs supported by a lot of organizations. Special attention is given to the evolution with burnup of fuel neutronic characteristics and of in-reactor rod thermal mechanical behavior.

## Results

Programs are described in the Belgian VENUS criticality facility as well as other investigations related to fuel rod behavior under normal conditions obtained through large scale irradiations in various reactors like BR3, DODEWAARD, BEZNAU-1 and GUNDREMMINGEN and under off-normal conditions, which are simulated in BR2, OSIRIS, HALDEN and HFR. Important characteristics as fission products, helium production, actinides inventory, thermal conductivity, fuel central temperature, pellet-cladding interaction, fission gas release, micro-structure, are overviewed.

These characteristics demonstrate the good and safe behavior of MOX fuel under irradiation and the similar behavior of MOX and UO<sub>2</sub> with similar burnups. The MIMAS fuel is now loaded in 36 reactors in Europe and has been supplied for two Japanese reactors.

## Bibliography

1. Basselier J. et al., "Validation of MOX Fuel through Recent BELGONUCLEAIRE International Programs," IAEA TCM on Recycling of Pu and U in WR fuel – Windermere UK, July. 1995.
2. J. van Vliet, P. Deramaix, J. L. Nigon, W. Fournier, "MOX Fuel Fabrication, in Reactor Performance and Improvement," ENC 1998.
3. J. Krellmann, D. Hagelmann, "MOX Fuel Fabrication in France: A Nature Industry," RECORD 1998.
4. P. Deramaix, Y. Vanderborck, M. Lippens, J. van Vliet, "MOX Fuel Fabrication and in Reactor Performance : Realisation and Prospects," RECORD 1998.
5. Lippens M. et al., "MOX Fuel Performance – BELGONUCLEAIRE Views3," OECD/NEA Workshop on the Physics and Fuel Performance of Reactor-Based Plutonium Disposition, Paris, France, September 1998.

## Some Less Conventional Options for Plutonium Disposal

Prof. Dr. Wolfgang  
Stoll  
Hanau, Germany

Disposition of weapons Pu (W-Pu) aims at the replacement of military access restrictions by inherent longlasting technical barriers to make the return into the weapons state difficult and not rewarding anymore. At the time of the NAS-study in 1994, two ways were perceived to be mature and selected: Fissioning of W-Pu as LWR-MOX and the disposal in a vitrified radionuclide-spiked form.<sup>1</sup> Both options since have been questioned for equality, met different acceptance at both superpowers and showed slow progress. A criterion to measure disarmament would be the amount of W-Pu in the different proliferation resistant forms, multiplied by the effort needed for each form to return to weapons quality. From this it might emerge that small steps done for large amounts of material soon are more efficient than perfect solutions delayed for years and with limited throughputs.

At the Obninsk Conference 1994<sup>2</sup> already different unconventional options were presented. They centered around advanced fuel cycles and storage forms of particular long-term stability. Most suggestions could not materialize soon but required long demonstration phases. This report discusses three out of a series of other alternatives, which are perhaps not perfect, but can be realized in a relatively short time.

The first one uses plutonium as an alloy fuel with 60% zirconium in LWR, the second uses the concept of the LW-high converter reactor as a hot plutonium storage facility, and the third suggests a storage concept of planar plutonium sources, to make use of its alpha energy, while stored.

40 atom % plutonium-metal forms a malleable (cubic) alloy with zirconium.<sup>3</sup> Small amounts of gallium do not interfere. The alloy exhibits a slow and benign reaction with hot water. Addition of thorium metal as a stand-in for plutonium does reinforce the corrosion resistance but may not be necessary. Pit metal could directly be alloyed and rolled into small stripes, which could be aligned by a simple rolling procedure as an annular cylinder inside a zircaloy cladding robe. Enough swelling volume could be provided, and the Pu-containing layer would exhibit some self-shielding to smooth out the reactivity over burnup. The technology, dependent on Pu-metal handling like in weapons facilities, would not lead into MOX plutonium economy. As relative small material volumes would have to be handled in existing facilities, no major plant building activity would be necessary. After one or two cycles in-pile, the fuel could be stored safely together with other LWR-fuel.

The second approach was the LW High Converting Reactor. Numerous studies between 1985 and 1988<sup>4,5</sup> recommended tightening the standard LWR lattice, resulting in a much lower water-to-fuel ratio and the utilization of epithermal and fast neutrons. The studies were made to overcome the delay of the FBR introduction. Near breeding should be reached within existing PWR pressure vessels. Reduced safety margins, like in void coefficient, were the apparent shortcomings. They could be overcome by lowering the burnup goal to about half of the originally attempted values. An additional plutonium inventory could replace frequent reloading to keep reactivity constant. With these modifications a standard 1000 MW PWR could house 9 to 15 tons of plutonium as a 8%–11% MOX ceramic,

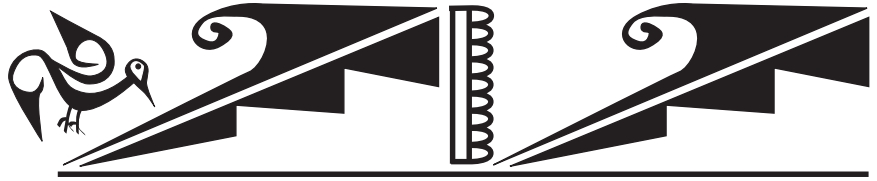
with or without thorium oxide as a discouraging addition for future reprocessing in steel-clad, rib-supported fuel rods. The burnup of some 25 MWD/kg would need only 2 to 3 standard PWR to take the whole load of the 33 tons of Pu to be inserted as MOX fuel. This "hot plutonium storage" would be particularly proliferation resistant and would also provide valuable data for future PWR development. Fuel could be made in a small (e.g., former FBR) facility and is dissimilar to commercial LWR MOX.

The third approach attempts utilizing Pu-alpha-energy, while in storage. The technology to produce plutonium radiation standards is well developed. Very stable thin layers are deposited either on steel or other foil, like aluminum. Layer formation by deposition methods like electrochemistry or radiocolloids<sup>6</sup> are industrially well established and could produce a large surface with a durable solid plutonium oxide layer. Foils are rolled and/or folded in a distance-giving geometry, to let fluids or gases pass over, where chemical reactions are initiated by radiolysis. One example would be water radiolysis, which gives a small, but very steady flow of gaseous hydrogen and some hydrogen peroxide. A second example is irradiation of a beryllium fluoride-ammonium fluoride solution and use of the alpha,n neutrons, producing via the (N15-n,p-C14) nuclear reaction in the fluid a carrier-free carbon-14 to be separated from the fluid.<sup>7</sup> In a tight geometry some fission and capture processes would downgrade the clean <sup>230</sup>Pu and <sup>235</sup>U with time also. Batteries of such foils would range in the safeguards terminology like alpha-waste. Size and dilution would make diversion for weapons purposes uninteresting. Technical descriptions for experimental setups and current literature will be given.

### References

1. Management and Disposition of Excess Weapons Plutonium, National Academy of Sciences, January 1994.
2. Unconventional Options for Plutonium Disposition, Proceedings of a Technical Committee meeting at Obninsk, IAEA - TECDOC 840, Nov. 1994.
3. O. J. Wick, Plutonium Handbook, Fig. 7.27, P. 227(1980).
4. Yigal Ronen. Melvin J. Leibson, The Multispectrum High Converter Water Reactor, Nuclear technology 79, (1987), p.20.
5. Milton C. Edlund, On High Conversion Ratio Light Water Reactors, Nuclear Technology 80 (1988)+ the following 12 articles of different authors, P9-161.
6. J. Schubert and E. E.Conn, Nucleonics 4(1949) p.6.
7. M. Calvin. C. Heidelberger, J. C. Reid, B. Tolbert, P. F. Yankwich, Isotopic Carbon, J. Wiley, New York 1949.





# Condensed Matter Physics





## The Electronic Structure and Elastic Properties of the Actinide Chalcogenides (U,Np,Pu,Am): the Puzzle of AmTe

Most people seem to agree that the 5f state in the uranium chalcogenides is a relatively broad (about 1 eV wide) band<sup>1</sup> and in Cm compounds the 5f state is localized. We follow the width and hybridization of the 5f states from the uranium chalcogenides to AmTe. The simple crystal structure and the availability of large single crystals permitted new and unusual measurements. The electrical transport properties (measured between dc and optical frequencies), the magnetic susceptibilities and magnetization (between 1K and 1000 K, and between 10 Oe and 100 kOe), and the specific heat and its  $\gamma$  value are correlated to derive the electronic structure and relative arrangement of p, d and f states. In addition to electronic properties the elastic and phononic properties are measured and used to support the electronic structure.

Naturally, measurements on the uranium chalcogenides are abundant.<sup>1,2</sup> The compounds are in a  $5f^36d^1$  configuration. Regarding the f states they are trivalent metals and ferromagnets with ordering temperatures between 178 K for US and 104 K for UTe. Within the uranium chalcogenide series, UTe has the narrowest 5f band, so that effects of hybridization of a narrow f band with a broad d band become visible, one can observe weak effects of intermediate valence with a valency near three<sup>3</sup> (evidence is a negative  $c_{12}$ , to be discussed below). The transport properties are governed by the Kondo effect.

The Np chalcogenides with a  $5f^46d^1$  configuration are antiferromagnetic metals with  $T_N$  between 23 K for NpS and 30 K for NpTe.<sup>2</sup> The magnetic structures are very complex with multi k-structures. Due to f-d hybridization with an already narrower 5f band, moment quenching and crystal field effects are very significant so that NpTe has no long-range order anymore. The optical properties appear normal as for a trivalent (regarding the f configuration) metal, with a plasma edge in the visible (NpS) or near infrared (NpTe). No indications of intermediate valence seem to be present.

In Pu chalcogenides the 5f state is already so narrow (meV wide) that the moment quenching is total, the susceptibility is a very large temperature independent Pauli term<sup>2</sup> due to a renormalized susceptibility of heavy 5f electrons.<sup>4</sup> The nearly free 6d electrons make a plasma resonance in the optical spectrum and cause the vivid colors—gold for PuS, copper for PuSe and black for PuTe—because in the latter compound the plasma edge is in the near infrared.<sup>5</sup> The Pu chalcogenides are the high-pressure phase of the corresponding Sm chalcogenides; they are intermediate valent with a valency of about 2.7<sup>+</sup> and a hybridization gap of 2.7 meV in an already narrow 5f band of 40 meV width.<sup>4</sup> Experimentally a g value of 69 mJ/mol K<sup>2</sup> has been measured for PuTe; our renormalized theory<sup>4</sup> yields 20 mJ/mol K<sup>2</sup>. The intermediate valence leads to a negative  $c_{12}$  of the elastic constants.

In AmTe the situation has changed completely. The susceptibility is the largest Pauli term ever observed and can only be explained with an effective mass of about 1000 m. There is no plasma resonance in the optical spectrum even in the near infrared, so that the concentration of carriers must be very small, or they must have a very large effective mass. In a special effort the optical range for the encapsulated single crystals could be extended into the far infrared, down to meV

**P. Wachter,**  
**M. Filzmoser**  
*Laboratorium für  
Festkörperphysik,  
ETH Zürich, 8093  
Zürich, Switzerland*

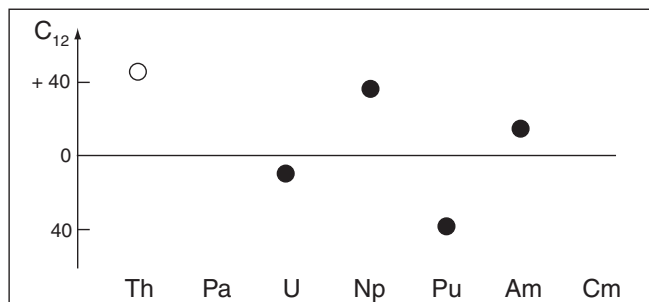
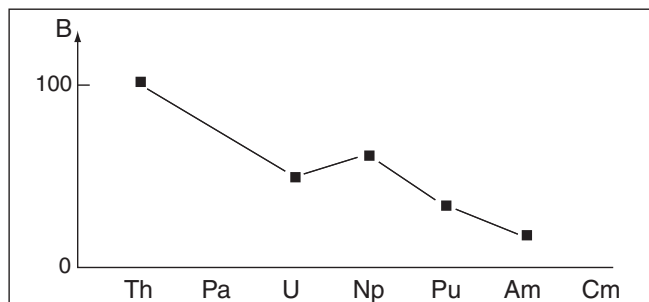
**J. Rebizant**  
*European Institute for  
Transuranium  
Elements, 76125  
Karlsruhe, Germany*

photon energy by using diamond windows.<sup>6</sup> There, finally, a plasma edge could be observed. So the samples are metals, but the carrier mass is extremely large, as for heavy fermions. The final result is that AmTe (and also the other Am chalcogenides) are in a divalent configuration with a 5 meV wide 5f band, half filled with 7 electrons, having an enormous mass, but being separated from the 6d band by about 0.1 eV. Thus AmTe is a new kind of heavy fermion, without hybridization, because the  $c_{12}$  is positive. A negative  $c_{12}$  is a clear-cut indication of intermediate valence, and this has been tested for about 50 materials, mostly rare earth compounds.

Using angle resolved Brillouin scattering the dispersion of the sound velocities (as function of the crystal orientation) could be measured and thus the 3 elastic constants of a cubic system could be determined. They are displayed for the An tellurides in the table. The bulk modulus can be calculated  $B = (c_{11} + 2 c_{12})/3$  and is also shown in the table, together with bulk moduli obtained from measuring the lattice constant with X-rays under pressure. The agreement is very good. The bulk modulus is a zigzag curve, but the reason for this is the alternatively positive or negative  $c_{12}$  as shown in the lower part of the table. This in turn is related with an even or odd 5f occupation and is a consequence of the Luttinger theorem. AmTe has a very low bulk modulus; it is extremely soft due to the narrow and half filled 5f band. In AmTe also the TO and LO phonon modes could be determined, just as the very slow sound velocity.

#### Mono - Tellurides

B	<sup>102</sup>		<sup>48</sup> 41.8	<sup>52</sup> 67	<sup>34</sup> 37	<i>U. Benedikt et al 1988</i> 15	
$C_{11}$			143	129	177	25	
$C_{44}$			11.9	10.6	30	8	
$C_{12}$	+		- 8.7	+ 37	- 32	+10	
	Th	Pa	U	Np	Pu	Am	Cm



ETH/PW/AmTe/fig04.cdr

In summary a vast amount of physical data has been obtained on the An chalcogenides up to AmTe, and the gradual narrowing of the 5f band could be observed and interpreted in the series. The elastic properties are used to support the electronically derived model.

### References

1. J. Schoenes, Phys. Reports **66** 187 (1980).
2. K. Mattenberg and O. Vogt, Physica Scripta **T45** 103 (1992).
3. J. Neuenschwander, O. Vogt, E. Voit and P. Wachter, Physica **144B** 66, (1986).
4. P. Wachter, F. Marabelli and B. Bucher, Phys. Rev. **B43** 11136 (1991).
5. M. Mendik, P. Wachter, J.C. Spirlet and J. Rebizant, Physica B 186-188,678 (1993).
6. P. Wachter and J. Rebizanz, 29th Journées des Actinides, 15–17 April, 1999, Luso, Portugal (unpublished).

## Phase Transitions in Plutonium: New Insights from Diffraction

**A. C. Lawson,  
B. Martinez,  
J. A. Roberts,  
R. B. Von Dreele,**  
*Los Alamos National  
Laboratory, Los  
Alamos, NM 87544*

**J. W. Richardson, Jr.,**  
*Argonne National  
Laboratory, Argonne,  
IL 60439*

**A. Mehta,  
J. Arthur**  
*Stanford Synchrotron  
National Laboratory,  
Stanford, CA 94025*

We are using the techniques of neutron and x-ray powder diffraction to learn more about the driving forces for structural transformations in Pu metal. This research is currently being conducted in three areas: (1) understanding the low melting point of Pu, (2) measuring the intergranular stresses that arise in solid-solid phase transitions of Pu, and (3) determining whether the idiosyncratic crystal structures of Pu are stabilized by Pu atoms in different valence states at different crystallographic sites.

Recently we showed that the anomalously low melting point of Pu is related via the Lindemann melting criterion to the temperature dependence of its elastic properties. The Lindemann criterion states that a metal melts when the amplitude of thermal vibration exceeds about 8% of the interatomic distance as the temperature is raised. Although this criterion is quite reasonable and works well for most of the elements, there has not so far been a theoretical explanation for its success. In fact, Pu was one of its failures, as the Lindemann criterion predicted a melting point that was much higher than the experimentally determined value. In other words, the elastic constants appeared to be too high for the low melting point. We have resolved this discrepancy by showing that the elastic constants vary with temperature in just such a way that the elastic constant at the melting point has decreased enough to predict the correct low melting point. In this work we have characterized the elastic properties of Pu with the "Debye-Waller temperature," which is the temperature characteristic of the temperature dependence of the intensities of neutron or x-ray diffraction reflections, and our conclusions are in agreement with those reached on the basis of more conventional elastic measurements.

A second area of research is based on the measurement of diffraction peak broadening to determine the intergranular stresses in Pu as temperature variations drive the metal through its various phase transitions. The diffraction technique permits us to determine the microstrain, which is the RMS variation of the local strains experienced by individual crystal grains. This quantity has a characteristic anisotropy in crystal space that can be determined by diffraction techniques. A spectacular effect is observed in  $\delta'$ -Pu in the  $\delta$ - $\delta'$ - $\epsilon$  sequence encountered in the heating of pure Pu metal.

A third research area is concerned with the idiosyncratic structures found in several allotropes of pure Pu and in some of its alloys. For example, the  $\alpha$ -phase of Pu has sixteen atoms in the monoclinic unit cell, and these are distributed among 8 distinctly different crystallographic positions in the crystal structure. The  $\zeta$ -phase in the Pu-U system is even worse. Why should nature favor such a complicated structure? Part of the answer comes from electronic band structure calculations, which show that complicated structures are generally favored by narrow electronic bandwidths. In the cases where several distinct crystallographic sites are involved, we have been interested in finding out whether the atoms on these different sites are in different valence states, and, if so, how these valence differences contribute to the stabilization of complicated structures. This work is being conducted by resonant x-ray diffraction studies on the  $\alpha$ -phase structure of Mn metal. Mn is a good model for Pu for this problem, as its structure includes four distinct crystallographic sites.

# Magnetic Properties of $\text{Pu}_{(1-x)}\text{Am}_x$ Solid Solutions

## Introduction

Substitution of plutonium (Pu) by so-called deltagen elements (Ga, Al, Am, Ce...) allows us to stabilize the high-temperature expanded fcc  $\delta$ -phase of Pu at room temperature or down to 4 K, depending on the concentration of the deltagen.<sup>1</sup> The nature of this stabilization is still a question of fundamental interest. It is possible to separate the deltagen elements in two sub-classes:

atoms smaller than Pu atoms (Ga, Al...);

atoms larger than Pu atoms (Ce, Am).

In the first case, the stabilization of the expanded  $\delta$ -phase (compared to the  $\alpha$ -phase) necessarily involves electronic effects (5f-p hybridization) which have been observed in particular by EXAFS.<sup>2</sup> In the second case, and especially in the case of Am, the 5f electrons are well localized and its valence band is the same as Pu one. One thus expects only a steric effect.

## Experimental

Six  $\text{Pu}_{(1-x)}\text{Am}_x$  alloys were prepared with Am content ranging from 6 to 25 at. %. The Am content was determined both by chemical analyses and X-ray microanalysis. Cell parameters, deduced from X-ray diffraction, are in agreement with published data.<sup>3</sup> These are compared to a Vegard's law considered between  $\delta$ -Pu and  $\beta$ -Am lattice parameters (extrapolated to room temperature). Susceptibility measurements were performed on a Faraday-type balance. Before measurements, the samples were confined in a silica tube (first confinement) and in an aluminum tube (second confinement), both laser sealed. A gold shield was inserted between the two confinements to reduce the magnetic susceptibility of the sample holder and to limit the Am  $\gamma$ -irradiation. Before confinement, samples were electropolished in order to remove surface oxides and possible other impurities.

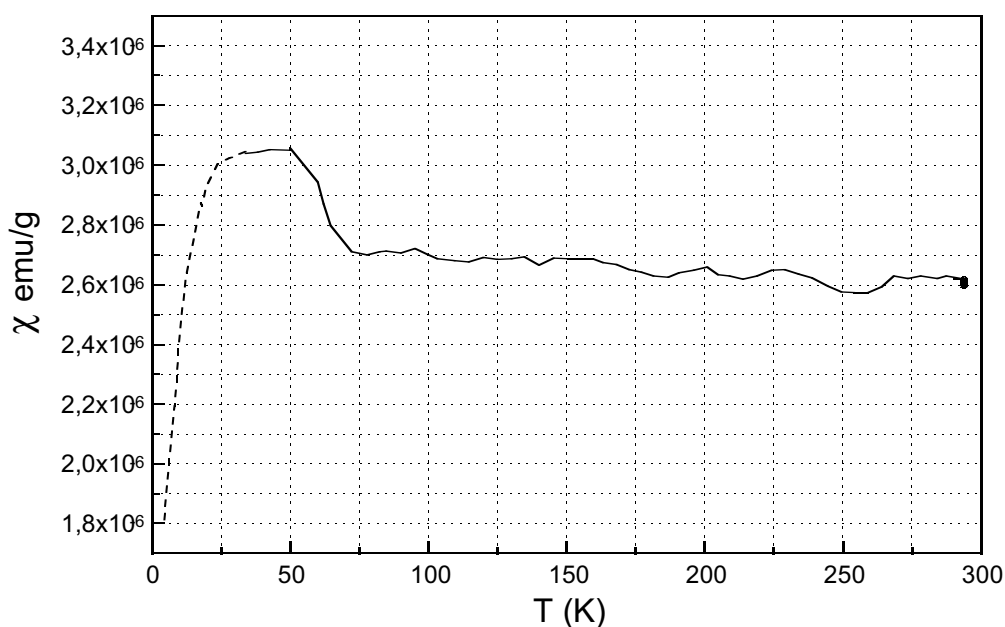
## Results and Discussion

The magnetic properties of the six binary  $\text{Pu}_{(1-x)}\text{Am}_x$  alloys have been studied from 4 K to 300 K in fields up to 1.8 T. A typical susceptibility versus temperature curve ( $\chi(T)$ ) is presented in Figure 1. For the analysis of the susceptibility, it is assumed that the two contributions of Pu and Am are additive. Indeed, the 5f electrons of Am being localized, the  $J = 0$  ( $5f^6$ ) configuration gives rise to a Van Vleck susceptibility, independent of its environment. It is then assumed that, in a  $\text{Pu}_{(1-x)}\text{Am}_x$  solid solution,  $\chi_{\delta\text{-Pu}} = \frac{\chi_{\text{mes}} - x \cdot \chi_{\beta\text{-Am}}}{1 - x}$  where  $\chi_{\text{mes}}$  is the measured susceptibility of the solid solution.  $\chi_{\beta\text{-Am}}$  is supposed to be close to  $\chi_{\alpha\text{-Am}}$  since the susceptibility is a Van Vleck one ( $\chi_{\alpha\text{-Am}} \sim 3.32 \text{ emu}\cdot\text{g}^{-1}$ ).<sup>4</sup> In the example of Figure 1, this leads to a susceptibility of  $\chi_{\delta\text{-Pu}} = 2.37 \cdot 10^{-6} \text{ emu}\cdot\text{g}^{-1}$  at room temperature (very close to the pure  $\alpha$ -Pu value). The evolution in  $\chi_{\delta\text{-Pu}}(T)$  with Am concentration will be discussed with respect to 5f localization in Pu.

Marion Dorneval,  
Nathalie Baclet,  
CEA-Centre de  
Valduc 21120 IS-SUR-  
TILLE, FRANCE

Jean-Marc Fournier  
Université Joseph  
Fourier LEG-INPG,  
BP 46, 38402 AINT  
MARTIN D'HERES  
Cedex, FRANCE

Figure 1.  
Susceptibility  
versus  
temperature of  
 $\text{Pu}_{0.8}\text{Am}_{0.2}$



Moreover, it can be seen in Figure 1 that, below 65 K, the behavior is anomalous. Comparison with results obtained on pure two-years aged  $\alpha$ -Pu, before and after annealing, leads to tentatively attribute this anomaly to self irradiation effects. Annealing effects on the susceptibility of  $\text{Pu}_{(1-x)}\text{Am}_x$  solid solutions will be also presented and discussed.

### References

1. R. Lallement, R. Pascard, *Plutonium : métallurgie et propriétés physiques du métal, Nouveau traité de chimie minérale (P. Pascal) XV, 5*, pp217-292, Masson et Cie Ed. (1970).
2. Ph. Faure, B. Deslandes, D. Bazin, C. Tailland, J.M. Fournier, A. Falanga, *J. Alloys Comp.* 244, p131 (1996).
3. F. H. Ellinger, K. A. Johnson, V. O. Struebing, *J. Nuc. Mat.* 20, pp83-86 (1966).
4. B. Kanellakopoulos, J. P. Charvillat, F. Maino, W. Müller, *Transplutonium Elements*, Eds. W. Miller and R. Lindner, North-Holland Publishing Company, Amsterdam (1976).



## X-Ray Magnetic Scattering from Transuranium Systems

The magnetic scattering of x-rays is a weak process, difficult to observe even with present day synchrotrons if heavy elements, with their associated high absorption cross sections, are used. A decade ago it was discovered that by tuning the photon energy to an absorption edge there is often a large enhancement of the magnetic signal. Some of the largest signals are, in fact, found at the M edges (which lie around 4 keV) of the actinides. This is because these resonant energies signify transitions from core  $3d$  to empty orbits in the  $5f$  shells, and it is electrons in the  $5f$  shells of the actinides that give rise to their magnetism.

Many experiments have now been done on uranium compounds. We first extended this technique to Np at Brookhaven National Laboratory (BNL) in 1994 [1], and recently a number of Np systems [2,3] have been examined at the European Synchrotron Radiation Facility in Grenoble. These measurements probe the electronic structure of the actinide. An important additional feature as compared to either bulk or other diffraction (i.e. neutron) techniques is that the technique is element specific. For example, we have measured separately the temperature dependence of the U and Np ordered moments in the solid solutions  $(U,Np)Ru_2Si_2$ , and they are not the same for the two actinide ions [3].

A further advantage of the technique is that only very small crystals are required. For example, samples are often less than 1 mg, and we have detected quantities of actinide at the microgram level.

Recently we have extended the technique at BNL to Pu compounds. This caused initially some difficulty due probably to the chemical products produced by radiolysis of the surrounding organic glue by the Pu alphas [4]. However, the first successful results were obtained in 1999 [5]. Interestingly, there is an additional feature in the Pu energy spectrum at the M5 resonance that may be related to the hybridization of the Pu  $5f$  states with the  $p$  states of Sb. This has not been seen previously in actinide materials. More experiments will take place in 2000.

We will discuss some of these results and what they bring to our basic understanding of the behavior of the  $5f$  electrons in transuranium systems.

Some of the high-purity Np and Pu metal required for the fabrication of these compounds was made available through a loan agreement between Lawrence Livermore National Laboratory and EITU, in the frame of a collaboration involving LLNL, Los Alamos National Laboratory, and the US Department of Energy.

### References

1. S. Langridge et al., *Europhysics Lett.* **25** 137 (1994); *Phys. Rev. B* **49**, 12010 (1994); *ibid B* **49**, 12022 (1994).
2. D. Mannix et al., *Phys. Rev. B* **60** 15187 (1999).
3. E. Lidström et al., *Phys. Rev. B* **61**, 1375 (2000).
4. D. Mannix et al., *Physica B* **262**, 125 (1999).
5. P. Normile et al., unpublished results.

**G. H. Lander,**  
**D. Mannix,**  
**F. Wastin,**  
**J. Rebizant**  
*European*  
*Commission, JRC,*  
*Institute for*  
*Transuranium*  
*Elements, Karlsruhe,*  
*Germany*

**D. Mannix,**  
**E. Lidström,**  
**C. Vettier**  
*European Synchrotron*  
*Radiation Facility,*  
*Grenoble, France*

**R. Caciuffo**  
*Istituto Nazionale per*  
*la Fisica della Materia,*  
*Dipartimento di*  
*Scienze dei Materiali*  
*della Terra, Università*  
*di Ancona, Ancona,*  
*Italy*

**N. Bernhoeft**  
*Dépt. de Recherche*  
*Fond. sur la Matière*  
*Condensée, SPSMS/*  
*LCP, CEA-Grenoble,*  
*IF-38054 Grenoble,*  
*France*

**P. Normile,**  
**W. G. Stirling**  
*Oliver Lodge*  
*Laboratory, University*  
*of Liverpool, Liverpool,*  
*UK*

**A. Hiess,**  
**C. Vettier**  
*Institut Laue Langevin,*  
*156X, 38042*  
*Grenoble, France*

## The Stabilization of fcc Plutonium: A Solid-State-Solution-Like Phase of Stable and Fluctuating Configuration Plutonium

Bernard R. Cooper  
West Virginia  
University,  
Morgantown, WV  
26506-6315, USA

It has been evident for some time that the unusual structural behavior found in plutonium is related to the localization mechanism for the 5*f* electrons in going from alpha to delta plutonium. The atomic volume<sup>1</sup> expands by sharply defined steps at the alpha-to-beta, beta-to-gamma, and gamma-to-delta transition temperatures. Here we explain this behavior on the basis of a multistep 5*f* localization process involving spatially nonuniform localization. That is, we suggest that a disordered array of two types of plutonium on crystallographically equivalent fcc sites breaks the translational symmetry and provides an entropy generating mechanism that drives the transition to the delta structure. The two types of plutonium sites are first the fluctuating para (spin-singlet two-electron state) sites, at which the number of localized *f* electrons fluctuates between  $f^4$  and  $f^5$  because of hybridization with non-*f* band electrons, and second the localized ortho (spin-triplet two-electron state) sites, at which the number of localized *f* electrons remain stable at  $f^5$ . It is the entropy of mixing between these two types of sites that drives the thermal stepwise transition from the monoclinic alpha ground state to the face-centered-cubic delta phase.<sup>2-5</sup>

This is a type of Anderson (disorder-induced) localization<sup>6</sup> and is self-induced in pure Pu when atoms on some sites assume an occupied ortho state (the *f* electrons at these sites are almost fully localized) and thereby provide sufficiently strong scattering of the itinerant 5*f* electrons originating from the remaining sites (with fluctuating 5*f* configuration) so that these itinerant electrons lose their coherent-wave character, while the plutonium atoms at these remaining sites retain a fluctuating (para) 5*f* configuration. This partially localized phase is stabilized against total localization by maximizing the entropy gain and thereby lowering the free energy. Likewise, this self-induced partial localization replaces 5*f* bonding when it lowers the free energy relative to the coherent 5*f* bonding that it destroys. Presumably which sites are ortho and para will vary with time, but with a mean time sufficiently long to establish a configurational free energy and hence entropy.

For unalloyed Pu, maximizing the entropy favors exact bifurcation into the two types of sites. If  $E_{fbond}$  denotes the *f*-electron contribution to the bonding energy per atom in mRy, then the temperature at which we would observe the delta transition, considering only the entropy change from the site disorder, is given by,

$$T_{Aloc} \approx 158E_{fbond} / \ln 2 \approx 228E_{fbond} \quad (1)$$

At this temperature, the loss of bonding energy per atom would be balanced by the increase in entropy per atom. Equation (1) predicts that the delta transition at 592 K corresponds to a loss of 5*f* bonding energy per atom of 2.6mRy, which falls at the expected value about 1percent of the<sup>7</sup> total cohesive energy per atom.

For gallium (or other IIIB elements) substituted in plutonium the valence 4*p* electrons from the gallium compete with the plutonium 5*f* electrons to hybridize with the plutonium 6*d* band electrons. This not only effectively *decreases* the 6*d* hybridization per Pu 5*f* electron, it provides a severe disordered disruption of the 6*d*-mediated 5*f* banding; and the effect is to localize the 5*f* electrons, thereby stabilizing the delta structure at low temperatures. Given the highly nonlinear



nature of the effects of alloying in driving the restructuring of the ground state, the nucleation of localized sites by the addition of gallium is likely to give rise to an avalanche effect, with the formation of randomly located stable  $f^5$  (ortho) Pu sites further breaking up the  $f$  bonding coherency between the fluctuating  $f^5/f^4$  Pu (para) sites. The Ga-Pu bond shortening observed<sup>8</sup> by extended x-ray absorption fine structure (EXAFS) and x-ray diffraction has a minimum near or at the 7.7 percent Ga corresponding to one Ga for every 12 Pu. It is possible that the avalanche effect provides an explanation for the increase in bond shortening beyond 7.7 at % by providing a reinforcement of the effect of the Ga nucleation centers in breaking up the Pu-Pu bonding.

Delta-stabilized (fcc) plutonium (which does not have magnetic ordering) and similarly behaving uranium magnetically-ordered materials share the experimental signature of the solid-solution-like two-site phase, a high-temperature magnetic susceptibility that combines Curie-Weiss and enhanced Pauli-like contributions.<sup>9,10</sup> A possible way to quantify the distribution between para and ortho plutonium as a function of gallium content is based on the prediction that an increase of hybridization (with consequent increase in number of para sites) would lead to an increase in the Pauli-like paramagnetic component, and a corresponding decrease in the Curie-Weiss component. This behavior is presently being experimentally validated for a number of magnetically-ordered uranium compounds.

### References

1. See pp. 158-169 (especially Fig. 94-8) in *The Structures of the Elements* by Jerry Donohue, Robert E. Krieger Publishing Co., Malabar, FL (1982).
2. B. R. Cooper, O. Vogt, Q.-G. Sheng, and Y. L. Lin, *Phil. Mag. B* **79**, 683 (1999).
3. B. R. Cooper and Y. L. Lin, pp 251-265 in *Electron Correlations and Materials Properties* (A. Gonis, N. Kioussis, and M. Ceftan eds, Kluwer Academic, Plenum Publishing, 1999).
4. B. R. Cooper, to appear in *Los Alamos Science*, 2000.
5. B. R. Cooper, Chapter 5 in *Magnetism in Heavy Fermion Systems* (ed, Harry Radousky, World Scientific Publishing Co., Singapore, 2000).
6. P. W. Anderson, *Phys. Rev.* **109**, 1492 (1958).
7. See Fig. 3 page 158 in M. S. S. Brooks, B. Johansson, and H. L. Skriver, vol. 1 *Handbook on the Physics and Chemistry of the Actinides* (eds, A. J. Freeman and G. H. Lander, Elsevier Science Publishers, Amsterdam, 1984).
8. Ph. Faure, B. Deslanders, D. Bazen, C. Tailland, R. Doukhan, J. M. Fournier, and A. Falanga, *J. of Alloys and Compounds* **244**, 131 (1996).
9. S. Méot-Reymond and J. M. Fournier, *J. of Alloys and Compounds* **232**, 119 (1996).
10. J. Schoenes, O. Vogt, J. Löhle, F. Hulliger, and K. Mattenberger, *Phys. Rev. B* **53**, 14,987 (1996).

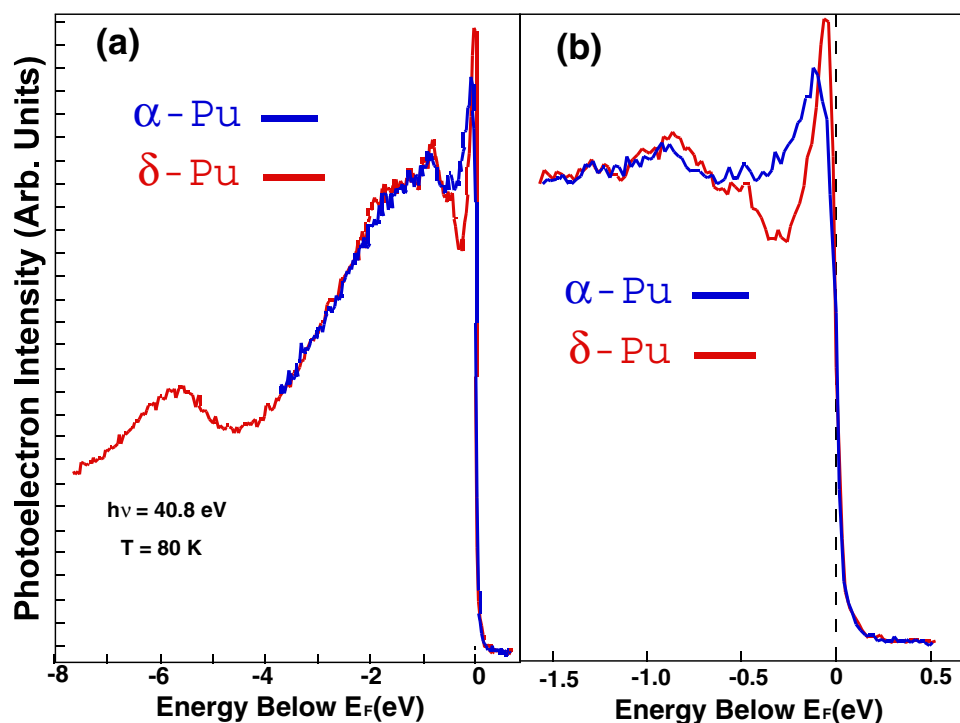
## Electronic Structure of $\alpha$ - and $\delta$ -Pu from PES Measurements

A. J. Arko,  
J. J. Joyce,  
L. Morales,  
J. Wills,  
J. Lashley  
Los Alamos National  
Laboratory, Los  
Alamos, NM 87545,  
USA

Despite extensive work over several decades, the electronic structure of Pu in its various allotropes is not yet understood in detail. It is generally accepted that f-bands in  $\alpha$ -Pu are strongly hybridized with 6d bands, and moreover that there may exist direct f-f overlap, while in  $\delta$ -Pu there is a much greater tendency toward localization of the 5f electrons. Since photoemission spectroscopy (PES) is the most direct experimental tool for probing the electronic structure of materials, it is utilized to observe the assumed differences described above. We report PES results on  $\alpha$ - and  $\delta$ -Pu using a laser plasma light source (LPLS) as well as HeI and HeII radiation. Surprisingly, we find only minimal differences in the electronic structures of  $\alpha$ - and  $\delta$ -Pu (except near the Fermi energy) despite large differences in structural and mechanical properties.

The LPLS (together with HeI and HeII) provides photon energies from 21.2 to 140 eV in a bench-top laboratory system. The surfaces of the specimens were prepared by laser ablation through a quartz window. With this technique the surface can be ablated (and simultaneously annealed) while the sample is at cryogenic temperatures so that any impurities in the bulk do not re-migrate to the surface after cleaning.

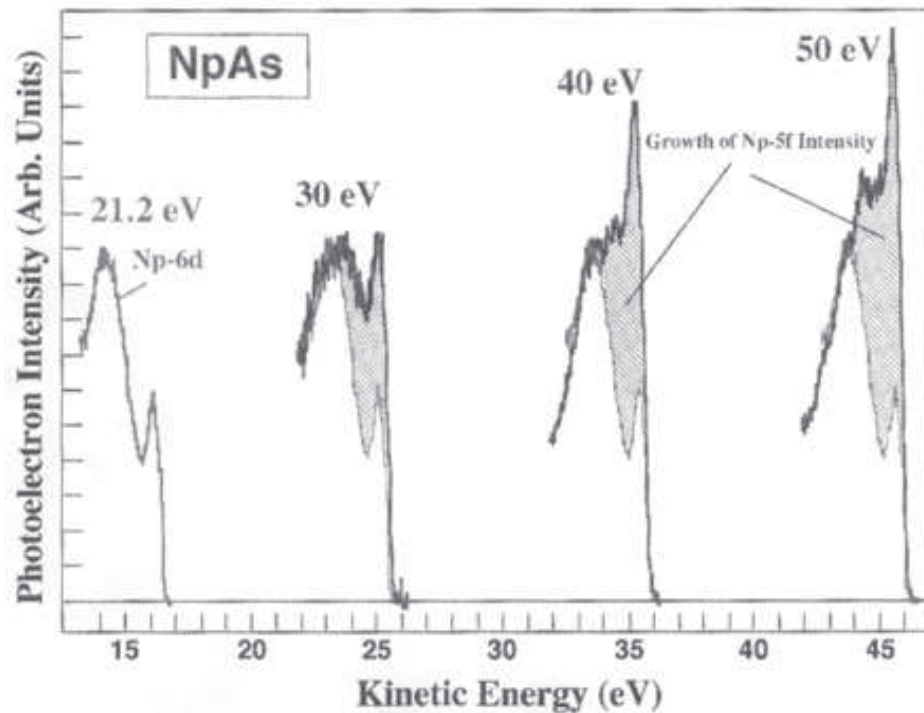
In Fig.1 we show EDCs for the two Pu allotropes using HeII radiation with the specimens at 80K. At a photon energy of 40.8eV the 6d and 5f cross sections per electron are nearly equal so that we obtain a good representation of the DOS in the PES spectra. With the exception of the feature near the Fermi energy, the spectra nearly overlay each other. There are some very subtle differences in the  $-2$  eV range (possibly related to a two hole satellite in  $\delta$ -Pu), which require further investigation. The intensity at about  $-6$ eV is due to adsorbed oxygen from the edge portions of the sample not fully cleaned by ablation.



In the expanded view in Fig. 1b where only the near  $E_F$  data are shown, we find the only truly significant and understandable differences between  $\alpha$ -Pu and  $\delta$ -Pu in the valence band data. In particular, the sharp feature in  $\delta$ -Pu (FWHM  $\leq 100$  meV) is clearly much narrower than that found in  $\alpha$ -Pu (FWHM  $\geq 200$  meV) and, to within our resolution, crosses  $E_F$ , while the much broader peak in  $\alpha$ -Pu reaches maximum intensity at about 50 meV below  $E_F$ . This is consistent with the larger specific heat  $\gamma$ -value of  $\delta$ -Pu [27] relative to  $\alpha$ -Pu.

Data taken at 21.2 eV light (HeI radiation), where one should be sensitive to  $\delta$ -electron emission (as well as greater bulk sensitivity), are very similar to those of Fig. 1. Indeed, they are similar at all  $h\nu$ . Thus it is reasoned that the sharp features at the Fermi energy in both  $\alpha$ - and  $\delta$ -Pu must contain substantial 6d admixture and are bulk related. Only the intensity in the  $-1$  eV range increases more rapidly with  $h\nu$  than the near- $E_F$  feature, and is thus assumed to be of purer 5f character. This is different from typical 5f materials, such as the spectra of antiferromagnetic Np As shown in Fig. 2, where the 5f intensity is clearly identifiable and separated from the 6d intensity, and whose intensity increases dramatically relative to the 6d features with  $h\nu$ .

Comparisons will be made to band calculations where at present the constrained LDA calculation for  $\delta$ -Pu yields somewhat better agreement with experiment than the non-constrained LDA calculation for  $\alpha$ -Pu. The disagreements are presently not understood.



## Resonant Ultrasound Studies of Pu

**A. Migliori,  
J. P. Baiardo,  
T. W. Darling,  
F. Freibert,  
B. Martinez,  
H. Roder,  
D. A. Dimitrov**  
Los Alamos National  
Laboratory, Los  
Alamos, NM 87545,  
USA

The measurement of elastic moduli can provide crucial input to fundamental descriptions of the electronic structure and thermodynamics of Pu because elastic moduli play a leading role in determining how thermal energy is distributed among internal vibrations, which, for the most part, control the entropy at ambient temperatures and above. In addition, elastic moduli are important parameters for engineering processes related to the fabrication and function of Pu components and are often the most sensitive of physical parameters to changes in material properties with age, composition or temperature. We describe here the rationale, techniques, and results for recent studies of the elastic moduli of Pu.

The fundamental electronic structure of a homogeneous solid determines, of course, all of its properties. However, it is not, at present possible to perform an *ab initio* electronic structure calculation at finite temperature with anything approaching an accuracy adequate to explain completely such things as structural phase transitions as in Pu metal.

We can, however, compute the elastic (harmonic phonon) entropy for Pu, by far the largest part but a 3-D phonon average  $\Theta_0 = \Sigma \omega_{average} / k_b$  is needed. At temperatures such that  $k_b T / \Sigma \gg w_{max}$ , the highest phonon frequency, all the phonon modes are fully populated and we define  $\Theta_0$  by

$$TS \approx 3 N k_b T [1 + \ln(T/\Theta_0)]. \quad (1)$$

Equation 1 describes the total vibrational entropy of a solid of  $N$  atoms at high temperatures, and can be calculated for Pu from a measurement of the speed of sound at all wavelengths and in all directions.

This simple approach, especially in the high temperature limit, can quickly establish if a theoretical model is sufficiently robust to be worth pursuing. For Pu metal, a mysterious material with at least five zero-pressure stable phases, electronic structure calculations predict with reasonable certainty the low-temperature monoclinic  $\alpha$  phase, but have considerable difficulty with the two highest temperature structures, fcc  $\delta$  and bcc  $\epsilon$ . Can we understand why quantitatively from sound speed measurements?

Although the pure fcc phase is not stable at temperatures below 583 K, the addition of 3.3 at. % Ga will stabilize that phase with very few, if any, side effects at room temperature, so that not only can single crystals be grown, but measurements can be made as well. The only known single crystal elasticity data (Table I) for Pu 3.3 at. % Ga, were taken by Moment and Ledbetter in 1975. They found the utterly surprising result that Pu has the highest shear anisotropy and lowest bulk modulus of any fcc metal. An interesting unanswered question raised by their work was an accurate prediction for the polycrystal averages. More recently we have made high-accuracy resonant ultrasound spectroscopy (RUS) measurements on polycrystal samples with varying Ga concentrations, the first such measurements since 1975. In Figure 1 we show typical

$c_{11}$	36.28±0.36 GPa
$c_{44}$	33.59±0.11 GPa
$1/2(c_{11}-c_{12})=c^*$	4.78±0.38 GPa

**Table I. The Elastic Moduli of Pu-3.3 at. % Ga  $\delta$ -Phase at Ambient Temperature as Measured by Moment and Ledbetter.**

resonances for Pu and the apparatus used. Interestingly enough, radioactive damage appears to be a stronger effect than Ga concentration, as shown in Table II, where we compare a Kroner average of the single crystal data to our measurements. Note the extremely good agreement between samples of the same age and composition, an encouraging result for accurate thermodynamic analysis. These results indicate directly and quantitatively that aging effects associated with Pu and its radioactive decay processes are present.

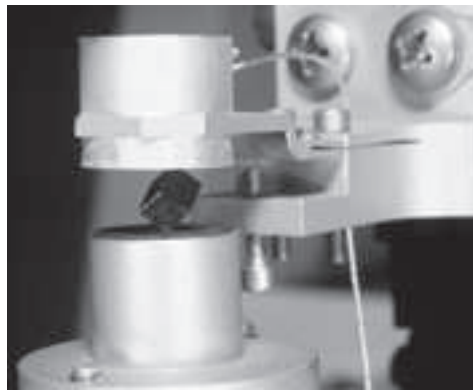
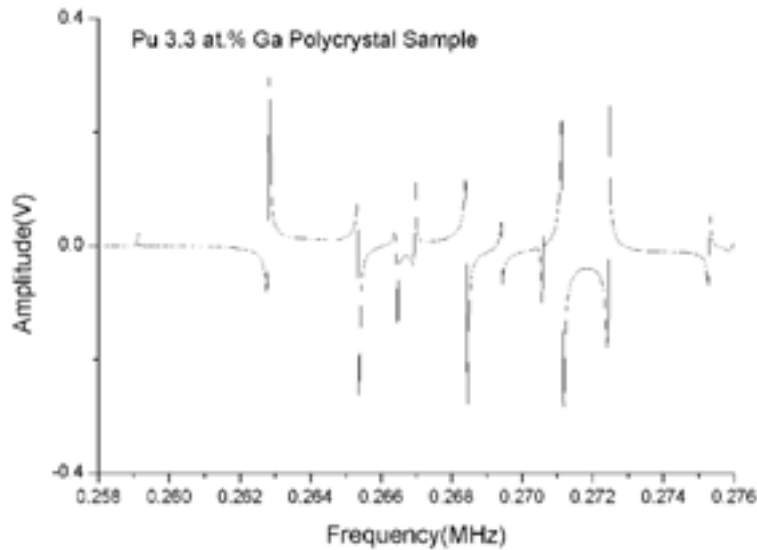
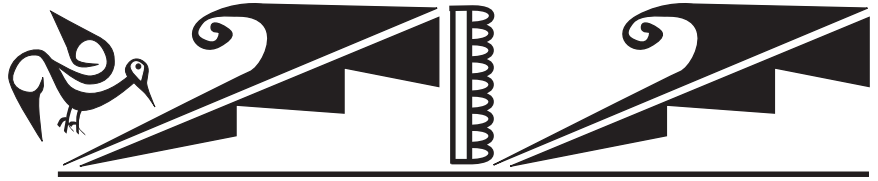


Figure 1. Top: Typical resonances of a Pu 3.3 at.% Ga new chill-cast polycrystal sample. The sharpness of the modes will enable real-time studies of the aging of  $^{239}\text{Pu}$ . Right: apparatus typically used for such RUS measurements.

Sample	$C_{11}$ (GPa)	Bulk(GPa)	Shear (GPa)
single crystal $\delta$ -Pu 3.2 at.% Ga new	51.4	29.9	16.2
<b>polycrystal <math>\delta</math>-Pu 1.73 at. % Ga 15y</b>	<b>47.5</b>	<b>26.7</b>	<b>16.3</b>
<b>polycrystal <math>\delta</math>-Pu 2.36 at. % Ga new</b>	<b>52.3<math>\pm</math>0.15</b>	<b>30.6</b>	<b>16.3<math>\pm</math>0.006</b>
<b>polycrystal <math>\delta</math>-Pu 3.3 at. % Ga new</b>	<b>51.8<math>\pm</math>0.44</b>	<b>29.6</b>	<b>16.7<math>\pm</math>0.018</b>
<b>polycrystal <math>\delta</math>-Pu 3.902 at. % Ga 15y</b>	<b>58.4</b>	<b>34.3</b>	<b>18.1</b>
<b>polycrystal <math>\delta</math>-Pu 5.53 at. % Ga 44y</b>	<b>50.0</b>	<b>27.0</b>	<b>17.2</b>
cast $\alpha$ -Pu (Laquer)	104.6	46.6	43.5
<b>cast <math>\alpha</math>-Pu (new)</b>	<b>109.1</b>	<b>55.8</b>	<b>40.0</b>
cast $\alpha$ -Pu (DeCadenet)	109.0	54.5	40.9

Table II. A summary of ours and other measurements of the elastic moduli of Pu. Our results are shown in bold. All measurements were at ambient temperature. Error bars where not noted for our measurements were less than 1% for  $c_{11}$  and less than 0.3% for  $c_{44}$ .

More recently, analysis of diffuse neutron scattering data by Roder and Dimitrov has produced tentative force constants. Although these data have serious problems associated with container wall corrections and neutron absorption by  $^{239}\text{Pu}$  impurities, an estimate can be made using sound speeds as initial slope constraints. From this we obtain  $\Theta_0 = 84\text{K}$ , yielding a value for  $TS = 625\text{meV/K}$ . There are, however, specific heat data available for this system from which the actual entropy can be calculated, including electronic and other components. These data, analyzed by Wallace, show that at the  $\delta$ - $\epsilon$  phase boundary in the  $\delta$  phase,  $TS = 740\text{ meV/atom}$ . The difference,  $115\text{ meV/atom}$ , though not expected to be very accurate just yet, is probably a good (and the first) measure of the entropic contribution of the free electrons. It is this number that must be dealt with via electronic structure calculations, not  $740\text{ meV/atom}$ , a much easier task. From this analysis, it is very likely that it is not the details of the electronic structure that stabilize the high temperature phases of Pu, but in fact it must be vibrational entropy.



# **Actinides in the Environment/Separation and Analysis**





## Aquatic Chemistry of Actinides: Is a Thermodynamic Approach Appropriate to Describe Natural Dynamic Systems?

The worldwide civilian use of nuclear energy generates yearly about 11,000 tons of spent-fuel from 433 nuclear power plants (NPP) in operation for the moment with an installed capacity of approximately 350 GWe (36 NPP are being under construction). This contributes to the world electricity production about 17%. The hitherto discharged spent-fuel is estimated to be around 220,000 tons, which contain about 1,400 tons of plutonium and a considerable amount of minor actinides and fission products. The total quantity of long-lived radioactive elements, mostly actinides, increases steadily. The foreseeable solution for their isolation from the biosphere is a geological disposal with safe confinement. The long-term safety assessment of such containment entails well-founded knowledge on the aquatic chemistry of actinides, most of all, their thermodynamic properties in the geochemical environment.

A thermodynamic approach is indispensable for the appraisal of the chemical behavior of actinides in natural aquatic systems. However, the real natural systems are dynamic and "open" for a variety of geochemical reactions. Actinide ions exposed once to natural dynamic systems undergo a multiplicity of nanoscopic chemical reactions, in which individual processes may not be equilibrated or may appear irreversible. For the assessment of such complexities, a challenging question arises indubitably: "Is a thermodynamic approach capable of describing the actinide behavior in natural dynamic systems?"

Actinides to be disposed of are immobilized in different solid phases, called engineered barriers, which are then contained by back-fills known as geo-engineered barriers and further by natural geological barriers. Whatever the perceived scenarios are to come after disposal, the long-term performance assessment of such a multi-barrier system necessitates the quantification of the geochemical behavior of individual actinides in the environment of each barrier. The two characteristics are recognized for actinides in aquifer systems: the oxidation state specific chemical behavior, namely M(III), M(IV), M(V), and M(VI), on the one hand and the chemical reactions governed by the effective charge of individual ions on the other hand. These characteristics can be followed as a primary guide for understanding their general chemical behavior in both laboratory and natural systems. Under reducing conditions, which are mostly the case for deep aquifers, actinides of M(V) and M(VI) become reduced to M(III) or M(IV). Actinides of M(III) and M(IV) are sparingly soluble in water at neutral pH, and these particular chemical properties lead to their strong tendency toward the so-called pseudo-colloid formation. How can such processes be quantified? Can it be delivered by a thermodynamic approach?

Whatever the engineered barriers are made of, they are thermodynamically unstable in the near-field environment once water comes in contact with them and they undergo a variety of geochemical reactions. Solid phases of waste are first subject to corrosion, leaching and dissolution of individual components, the processes of which generate the *new* secondary solid phases that appear to be stable thermodynamically as compared to the primary solid phases in the near-field environment. Upon the phase conversion of engineered barriers, the actinides dissolved are submitted to hydrolysis, complexation, redox-reaction and

J. I. Kim  
Forschungszentrum  
Karlsruhe, Institut für  
Nukleare  
Entsorgungstechnik,  
76021 Karlsruhe,  
Germany

colloid generation, and largely immobilized by incorporation into the secondary solid phases that are partially equilibrated in the new environment. Under these conditions the chemistry of actinides in the aqueous phase is submerged into the geochemical condition evolved from water interactions with waste, backfill and surrounding geological matrices. Taking into account these conditions the source terms of individual actinides are to be quantified. How far is a thermodynamic approach capable for such quantification?

The so-called “Kd-concept” is often used to calculate the migration behavior of individual actinides in a given aquifer system. Since Kd is a simple operational parameter, which depends on various unknown geochemical effects involved, it has no solid thermodynamic foundation, and its applicability to the long-term performance assessment has become the subject of controversial debate. An alternative to the Kd-concept is to evaluate thermodynamic parameters for the complexation of individual radionuclides onto the surface of geo-matrices. This can be realized by the study of solid-water interface reactions for a given actinide ion on a number of single minerals and thereafter by a combination of the results proportionally into a composite model. The development of such a surface complexation model is in progress in a number of laboratories worldwide. Is such a model conceived for actinides applicable to natural dynamic systems?

The paper summarizes the present state of available thermodynamic approaches that can be applicable for the performance assessment of multi-barrier systems. Limitations of the approaches, as perceived for the moment, are to come into view simply as repercussions of the present discussion. To provide an overview on a multiplicity of convoluted chemical reactions in natural systems, the present discussion is separated into the following three areas:

- Laboratory systems (closed system),
- Natural dynamic systems (open systems),
- Applicability of laboratory knowledge to natural systems.

Along these subject areas, detailed discussion is further directed to the speciation of actinides in solution, in solid phase and in solid-water interface interaction for laboratory systems, and additionally to the quantification of source terms in the near-field and the migration behavior in the far-field.

# Sorption of Plutonium onto Clinoptilolite (Zeolite) Colloids

## Introduction

Colloids may play a major role in the migration of radionuclides e.g., plutonium from nuclear waste disposed of in a geologic repository.<sup>1</sup> Recent work by Kersting et al. (1999), detected plutonium 1.3 km from an underground nuclear test at Nevada Test Site (NTS), from which it was originally deposited.<sup>2</sup> The plutonium was associated with colloids that may enhance the transport of plutonium in the groundwater. These colloids consisted mainly of zeolite (mordenite, clinoptilolite/heulandite), clays (illite, smectite) and cristobalite (SiO<sub>2</sub>).

The Environmental Protection Agency (EPA) found that plutonium deposited near Maxey Flats, Kentucky, had migrated hundreds of feet in less than 10 years<sup>3</sup> In addition, plutonium was also detected in groundwater from test wells in West Valley, New York, suggesting that the plutonium had moved more than 50 feet in less than 25 years.<sup>4</sup> These field observations raise a number of questions regarding the dominant mechanisms that may control the plutonium migration. Kersting et al. (1999), suggested that the plutonium might sorb to colloids (zeolites or clays). In order to test this hypothesis, it is important to understand the effect of plutonium sorption and desorption onto the existing colloids found in NTS groundwater.

In the present work, we have performed a series of laboratory batch sorption experiments of plutonium (IV) on zeolite (clinoptilolite) colloids to understand the role of colloids in the transport of plutonium under groundwater conditions similar to those found at the NTS.

## Experiments

Laboratory batch experiments were carried out at room temperature to evaluate the effect of time, plutonium concentration and pH on the sorption of Pu(IV) onto clinoptilolite colloids.

Water samples were collected from a well (WW-20) located on the NTS that has water representative of the water hosted in the volcanic aquifers at the NTS. The samples were filtered prior to use. The chemical analysis of the water indicated the presence of HCO<sub>3</sub> (110 ppm), Na (60 ppm), SO<sub>4</sub> (32 ppm) and Si (21.9 ppm), the pH and the conductivity were 7.96 and 296 mS/cm, respectively.

Colloid particles were prepared in WW-20 water by grinding a pure amount of clinoptilolite. Final concentration and particles size were 0.3mg/ml and of  $90 \pm 10$  nm, respectively. Plutonium (IV) concentration was  $5 \times 10^{-9}$  M.

The zeta potential and the size variations of the colloids were measured as a function of pH by electrophoretic light-scattering and photon correlation spectroscopy (PCS), respectively.

**Nadia L. Hakem,  
Axel Brachmann,  
Mavrik Zavarin,  
Annie B. Kersting**  
*Lawrence Livermore  
National Laboratory,  
Livermore, CA 94550*

## Results

The zeta potential of the colloids was always negative for pH ranging between 2.7 and 10.5. This negative charge is assigned to the progressive deprotonation of the surface of the colloids as the pH increased. The size of the particles increased at the lower pH range, from the original 90 nm of the starting material to approximately 342 nm indicating a partial coagulation of the colloids at low pH where their surface charge is minimum.

Using the software Mineql+, we determined the speciation of plutonium Pu(IV) in WW-20 water as a function of pH.  $\text{Pu}(\text{CO}_3)_4^{4-}$  and  $\text{Pu}(\text{CO}_3)_6^{5-}$  are the dominant species around pH 8.

At the WW-20 water pH (8), the clinoptilolite colloids have a negative charge, a size of 90 nm and Pu(IV) is highly carbonated.

A kinetic study showed that the Pu(IV) sorption reached the equilibrium after four days. It was found that the sorption was dependent of the pH variation, e.g., the sorption ratio increased from 30% to 90% as the pH increased from 2.4 to 11.8 for a concentration of Pu(IV) equal to  $5 \times 10^{-9}$  M.

We are presently fitting the sorption data to several surface complexation models using the FITEQL code.<sup>5</sup> Initial data fits indicate that the sorption is comparable to Pu(IV) sorption to smectite reported by Sanchez.<sup>6</sup>

## References

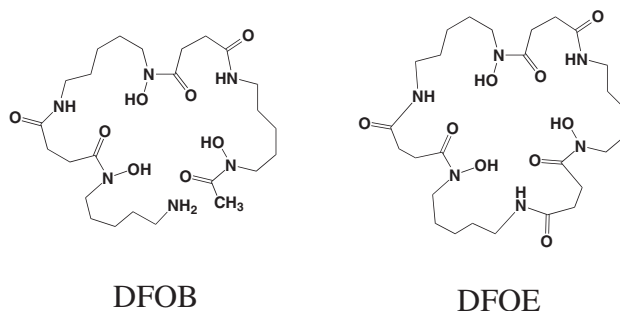
1. Buddemeier R. W. and Hunt J. R. (1988), Transport of Colloidal Contamination in Groundwater: Radionuclides Migration at the Nevada Test Site, Applied Geochemistry, Vol 3, 535-548.
2. Kersting, A. B., Efurud, D. W., Finnegan, D. L., Rokop, D. J., Smith, D. K. and Thompson, J. L. (1999), Migration of Plutonium in Groundwater at the Nevada Test Site, Nature, 397:56-59.
3. Cleyeland J. M., Rees T. F. (1981), Characterization of Plutonium in Maxey Flats Radioactive Trench Leachates, Science Vol. 212, 1506-1509.
4. State of Nevada Nuclear Waste Project Office (1998), Plutonium Migration Has Significant Implications For Waste Isolation At Yucca Mountain, Report, <http://www.state.nv.us/nucwaste/yucca/plut01.htm>.
5. Herbelin A. L. and Westall J. C. (1994), FITEQL, A computer program for determination of chemical equilibrium constants from experimental data. Department of Chemistry, Oregon State University, Corvallis, OR.
6. Sanchez A. L. (1983) Chemical speciation and adsorption behavior of plutonium in natural waters, Thesis, University of Washington, Seattle, WA.

## Actinide (Pu, U) Interactions with Aerobic Soil Microbes and Their Exudates: Fundamental Chemistry and Effects on Environmental Behavior

To understand the environmental behavior of metals we must consider a tremendous range of phenomena, from simple individual reactions, such as ligand complexation and solubility equilibria, to quite complicated and collective processes, such as metal-mineral-microbial interactions. Because of pressing contamination problems at DOE sites and the paucity of relevant actinide chemistry knowledge, research is needed in this entire range of science. The determination and evaluation of key thermodynamic data for actinide species and the development of geochemical, hydrological, and environmental transport models are progressing. In contrast, we know almost nothing about how actinides interact with microorganisms. Ubiquitous microorganisms can absorb, reduce, oxidize, solubilize, or precipitate actinides, thereby affecting their speciation, solubility, bioavailability, and migration. These effects are due to both direct and indirect interactions, such as sorption to the cell wall and reaction with microbial byproducts, respectively. Our goal is to fully characterize specific microbial-actinide interactions, both to develop this area of fundamental research and to determine how the interactions may be exploited to affect environmental actinide mobility/immobility and remediation efforts.

We are initially studying the interactions of plutonium and uranium with very common aerobic soil bacteria with focus on binding by extracellular polymers and complexation and uptake by siderophores. Extracellular polymers are produced by microorganisms for a variety of functions, including surface adhesion, nutrient acquisition, and desiccation protection. Siderophores are excreted by microorganisms to acquire Fe(III) and transport this nutrient across the cell wall. Both of these naturally-produced chelators have the potential to strongly bind actinide ions. The specific systems we are studying include (1) the polyglutamic acid polymer of *Bacillus licheniformis* and the previously uncharacterized polymer of *Rhodococcus erythropolis* and (2) siderophore complexation and uptake using *Streptomyces pilosus*, which produces desferrioxamine B (DFB, Figure 1), *Pseudomonas stutzeri*, which produces desferrioxamine E (DFE), and *Rhodococcus rhodochrous* strain OFS, which produces a previously uncharacterized siderophore. Results on each of these systems and implications for the environmental behavior of actinides will be presented.

One of the first questions we addressed is, "To what extent can these strong chelating agents solubilize generally insoluble Pu(IV) phases?" Counter to conventional wisdom, we have shown that stability constants are not sufficient for predicting solubilization. Surprisingly, the siderophores DFE and DFB do not readily solubilize Pu(IV) hydroxide or oxide. They are 100 times slower than EDTA, despite having signifi-



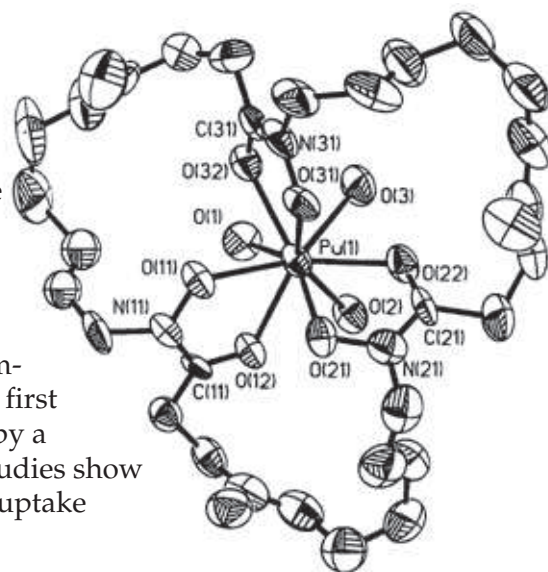
M. P. Neu,  
C. E. Ruggiero,  
M. T. Johnson,  
J. R. Fairlee,  
J. H. Matonic,  
L. A. Vanderberg,  
L. E. Hersman,  
L. He, M. M. Cox,  
D. J. Chitwood,  
P. D. Gladden,  
G. L. Wagner  
Los Alamos National  
Laboratory, Los  
Alamos, NM 87545,  
USA

Figure 1. DFO-B and DFO-E



**Figure 2. ORTEP of Pu(IV)DFO-E complex**

cantly higher solution Pu(IV) complex formation constants. Despite being unable to rapidly solubilize Pu(IV), desferrioxamine-Pu(IV) complexes are thermodynamically favored. No matter what oxidation state of Pu is present initially (III, IV, V, VI), desferrioxamines rapidly and irreversibly form the Pu(IV)DFO complex at environmentally relevant solution pH. We have crystallized a Pu(IV)-DFE complex (Figure 2) thereby performing the first characterization of Pu(IV) complexed by a biomolecule. Initial bacterial uptake studies show that Pu-DFB and Fe-DFB have similar uptake profiles, suggesting Pu-DFO complexes are taken up by bacteria.



We have optimized production and purification of the siderophore of *Rhodococcus rhodochrous*. <sup>1</sup>H-NMR spectroscopy shows that there are two distinct catechols in the siderophore in a 1:1 ratio. Mass spectral results confirm the catecholate functionality and are consistent with a siderophore composed of 2,3 dihydroxybenzoyl arginine. Metal binding experiments with Fe(III) and Pu(IV) have been completed.

We have optimized the production and purification of the exopolymers produced by *Bacillus licheniformis* and *Rhodococcus erythropolis*. The *B. licheniformis* polymer has a molecular weight of approximately 800 KDa, with approximately 6200 subunits. The *R. erythropolis* polymer has been identified to be a polysaccharide composed of glucose, mannose, pyruvic and glucouronic acid with a molecular weight of approximately 900 KDa. We have studied the structural and chemical behavior of the *B. licheniformis* polymer. The surface charge of this polymer varies with ionic strength and ion type with behavior very different from that typically measured for mineral surfaces. The polymer forms a water soluble U(VI) complex at 1: 10 U:glutamate ratios, but forms insoluble complexes at lower ratios. The conformation of the polymer changes (helical to beta) with varying metal binding, pH, and ionic strength. We have determined the metal ion capacity for Fe(III), Pu(IV) and U(VI) and found the polymer binds 0.38  $\mu\text{mol Fe(III)}$  per milligram of polymer and approximately one third less Pu(IV).

## The Interaction of Plutonium with Bacteria in the Repository Environment

Microorganisms in the nuclear waste repository environment may interact with plutonium through (i) sorption, (ii) intracellular accumulation, and (iii) transformation of chemical speciation. These interactions may retard or enhance the mobility of Pu by precipitation reactions, biocolloid formation, or production of more soluble species. Current and planned radioactive waste repository environments, such as deep subsurface halite and granite formations, are considered extreme relative to life processes in the near-surface terrestrial environment. There is a paucity of information on the biotransformation of radionuclides by microorganisms present in such extreme environments. In order to gain a better understanding of the interaction of plutonium with microorganisms present in the waste repository sites we investigated a pure culture (*Halomonas* sp.) and a mixed culture of bacteria (*Haloarcula sinaiiensis*, *Marinobacter hydrocarbonoclasticus*, *Altermonas* sp., and a  $\gamma$ -proteobacterium) isolated from the Waste Isolation Pilot Plant (WIPP) site and an *Acetobacterium* sp. from alkaline groundwater at the Grimsel Test Site in Switzerland.

We examined the effects of various concentrations of  $^{239}\text{Pu}$ -perchlorate and 1:1  $^{239}\text{Pu}$ -EDTA(ethylenediaminetetraacetic acid) ( $10^{-8}$  to  $10^{-6}$  M) on the growth of pure and mixed cultures of halophilic bacteria grown in medium containing 4 M NaCl and 1.7 M NaCl/1.4 M  $\text{MgCl}_2$ , respectively, under anaerobic (denitrifying) conditions. In addition, to eliminate effects of growth media and pH change on Pu speciation, experiments were performed with washed resting cells of *Halomonas* sp. suspended in high ionic strength solution and *Acetobacterium* sp in low ionic strength solution and contacted with  $10^{-11}$  to  $10^{-9}$  M  $^{241}\text{Pu}$ -nitrate at a constant pH of 5.

Figure 1 shows  $^{239}\text{Pu}$  association with the cells of *Halomonas* sp. and the mixed culture during growth in the presence of various concentrations and forms of Pu. During the growth of *Halomonas* sp., the pH of the medium changed from 7.0 to 8.5 as a result of bacterial action. Plutonium association with the bacterial cells was determined by separating the cells after filtration through a  $0.4\ \mu\text{m}$  membrane

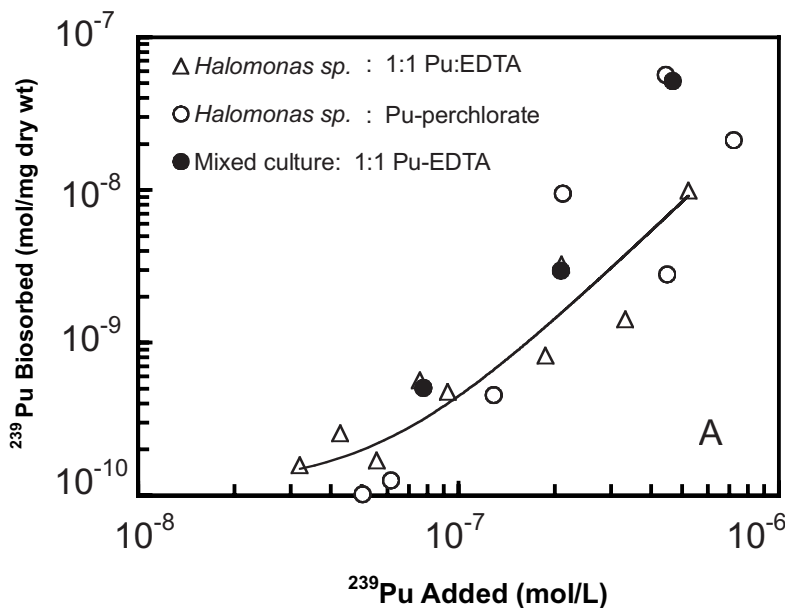


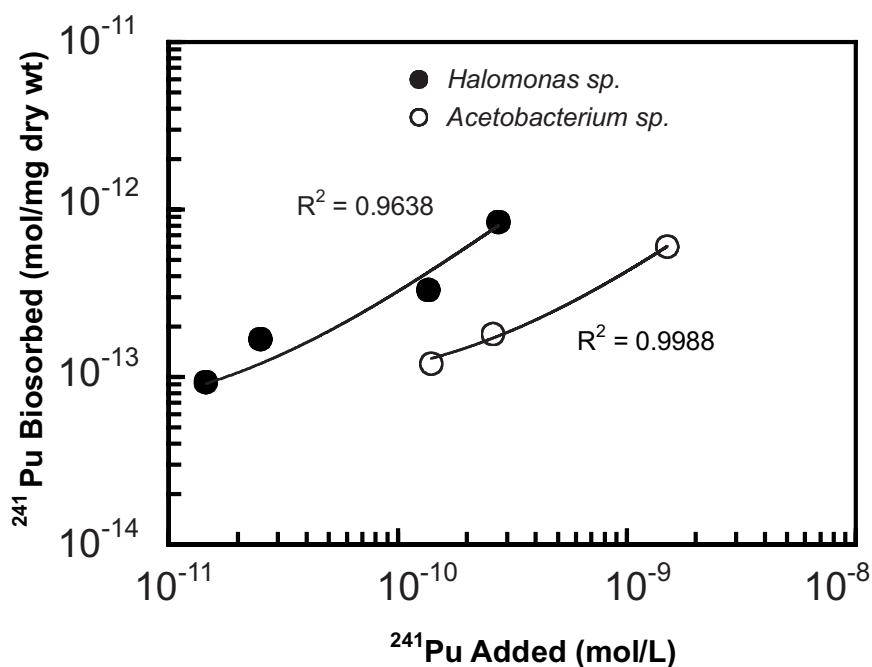
Figure 1. Uptake of various concentrations of  $^{239}\text{Pu}$  by a growing culture of *Halomonas* sp. and a mixed culture of halophilic bacteria (*Haloarcula sinaiiensis*, *Marinobacter hydrocarbonoclasticus*, *Altermonas* sp., and a  $\gamma$ -proteobacterium).

J. B. Gillow,  
A. J. Francis  
Brookhaven National  
Laboratory, Upton, NY,  
11973, USA

D.A. Lucero,  
H. W. Papenguth  
Sandia National  
Laboratories,  
Albuquerque, NM,  
87185, USA



Figure 2. Uptake of  $^{241}\text{Pu}$ -nitrate by resting cells of *Halomonas* sp. and the non-halophilic culture *Acetobacterium* sp.



filter and analysis of Pu in solution before and after filtration. Samples containing Pu but without bacterial cells were used as controls. *Halomonas* sp. sorbed 0.013 to  $2.1 \times 10^{-8}$  mol Pu added as perchlorate per mg cells dry wt., and 0.057 to  $0.99 \times 10^{-8}$  mol Pu added as the EDTA complex per mg cells dry wt., depending upon the concentration of Pu added. On the other hand, with the mixed culture the pH of the medium did not change and remained constant at 6.5. The mixed culture sorbed 0.05 to  $5 \times 10^{-8}$  mol Pu added as the EDTA complex per mg cells dry weight. Toxicity of Pu to both the pure (*Halomonas* sp.), and mixed culture was observed at  $\sim 2$  to  $3 \times 10^{-6}$  M as evidenced by a reduction in the optical density of the cell suspension, cell numbers and cell dry wt. It appears that at a lower cell density the bacteria may be able to sorb more Pu due to the absence of both clumping of cells and shielding of sorption sites at the cell-surface, hence the skewed data at higher Pu concentrations. An increase in Pu sorption by the growing cells may also increase the toxic effects.

Figure 2 shows association of  $^{241}\text{Pu}$  with the resting cells of *Halomonas* sp. and *Acetobacterium* sp. that had been contacted with various concentrations of  $^{241}\text{Pu}$  nitrate at pH 5 for 30 min. The halophile *Halomonas* sp. showed  $\sim 36\%$  removal of the added Pu at both the lowest and highest concentrations tested ( $0.96$  to  $8.3 \times 10^{-13}$  mol mg cells dry wt.). In contrast, the non-halophilic *Acetobacterium* sp. showed only  $\sim 14\%$  removal of the added Pu at the lowest concentration and  $\sim 7\%$  at the highest concentration tested. When the same amount of Pu was added to the two cultures, there was greater Pu uptake by the halophile. Additional studies are under way to determine the functional groups involved in surface complexation and the chemical speciation of Pu.

These results show that the halophiles have a greater capacity for Pu removal than the non-halophilic bacterium. The oxidation state and chemical form of Pu, and possible intracellular transport processes, may regulate the amount of Pu taken up by microorganisms. Further studies are needed to determine the factors regulating the microbial mobilization and immobilization of Pu in the repository environment.

# Transuranium Removal from Hanford High Level Waste Simulants Using Sodium Permanganate and Calcium

## Introduction

Plutonium and americium are present in the Hanford high level liquid waste complexant concentrate (CC) due to the presence of complexing agents including di-(2-ethylhexyl) phosphoric acid (D<sub>2</sub>EHPA), tributylphosphate (TBP), hydroxyethylene diamine triacetic acid (HEDTA), ethylene diamine tetraacetic acid (EDTA), citric acid, glycolic acid, and sodium gluconate.<sup>1</sup> The transuranic concentrations approach 600 nCi/g and require processing prior to encapsulation into low activity glass. BNFL's (British Nuclear Fuels Limited's) original process was a ferric co-precipitation method based on earlier investigations by Herting and Orth, *et al.*<sup>2</sup> Furthermore, flocculation and precipitation are widely used for clarification in municipal water treatment. Co-precipitation of Np, Am, and Pu with ferric hydroxide is also used within an analytical method for the sum of those analytes.<sup>3</sup>

Tests to evaluate BNFL's original precipitation process indicated the measured decontamination factors (DFs) and filter fluxes were too low.<sup>4</sup> Therefore, an evaluation of alternative precipitation agents to replace ferric ion was undertaken. Agents tested included various transition metals, lanthanide elements, uranium species, calcium, strontium, and permanganate.<sup>5</sup>

Moreover, the association of manganese and calcium for synergistic adsorption of water contaminants is prevalent in the literature. Aziz and Smith found that limestone was better for treating manganese-containing water than gravel or crushed brick at the same pH.<sup>6</sup> Goel and Chaudhuri also demonstrated the ability of calcium plus manganese to remove humic acids from water.<sup>7</sup> This adsorption property of hydrated manganese oxides could potentially be used in the decontamination of the Hanford CC wastes.

## Description

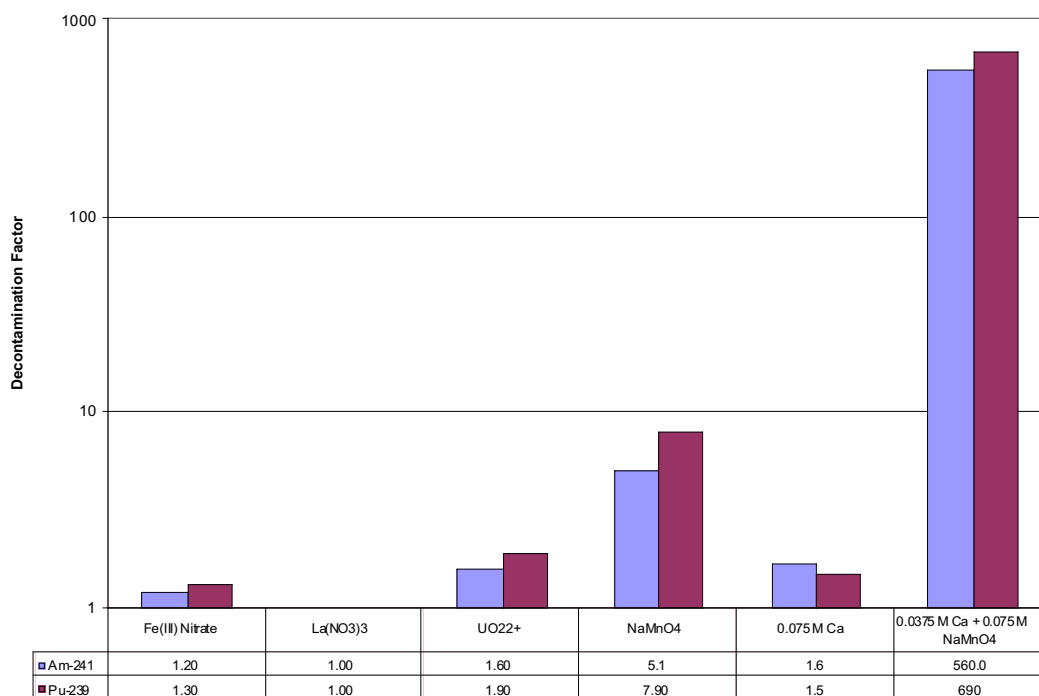
The various precipitating agents were added to 50 mL of the actinide-spiked simulant that had been adjusted to 5.5 M Na<sup>+</sup>, 1.0 M OH<sup>-</sup> and 0.4 M Al. The slurry was stirred for 15 minutes and then heated 4 h at 50°C. The samples were filtered through a 0.45-micron filter. The filtrate was collected for 1 minute and weighed or volumetrically measured. Samples were analyzed by gamma and alpha pulse height analysis. Decontamination factors (DFs) for each isotope are the initial concentration divided by the final concentration. Infrared spectra were obtained using a Nicolet 200 spectrometer and a DRIFT accessory.

## Results

Shown in Figure 1 are the decontamination factors for <sup>239</sup>Pu and <sup>241</sup>Am for a series of precipitation agents including the ferric nitrate baseline. The actinide decontamination was low with the exception sodium permanganate and the mixed agents of sodium permanganate and calcium nitrate. Orth<sup>2</sup> had originally examined the use of potassium permanganate for strontium decontamination. During this testing, a permanganate test with an actual sample from Tank 241-SY-101

W. R. Wilmarth,  
S. W. Rosencrance,  
C. A. Nash,  
F. F. Fonduer,  
D. P. DiPrete,  
C. C. DiPrete  
Savannah River  
Technology Center  
Westinghouse  
Savannah River  
Company, Aiken, SC  
29808 USA

Figure 1. DF Data for Actinide Removal from CC Waste.



showed plutonium decontamination in addition to the strontium removal. The applicability of this process to other complexant concentrated waste was not tested.

Interestingly, the combination of calcium and permanganate exhibited a phenomenal decontamination for both actinides. An apparent synergism between Ca and  $\text{MnO}_4^-$  yielded decontamination efficiencies of 99.9% for both Am and Pu. Decontamination factors for  $^{239}\text{Pu}$  and  $^{241}\text{Am}$  were 690 and 560, respectively. Additionally, this pretreatment strategy produces a slurry that is filterable in contrast to the iron decontamination sequences that proved not to be filterable.

Shown in Figure 2 are the infrared spectra of reagent-grade manganese dioxide, hydroxyethylene diamine triacetic acid (HEDTA), and the precipitate from the addition of calcium nitrate and sodium permanganate to the Hanford CC waste simulant. The spectrum of reagent grade  $\text{MnO}_2$  is dominated by an intense absorption band centered at  $550\text{ cm}^{-1}$ .<sup>8</sup> The spectrum of the HEDTA agrees with previously published results in Nakamoto.<sup>9</sup> The bottom spectrum is the manganese oxide precipitate produced from the newly developed calcium/permanganate treatment scheme. The characteristic vibration of the Mn-O stretch is observed ca.  $550\text{ cm}^{-1}$ . Additionally, bands at 1590, 1410, and  $1350\text{ cm}^{-1}$  are observed and can be attributed to coordinated carboxylate vibrations.<sup>10</sup> This suggests that plutonium and americium could be removed via an interaction between the newly formed oxide surface and an actinide-EDTA complex. Additional work is underway to examine these interactions.

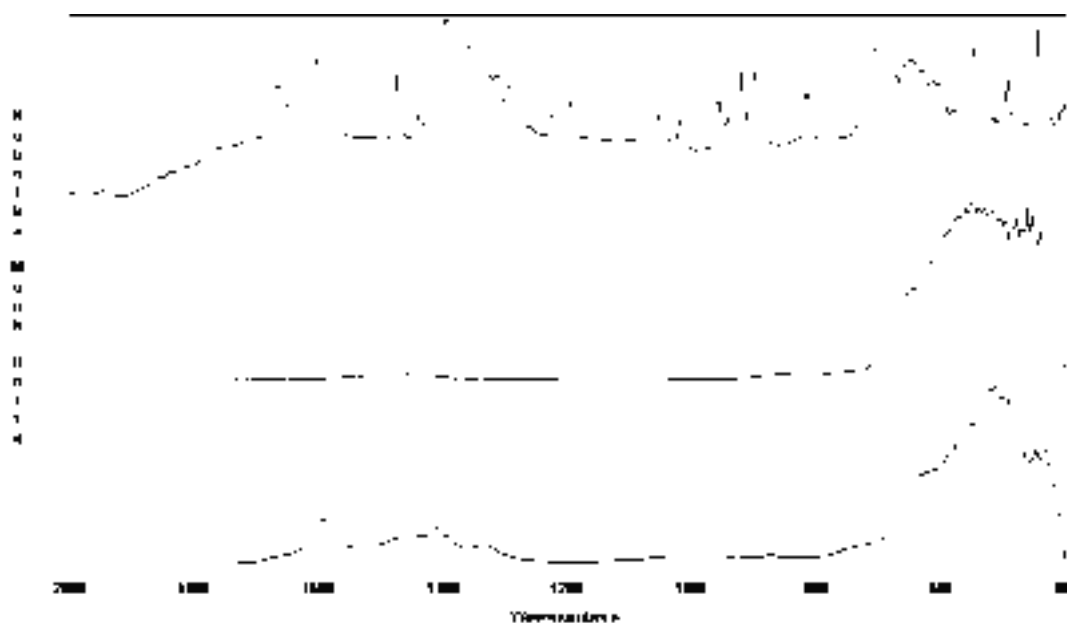


Figure 2. Infrared spectra of Ca/NaMnO<sub>4</sub> precipitate.

### References

1. M. J. Klein and W. G. Wilson, "Strontium Recovery from Purex Acidified Sludge," ARH-CD-691, May 1976, [www.osti.gov/bridge/](http://www.osti.gov/bridge/).
2. R. J. Orth, A. H. Zacher, A. J. Schmidt, M. R. Elmore, K. R. Elliott, G. G. Neuenschwander, S. R. Gano, "Removal of Strontium and Transuranics from Hanford Tank Waste via Addition of Metal Cations and Chemical Oxidant – FY1995 Test Results," PNL-10766, UC-721, September, 1995, [www.osti.gov/bridge/](http://www.osti.gov/bridge/).
3. Maiti, T. C., and Kaye, J. H., "Measurements of Total Alpha Activity," Journal Of Radioanalytical And Nuclear Chemistry, Articles, vol. 190, no. 1 (1995), pp. 175-180.
4. W.R. Wilmarth, S. W. Rosencrance, C. A. Nash, and T. B. Edwards, "Sr/TRU Removal from Hanford High Level Waste," Submitted to J. Sep. Sci.
5. W. R. Wilmarth, S. W. Rosencrance, C.A. Nash, D. P. DiPrete, and C. C. DiPrete, "Transuranium Removal from Hanford High Level Waste Simulants Using Sodium Permanganate and Calcium," Submitted to J. Radioanal. Nucl. Chem.
6. Aziz, Hamidi A., and Smith, Paul G., "Removal of Manganese from Water Using Crushed Dolomite Filtration Technique," Water Research, vol. 30, no. 2, pp. 489-492, 1996.
7. Goel, P. K., and Chaudhuri, M., "Manganese-Aided Lime Clarification of Municipal Wastewater," Water Research, vol. 30, no. 6, pp. 1548-1560, 1996
8. Y. H. Ikuhara, et al., J. Mater. Res., 14, 3102, 1999.
9. K. Nakamoto, "Infrared and Raman Spectra of Inorganic and Coordination Compounds," 3rd Ed., John Wiley & Sons, New York, 1978.
10. F. Verpoort, T. Haemers, P. Roose, and J.-P. Maes, Appl. Spectrosc. 53, 1528, 1999.

## Radiolysis of Hexavalent Plutonium in Solutions of Uranyl Nitrate Containing Fission Product Simulants

**Peter J. W. Rance**  
*British Nuclear Fuels,  
Sellafield, Seasale,  
Cumbria, UK*

**B. Ya. Zilberman,  
G. A. Akopov**  
*V. G. Khlopin Radium  
Institute, St.  
Petersburg, Russia*

The effect of the inherent radioactivity on the chemical state of plutonium ions in solution was recognised very shortly after the first macroscopic amounts of plutonium became available and early studies were conducted as part of the Manhattan Project.<sup>1</sup> However, the behaviour of plutonium ions, in nitric acid especially, has been found to be somewhat complex, so much so that a relatively modern summary paper included the comment that, "The vast amount of work carried out in nitric acid solutions can not be adequately summarized. Suffice it to say results in these solutions are plagued with irreproducibility and induction periods..."<sup>2</sup> Needless to say, the presence of other ions in solution, as occurs when irradiated nuclear fuel is dissolved, further complicates matters. The purpose of the work described below was to add to the rather small amount of qualitative data available relating to the radiolytic behaviour of plutonium in solutions of irradiated nuclear fuel.

Previous work using upwards of 20 elements in solution showed that uranium and palladium in particular had very significant effects on the rate of reduction of Pu(VI) by radiolysis.<sup>3</sup> Consequently these elements together with Np, Ce, Fe and Tc, implicated in other works to have more minor effects, were added to nitric acid solutions containing hexavalent plutonium for radiolysis studies. These studies investigated both the inherent alpha radiolysis and also external irradiation using a <sup>60</sup>Co gamma source.

### Alpha Radiolysis

Four solutions of uranium, plutonium and the other elements listed above were made up in nitric acid. The plutonium used in each of these solutions had a different proportion of the 238 isotope in order to enable dose rate effects to be studied, <sup>238</sup>Pu contents of 0.12%, 1.00%, 2.94% and 9.20% were used, the balance being essentially all <sup>239</sup>Pu. Prior to the start of each experiment, plutonium was converted to the hexavalent form by ozonolysis. The change in the proportion of hexavalent and tetravalent plutonium was then determined over a two month period by extraction of Pu(IV) using TTA from samples of each solution. Results are shown in Figure 1.

These results are interesting in that the rate of reduction of Pu(VI) to Pu(IV) appears to have been accelerated by the presence of the other ions. Vladimirova<sup>4</sup> indicates that in 4 molar nitric acid in the absence of other species a 10<sup>-2</sup> molar solution of hexavalent <sup>238</sup>Pu reduces with a G value of approximately 0.01. Our results indicate G values of approximately 0.7 and 0.5 for solutions containing 2.9% and 9.2% <sup>238</sup>Pu respectively. Vladimirova's results would be expected to show slightly smaller G values due to the higher dose rates (x10) used but this effect is not large enough to explain the fifty-fold increase in G values shown by this work. It appears that the accelerative effects of uranium and palladium on the reduction of hexavalent plutonium by gamma radiolysis may also apply during autoradiolysis.

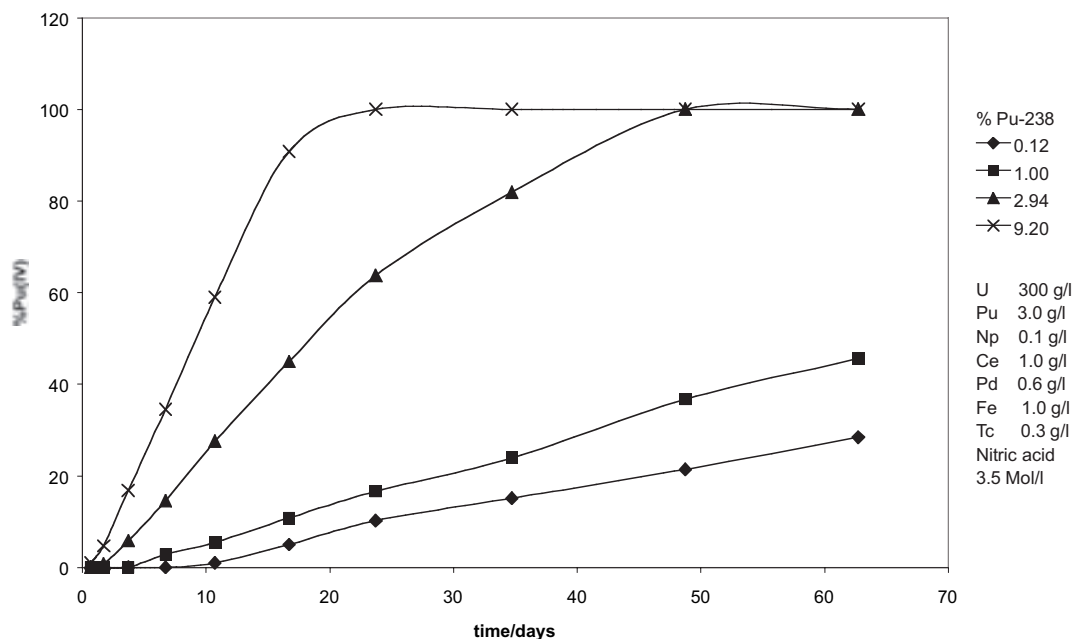


Figure 1. Autoradiolytic reduction of Pu(VI) to Pu(IV) in nitric acid.

### Gamma Radiolysis

Solutions of similar composition to those used for the alpha radiolysis experiments were made up, with the exception that only  $^{239}\text{Pu}$  was used and that the acidity and uranium concentration were varied. Samples were irradiated using a  $^{60}\text{Co}$  source for a number of days. Reduction of Pu(VI) to Pu(IV) was again determined using TTA extraction and alpha counting of evaporated samples; results are shown in Figure 2.

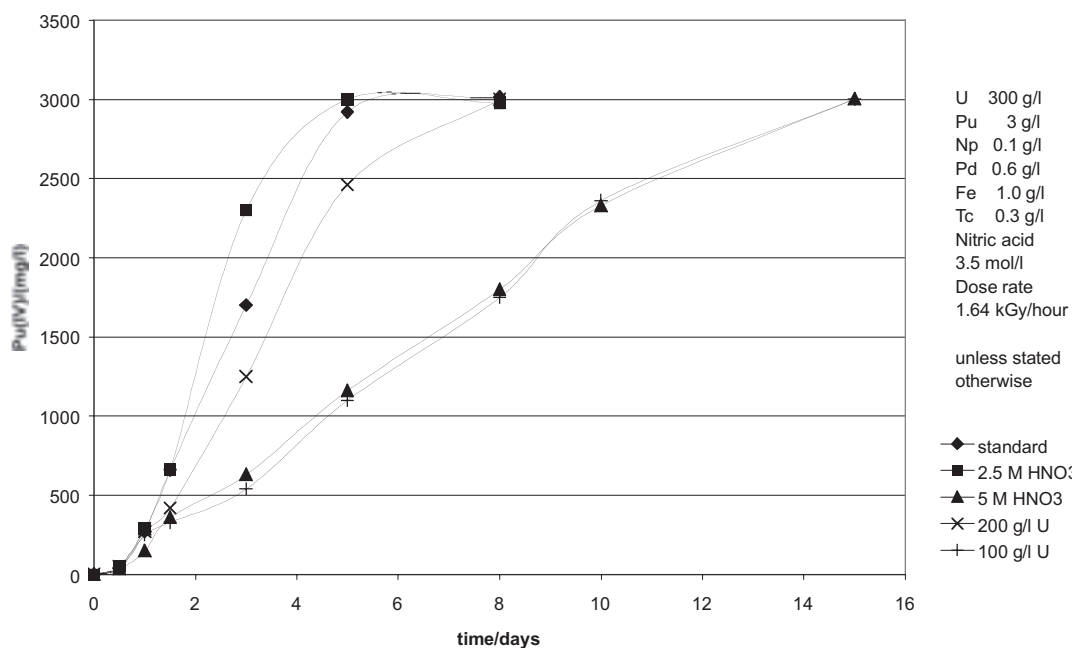


Figure 2. Reduction of Pu(VI) to Pu(IV) by gamma radiolysis.

The results indicate that increasing the acidity from 2.5 to 5 mol/l decreases the rate of reduction of Pu(VI) to Pu(IV) and that reducing the uranium concentration also reduces the rate of Pu(VI) reduction. Other elements such as technetium and zirconium had no discernible effect on the rate of Pu reduction and likewise no change was observed when using de-aerated solutions. These findings are in line with previous results from experiments<sup>3,5</sup> conducted at dose rates three orders of magnitude higher than those used in this present study and show that the accelerated reduction of Pu(VI) by uranium and palladium ions occurs irrespective of dose rate.

In conclusion, this work confirms the accelerative effect of uranium and palladium on the radiolytic reduction of Pu(VI) in nitric acid solutions and suggests that the effect is applicable to both external gamma radiolysis and alpha autoradiolysis. The effect has also been shown to occur at much lower dose rates than previously demonstrated.

### References

1. See for example papers by S. C. Carniglia, M. Kasha, W. H. McVey, G. E. Moore, G. E. Sheline and V. K. Wilmarth, *Transuranium Elements*, NNES, IV-14-B (1944).
2. J. C. Sullivan, *Plutonium Chemistry*, ACS Symposium Series 216 (1983).
3. G. P. Tkhorznitskii *et al.*, *Radiokhimiya* 5, 724-728 (1975).
4. M. V. Vladimirov, *Radiokhimiya* 22, 686-691 (1980).
5. G. P. Tkhorznitskii and G. F. Egorov, *Radiokhimiya* 27, 194-205 (1985)



## Contribution of the Surface Contamination of Uranium Materials on the Quantitative Analysis Results by Electron Probe Microbeam Analysis

The control of analysis of uranium materials is necessary for the research and development quality of the nuclear industry applications (enrichment, safety studies, fuel, etc.). Among the dependable analytical technologies, electron probe microbeam analysis wavelength dispersive spectrometry (EPMA-WDS) is a non-destructive analytical technology. The characteristic X-ray signal is measured to identify and quantify the sample constituents, and the analyzed volume is about one micron cube. The surface contamination of uranium materials modifies and contributes to the quantitative analysis results of the EPMA-WDS. This contribution is nonrepresentative of the bulk. A thin oxidized layer appears in the first instants after the preparation (burnishing, cleaning) [1-7] as well as a carbon contamination layer, due to the metallographic preparation and the carbon cracking under the impact of an electron probe [8]. Several analytical difficulties occur such as an overlapping line between the carbon Ka ray and the Uranium  $UN_{VI}O_{IV}$  ray. Moreover, the sensitivity and the precision on light element (i.e., carbon and oxygen) quantification are reduced by the presence of uranium. The aim of this study is to improve the accuracy of quantitative analysis on uranium materials by EPMA-WDS by taking into account the contribution of the surface contamination.

The first part of this paper is devoted to the study of contaminated surface of the uranium materials U,  $UFe_2$  and  $U_6Fe$  a few hours after the preparation. These oxidation conditions are selected with the aim to reproduce the same contamination surfaces that occurred in microprobe analytical conditions. The surface characterisation techniques are SIMS and Auger spectroscopy. The contaminated surfaces are described. They are made of successive layers: a carbon layer, one oxidised iron layer followed by an iron depletion layer (only in  $UFe_2$  and  $U_6Fe$ ), and a ternary oxide layer ( $U-Fe-O$  for  $UFe_2$  et  $U_6Fe$  and  $UO_{2+x}$  for the uranium).

The second part of this paper is devoted to estimating errors caused by surface contamination during quantitative analysis. EPMA-WDS is used to make the estimation. The analyses were carried out with a CAMECA SX100 and the simulation with the X-Film software. The experimental conditions are chosen in order to optimise the precision and the reproducibility of the measurements. The analytical procedure is the following: the bulk elements U, Fe and the contamination elements C, O are quantified. Quantitative analysis results by EPMA-WDS in three cases are presented: ( $\alpha$ ) simulation of perfect sample (no-contamination surface), in which the quantitative analysis results are the bulk concentrations; ( $\beta$ ) simulation with the contamination surface contribution a few hours after preparation, which is the simulation of experimental measurements; and ( $\gamma$ ) experimental measurements a few hours after preparation.

The surface effects on quantitative results of uranium-materials by WDS are very important. A few hours after preparation, oxygen atomic concentrations, exclusively due to the contamination: 11% in U, 5% in  $UFe_2$  and 15% in  $U_6Fe$  and a few carbon atomic % are measured. The errors of analysis on  $UFe_2$  materials are 5% on the uranium concentration, 5% for the iron, 8% for oxygen and 2% for carbon. The influence of the accelerating voltage of the electron beam on the quantitative results has been simulated (case of  $UFe_2$ ). The contribution of the surface is proved and is very important whatever the experimental conditions are. This study is a

**Olivier Bonino,  
Cécile Fournier,  
Catherine Fucili,  
Olivier Dugne**  
DCC/DTE/SIM – CEA  
Valrho BP 111, 26702  
Pierrelatte Cedex –  
France

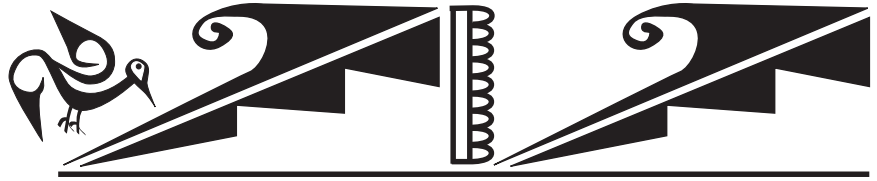
**Claude Merlet**  
ISTEEM, Université de  
Montpellier II, place  
Ugène Bataillon,  
34095 Montpellier  
Cedex 5 – France



progress in the understanding and control of quantitative analysis errors by EPMA-WDS on uranium materials. The perspective of this study is to more accurately remove errors in the results of quantitative analysis that had been caused by surface contamination. This work will contribute to the actions of CETAMA in enhancing the quality of analytical measurements.

### References

1. K.A. Winer, Dissertation, Abstracts International, 46 11B, (1985), 3975.
2. S. Orman, G. Picton, et J.C. Ruckman, *Oxydation of Metals*, 1(2), (1969), 199.
3. M.McD. Backer, L.N. Less et S. Orman, *Trans Faraday Soc.*, 62, (1966), 2513.
4. K. Winer, C. A. Colmenares, R. L. Smith, F. Wooten, *Surface Science* (1987), 67.
5. S. Orman et al., *Oxidation of Uranium and Uranium Alloys in Physical Metallurgy of Uranium Alloys*, Ed J.J. Shrier, Butterworths, London (1976).
6. W. McLean, C. A. Colmenares, R. L. Smith, *Physical Review B*, Vol 25, no 1 (1982), 8.
7. J. C. Schultz, C. A. Colmenares, J. Naegle, J. C. Spielet, *Surface Science* 198 (1988), 301.
8. A. J. Campbell and R. Gibbons, *Electron Microprobe* (1964).



## **Actinides/Processing**



## Oxidation/Reduction of Multivalent Actinides in the Subsurface

The U.S. Department of Energy (DOE) has the responsibility to remediate or stabilize existing subsurface contaminants on DOE sites. Additionally, strategies are being developed to deal with the disposal of nuclear waste and materials that are currently stored. Multivalent actinides are key constituents of this waste. A scientifically sound understanding of the environmental chemistry and key subsurface interactions of these multivalent actinides is needed to design cost-effective remediation and containment strategies.

The important role of oxidation state and redox chemistry on the mobility of multivalent actinides in the subsurface is beyond dispute. These actinides, primarily uranium, neptunium and plutonium, are likely to exist in more than one oxidation state that in many cases have very different mobility in the subsurface. An understanding of the key factors that influence the oxidation state distribution in the subsurface is essential to predicting actinide migration.

Our research here at Argonne has focused on two key factors that help define actinide speciation in the subsurface. These are microbiological interactions and interactions with anthropogenic organic complexants.

### Microbiological Effects on Actinide Speciation

Microbiological processes have an important role in defining the speciation of actinides in the subsurface. This influence has been largely ignored in assessments of subsurface actinide migration. Microbes play a major role in a wide variety of subsurface processes that lead to direct and indirect effects on actinide speciation. The most important of these are reduction/oxidation, the biodegradation of organic complexants, and the uptake/association of actinides in the cellular material.

We have investigated the fate of neptunium in the +5 oxidation state under a variety of anaerobic systems. This includes methanogenic consortia, sulfate-reducing bacteria and metal reducers – all of which are known to reduce multivalent metals. The oxidation state stability of neptunium was established by absorption spectrometry under both biotic and abiotic conditions. The neptunium precipitates formed subsequent to bioreduction were analyzed by XANES to determine the oxidation state. CCBATCH, a biodegradation model developed at Northwestern University, was used to track electron flow to assess and evaluate the mechanisms for the bioreduction noted.

The anaerobic systems investigated resulted in the reduction of Np(V) to form Np(IV) precipitates. Very little bioassociation was noted. The oxidation state of the precipitate, see Figure 1, was confirmed by XANES analysis to be Np(IV). So the result of biological activity in these systems was the immobilization of the neptunium as a neptunium (IV) precipitate. Modeling studies in support of these experiments showed that we could account for electron flow without including the actinide as an electron acceptor. This means that the neptunium (V) is not being reduced by direct enzymatic reaction. Alternative mechanisms, such as detoxification response and exocellular reduction by organics generated by the microbes, are under investigation.

**B. E. Rittmann**  
*Northwestern  
University, Evanston,  
IL 60208-3109, USA*

**D. T. Reed,  
S. B. Aase,  
A. J. Kropf**  
*Argonne National  
Laboratory, Argonne,  
IL 60439, USA*

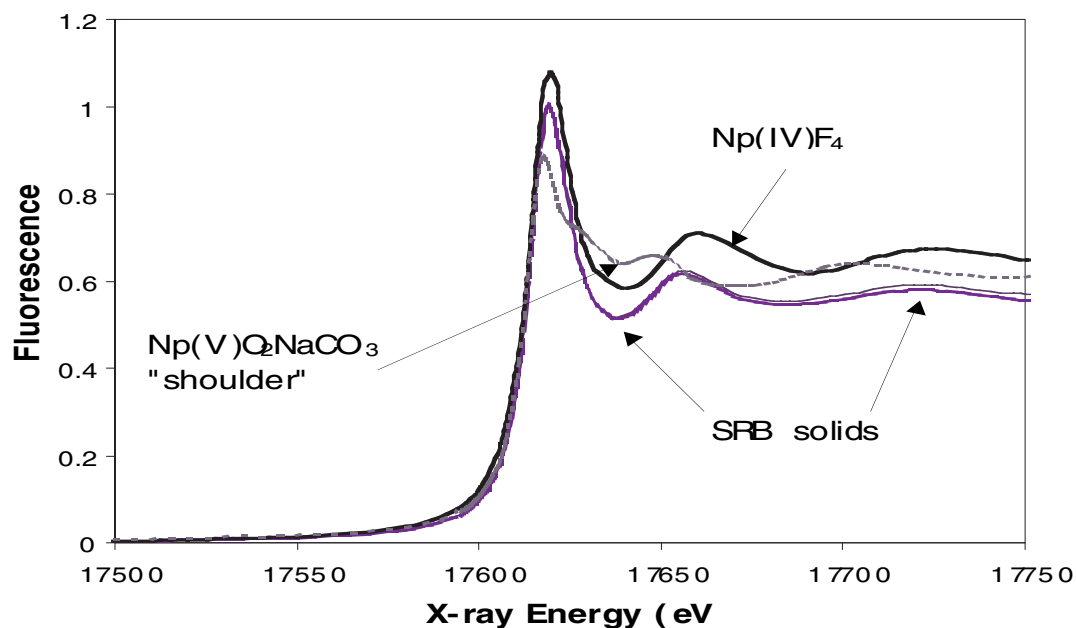
Actinide-microbiological studies of uranyl and plutonyl systems have also been completed. Pu(VI) is reduced under both aerobic and anaerobic systems to form low solubility Pu(IV) phases. We have not established uranyl reduction under aerobic conditions although uranyl precipitation is often noted. These results have also been confirmed by XANES analyses.

### Redox Effects of Organic Chelating Agents with Actinide

The important role of organic species in defining actinide speciation and mobility in subsurface is also beyond question. Organic species are present in the subsurface from both natural (e.g., hydro-geological and microbiological activity) and anthropogenic sources. Our research has focused on the role of anthropogenic organic complexants (e.g., edta, nta, citrate and oxalate) on actinide speciation and redox. Organic complexants directly affect the speciation of dissolved actinides in two ways. They can stabilize an oxidation state towards precipitation or reduction by forming complexes. The second, perhaps less recognized, effect is that many organic chelating agents reduce or facilitate the reduction of multivalent actinides.

The direct reduction of the higher oxidation states of multivalent actinides, not surprisingly, occurs rapidly under near-neutral conditions when the complexant is an amine. The oxidation state distribution, subsequent to reduction, however, depends on the stability of the various complexes formed, and complete reduction is not usually observed. The overall effect on redox, is not, however, straightforward, when the complexant is a carboxylic acid (e.g., oxalic and citric acid). Here the net reduction of the actinide depends on ligand/metal ratio, and radiolysis effects must be considered. So biodegradation of these organics will play a more important role in establishing their overall effect on actinide speciation.

Figure 1. Comparison of XANES spectra from neptunium precipitated during lactate fermentation by sulfate reducing bacteria to form Np(IV) phases with Np(V) and Np(IV) solid standards. The bio-precipitated neptunium spectra lack the near-edge shoulder associated with Np(V), confirming that Np(V) was reduced to Np(IV).



## Gas-Phase Plutonium Oxide Cluster Ions and Initial Actinide Ion Trapping Experiments\*

A thorough understanding of the chemistry of plutonium is needed to predict and manipulate environmental migration, degradation of stockpile and disposition forms, physiological effects, mixed-oxide (MOX) fuel behavior, etc. The complex chemistry of Pu is largely attributed to the accessibility of several common oxidation states, particularly Pu<sup>III</sup>, Pu<sup>IV</sup>, Pu<sup>V</sup> and Pu<sup>VI</sup>. Additionally, the quasi-valence 5f electrons can participate directly in bonding under suitable conditions, such as high atomic density or proximity to harmonious bonding partners. Although a plethora of solid compounds of Pu are known, the overall understanding of the nature of Pu bonding and reaction pathways is limited. Gas-phase reactions provide insights into fundamental chemistry; aspects of organoplutonium chemistry have been probed *via* studies of reactions between Pu<sup>+</sup> and organic molecules.<sup>1</sup> Lanthanide (Ln) studies<sup>2</sup> demonstrated that the compositions and abundance distributions of Ln<sub>x</sub>O<sub>y</sub><sup>+</sup> cluster ions were sensitive to the redox chemistry of the particular Ln—for example, divalent Eu and tetravalent Tb. In contrast to the predominantly trivalent Ln, the rich redox chemistry of Pu should be revealed in the formation of a variety of Pu<sub>x</sub>O<sub>y</sub><sup>+</sup> with diverse Pu oxidation states. Variations in chemistry among Pu<sub>x</sub>O<sub>y</sub><sup>+</sup> (and Pu<sub>x</sub>O<sub>y</sub>(OH)<sub>z</sub><sup>+</sup>) should illuminate interfacial and condensed phase processes. In the work described here, new plutonium oxide and oxyhydroxide cluster ions were synthesized by a technique previously applied to Ln<sub>x</sub>O<sub>y</sub><sup>+</sup>. In conjunction with this project, quadrupole ion trap (QIT) techniques are being developed to probe actinide atomic, molecular and cluster ion chemistries, and preliminary QIT results will be presented for uranium.

### Experiment

The actinide laser ablation mass spectrometry facility and *in situ* synthetic techniques employed to prepare Ln<sub>x</sub>O<sub>y</sub><sup>+</sup> have been described in detail,<sup>1,2</sup> and only a summary is included here. Cluster ions were produced by pulsed laser ablation of a Pu or Ce oxalate target and analyzed by a time-of-flight mass spectrometer. Based upon results for Ln<sub>x</sub>O<sub>y</sub><sup>+</sup>, f-element oxalates were selected as targets for the production of oxide cluster ions upon ablation into vacuum. The following hydrated oxalates were prepared by precipitation from chloride solutions: Pu<sup>III</sup><sub>2</sub>(C<sub>2</sub>O<sub>4</sub>)<sub>3</sub>-xH<sub>2</sub>O; Pu<sup>IV</sup>(C<sub>2</sub>O<sub>4</sub>)<sub>2</sub>-xH<sub>2</sub>O; Ce<sup>III</sup><sub>2</sub>(C<sub>2</sub>O<sub>4</sub>)<sub>3</sub>-xH<sub>2</sub>O; and Ce<sup>IV</sup>(C<sub>2</sub>O<sub>4</sub>)<sub>2</sub>-xH<sub>2</sub>O; the values of “x” were indeterminate, but x ≈ 10 for most Ln<sup>III</sup><sub>2</sub>(C<sub>2</sub>O<sub>4</sub>)<sub>3</sub>-xH<sub>2</sub>O. Cerium oxalates were studied because both Ce(III) and Ce(IV) are common oxidation states, and Ce is often employed as a surrogate for Pu. Whereas both the Pu(III) [yellow] and Pu(IV) [black] oxidation states were retained in air, Ce(IV) oxalate was rapidly reduced to Ce(III) oxalate. Greater cluster yields were obtained for Pu<sup>III</sup><sub>2</sub>(C<sub>2</sub>O<sub>4</sub>)<sub>3</sub>-xH<sub>2</sub>O compared with Pu<sup>IV</sup>(C<sub>2</sub>O<sub>4</sub>)<sub>2</sub>-xH<sub>2</sub>O, and most reported results are for the former. Targets were fabricated by compressing oxalate powders into small pellets.<sup>1,2</sup> A modified QIT with a glow discharge ion source was employed for the initial trapped uranium ion studies.

\*Research sponsored by Div. Chemical Sciences, U. S. Dept. of Energy, under Contract DE-AC0596OR22464 at Oak Ridge National Laboratory with Lockheed Martin Energy Research Corp.

John K. Gibson,  
Richard G. Haire,  
Douglas C. Duckworth  
Oak Ridge National  
Laboratory, Oak Ridge,  
TN, 37831-6375, USA

## Results and Discussion

Significant yields of  $\text{Pu}_x\text{O}_y^+$  and  $\text{Pu}_x\text{O}_y(\text{OH})_z^+$  were produced for values of  $x$  up to 6. The predominant ablated cerium oxide clusters were (average Ce valence in parentheses):  $\text{Ce}_2\text{O}_2^+$  (2.5);  $\text{Ce}_2\text{O}_3^+$  (3.5);  $\text{Ce}_3\text{O}_4^+$  (3.0); and  $\text{Ce}_3\text{O}_5$  (3.7). In contrast to the Ce results, a much wider variety of Pu clusters was produced in appreciable abundance, including several polyhydroxides and oxyhydroxides. A few of the more abundant Pu clusters were (average Pu valence in parentheses):  $\text{Pu}_2\text{O}_3^+$  (3.5);  $\text{Pu}_2\text{O}_2(\text{OH})^+$  (3.0);  $\text{Pu}_2\text{O}_4^+$  (4.5);  $\text{Pu}_2\text{O}_3(\text{OH})^+$  (4.0);  $\text{Pu}_2\text{O}_4(\text{OH})^+$  (5.0);  $\text{Pu}_3\text{O}_4^+$  (3.0);  $\text{Pu}_3\text{O}_5^+$  (3.7); and  $\text{Pu}_3\text{O}_6^+$  (4.3). As these representative small clusters illustrate, significantly higher valence states were obtained for Pu compared with Ce. The highest valence state definitively identified for Ce was +3.8 in  $\text{Ce}_4\text{O}_7^+$ , and that for Pu was +6.5 in  $\text{Pu}_2\text{O}_6^+$ . The highest common valence state of Ce is +4, and that of Pu is +6;  $\text{Pu}^{\text{VII}}$  can be produced under extreme conditions, and it is noteworthy that a the mixed valence species,  $\text{Pu}^{\text{VI}}\text{Pu}^{\text{VII}}\text{O}_6^+$  was identified here. Three primary differences between Pu and Ce cluster compositions and abundances were: 1) Pu produced clusters of a greater variety of compositions; 2) Pu clusters exhibited a tendency to incorporate hydroxide ligands; and 3) Pu clusters exhibited a wider range of average valences, notably valence states up to +6 and even +7. It is expected that future studies of actinide cluster synthesis and reactivity will provide new insights into fundamental chemistry and reaction pathways of central importance to understanding processes such as oxidation, hydrolysis and polymerization of Pu, and Pu-induced degradation of organics.

In distinct contrast to  $\text{Ln}_x\text{O}_y^+$ , where cluster ion intensities decreased monotonically with increasing values of  $x$ , small amounts of two “magic number” plutonium oxide clusters,  $\text{Pu}_{16}\text{O}_{22}\text{H}_z^+$  and  $\text{Pu}_{18}\text{O}_{23}\text{H}_z^+$  ( $z \approx 2$ ) were identified, well-isolated from the preceding largest cluster,  $\text{Pu}_6\text{O}_7(\text{OH})_2^+$ . Structures are proposed for these large clusters which might account for their special stabilities. Their formation suggests a link between the molecular and solid states, and provides a unique opportunity for examining the nature of bonding in plutonium molecules and solids.

A primary intent of this research program is to investigate the chemistries, stabilities and structures of actinide clusters. The laser ablation / time-of-flight approach is not particularly well-suited to this goal, and QIT techniques are being pursued to study mass-selected trapped actinide ions in a more controlled fashion. Preliminary results will be presented for reactions of atomic uranium and uranium oxide molecular ions with organic molecules such as pentamethylcyclopentadiene. Ultimately, the ability to produce, isolate and study Pu clusters of specific oxidation states and structures in the QIT should provide a powerful avenue to understanding valence and structural effects in Pu chemistry.

## References

1. J. K. Gibson, *J. Am. Chem. Soc.*, **120**, 2633 (1998).
2. J. K. Gibson, *J. Phys. Chem.*, **98**, 11321 (1994).

## Actinide Science with Soft X-Ray Synchrotron Radiation

The vacuum ultraviolet (VUV)/soft x-ray region of the synchrotron radiation (SR) spectrum that revolutionized the approach to surface materials chemistry/physics more than a decade ago, has long been recognized for its potential to investigate both fundamental and applied actinide science. Several workshops, some dating back fifteen years, have discussed the scientific impact that would be made possible by the capability to investigate actinides in this energy region but the actinide science community has been unable to take advantage of these SR methodologies, largely because of radiological safety concerns.<sup>1</sup> These safety issues stem from difficulties handling and preparing actinide materials in a manner compatible with experiments in ultra-high vacuum VUV/soft x-ray end stations. The advent of third-generation light sources operating in the VUV/soft x-ray region such as the Advanced Light Source (ALS) at LBNL, along with corresponding improvements in detector and vacuum technology, have made it possible to perform experiments with very small amounts of actinide material. Experimental safety considerations, based on a graded approach to hazard level and the use of actinide micro-samples, have enabled meaningful investigations to be performed.<sup>2-3</sup> Furthermore, the synchrotron radiation techniques used in this energy region also have matured, permitting more complicated investigations and enabling new spectroscopic approaches. Of particular importance are the microspectroscopy and spectromicroscopy capabilities that permit the handling of small amounts of actinide material and in addition, provide spatial information to complement the high resolution spectroscopic information.

The primary methods for the experimental investigation of actinide materials in the VUV/soft x-ray region are the complementary photoelectron spectroscopies, near-edge x-ray absorption fine structure (NEXAFS), and x-ray emission spectroscopy (XES) techniques. Resonant photoemission techniques capable of resolving the 5f electron contributions to actinide bonding along with angle-resolving measurements for band structure and surface structure determinations, have clear and immediate applications. Venerable angle-integrating core and valence band photoelectron spectroscopy are valuable for characterization and analytical purposes. Combined with results from NEXAFS measurements, these techniques will provide the information needed to develop improved understandings of the electronic structure of actinide materials and their surface chemistries/physics. A new and useful consequence of third generation source development is the renaissance of XES techniques in this energy region. XES is an atom specific probe, complementary to both photoemission and absorption, that is especially amenable to studies of buried, disordered, and bulk materials systems. All of these techniques yield experimental data that can be used within existing theoretical frameworks and efforts, as well as providing additional impetus to extend theoretical modeling methods with actinides into the soft x-ray region.

A significant amount of information about actinide materials chemistry and physics can be obtained from a comprehensive multi-technique approach in this energy region that will lead to an improved understanding of the materials. Examples from each of the aforementioned techniques, as applied to actinide materials, will be presented. Future scientific plans, directions (including the role of the ALS Molecular Environmental Science Beamline), approaches, and safety

**David K. Shuh**  
*The Glenn T. Seaborg  
Center, Lawrence  
Berkeley National  
Laboratory (LBNL),  
Berkeley, CA 94720,  
USA*



considerations for the investigation of actinide materials in this energy region will be discussed.

This work is supported by the Director, U.S. Department of Energy, Office of Science, Office of Basic Energy Sciences, Chemical Sciences Division and Materials Sciences Division under Contract No. DE-AC03-76SF00098.

### References

1. Perspective on the Use of Synchrotron Radiation in Transuranium Research, Workshop Report, Karlsruhe, Germany, (1985); Synchrotron Radiation in Transactinium Research, LBNL, LBNL Report-33049, Berkeley, CA, (1992); and Workshop on Scientific Directions at the Advanced Light Source: Summary and Reports of the Working Groups, LBNL Report-42014, July (1998).
2. D. K. Shuh, J. J. Bucher, N. M. Edelstein, A. Warwick, J. Denlinger, B. Tonner, E. Rotenberg, S. Kevan, and J. Tobin, Edited by A. Robinson, Researchers Use ALS for TRU Analysis, ER News, Office of Energy Research, U.S. Department of Energy, Vol. 4 (4) August (1994). pp. 4-6.
3. J. Terry, R. Schulze, J. Lashley, T. Zocco, J. D. Farr, E. Rotenberg, K. Heinzelmann, D. Shuh, M. Blau, and J. Tobin, Photoemission Studies at the Advanced Light Source Shed Light on Plutonium Phase Characteristics, Actinide Research Quarterly, Los Alamos National Laboratory, January (1999). pp. 1-3.

## Recent Achievements in the Development of Partitioning Processes of Minor Actinides from Nuclear Wastes Obtained in the Frame of the NEWPART European Programme (1996–1999)

Partitioning of long-lived minor actinides (americium and curium) from the nuclear wastes issuing from the reprocessing of nuclear spent fuels, in order to transmute them into short-lived nuclides, was the subject of intense research within the NEWPART research programme of the European 4<sup>th</sup> Frame Work Programme (1996–1999). The target waste considered was the acidic raffinate (HAR) issuing from the reprocessing of the used nuclear fuels by the PUREX process. A two-step separation process based on liquid-liquid extraction was designed. The first step consists of the co-separation of the mixture of trivalent actinides and lanthanides from the HAR by extraction with a malonamide extractant (DIAMEX process), while the second step relies on the actinides(III)/lanthanides(III) group separation (SANEX) process.

Several DIAMEX and SANEX processes were developed and successfully tested with cold, spiked and genuine high active effluents. The research carried out also included basic and fundamental work in order to better understand the relationships between the structures of the extractants and their affinities for the target metal ions. The lecture will highlight both the basic and applied aspects of the research.

**C. Madic**

*CEA/Saclay, France*

**M. J. Hudson**

*University of Reading,  
Reading, UK*

**J. O. Liljenzin**

*Chalmers University of  
Technology, Göteborg,  
Sweden*

**J. P. Glatz**

*ITU, JRC, Karlsruhe,  
Germany*

**R. Nannicini**

*ENEA, Ispra, Italy*

**A. Fraccini**

*Politecnico di Milano,  
Milano, Italy*

**Z. Kolarik**

*INE, KfK, Karlsruhe,  
Germany*

**R. Odoj**

*ISR, FZJ, Juelich,  
Germany*

## Actinide Chemistry: From Test Tube to Billion Dollar Plant – A BNFL Perspective

**Peter Parkes**  
*Research &  
Technology, British  
Nuclear Fuels plc,  
Sellafield, Seascale,  
Cumbria, CA20 1PG,  
England.*

British Nuclear Fuels (BNFL) is currently operating its third generation of nuclear plant for the management of irradiated nuclear fuel. Development for the fourth generation plant must meet requirements for processing higher burn-up fuel with lower unit costs, lower environmental impact, better process control, and more flexible control of actinides.

There is an ongoing need for focussed research and development on actinide chemistry to meet today's challenges for safety, process control, environmental impact, and cost reduction. Historically, nuclear research has been carried out in government organisations with huge levels of funding of similar magnitude to the facility costs themselves, often greater than a billion US dollars! BNFL on the other hand, is run as a private company and must fund research from its own profits and reserves. On the face of it, it cannot compete in resources with national laboratories. Experience has shown, however, that BNFL is unique in having within its organisation all aspects of the fuel cycle at all steps of the life cycle, from research through to decommissioning, feedback and organisational learning. This breadth then compensates for lower levels of funding. The role of research into actinide chemistry to help meet these challenges is described in broad detail, covering ligand design and selection, experimental determination of equilibria and kinetics, process modelling, and small-scale demonstration of active flowsheets.

## Robust Membrane Systems for Actinide Separations

A membrane is a semi-permeable structure separating two phases that can operate as an active or passive barrier to the transport of matter between the phases. The membrane can discriminate between the components of the phases based on differences in one or more properties of the components such as size, shape, electrical charge, solubility and diffusion rate. The resulting separation achieved by a membrane system is a function of both thermodynamic partitioning and kinetics. Control of the interaction of these features provides a wide range of separation possibilities with membranes, but is difficult to achieve in practical applications. Robust membrane systems that accomplish precise separations based on chemical properties would allow membrane separation technology to reduce separation costs for a much wider range of industrial needs, including many separation challenges faced by the U.S. Department of Energy.

Our focus in this effort is on membranes for selective separation of metal ions from solution. Supported liquid membranes (SLMs) have been investigated for many years to selectively separate metal ions and other species from aqueous solutions. The preparation of an SLM essentially involves placing a liquid-liquid extraction system into the pores of a thin membrane support. A carrier molecule dissolved in the organic layer contained in the pores acts as a shuttle for metal ions between an aqueous feed solution on one side of the membrane and an aqueous receiving solution on the other side. The SLM systems have illustrated that the selective chemistry developed for liquid-liquid extraction of metal ions could be applied in a membrane format, but the poor long-term stability of the SLMs has inhibited their industrial application. A number of approaches to mitigate the stability problem have been attempted, but none have yet been a significant commercial success. Our objective in this project is to develop very stable thin membrane structures containing ionic recognition sites that facilitate the selective transport of target metal ions, especially the actinides.

Most prior work with facilitated transport membrane systems has employed organic polymer membranes with pores that are generally variable in size, tortuous in shape, difficult to characterize and unstable under harsh conditions. The hybrid materials that we prepared eliminate or reduce many of these difficulties by using inorganic porous substrates that have rigid, uniform pore structures. We deposit a thin layer of metal or metal oxide onto the porous substrate to a prescribed depth. Selective receptors are attached to this coating. In this way, we can precisely control the thickness of the active membrane layer, a key factor in determining flux rates. The active layer must prevent nonselective convective flow through the pores, but be as thin as possible to maximize the rate of facilitated transport. Systematic chemical modification of this active layer enables us to perform experiments to define the mechanisms of transport.

For example, thin layers of gold (300-1000 Å) were deposited on commercial porous alumina supports. A self-assembled monolayer of a thiol compound was then attached to the gold surface. An SLM was prepared by dissolving an extractant such as tributylphosphate or trioctylphosphine oxide in the thiol layer.

For measuring metal ion transport rates the membrane was clamped in a holder where the membrane separated two compartments. One of the compartments

Gordon D. Jarvinen,  
T. Mark McCleskey,  
Elizabeth A. Bluhm,  
Kent D. Abney,  
Deborah S. Ehler,  
Eve Bauer,  
Quyen T. Le,  
Jennifer S. Young,  
Doris K. Ford,  
David R. Pesiri,  
Robert C. Dye,  
Thomas W. Robison,  
Betty S. Jorgensen,  
Antonio Redondo,  
Lawrence R. Pratt,  
Susan L. Rempe  
*Los Alamos National  
Laboratory, Los  
Alamos, NM 87545,  
USA*

contained a feed solution that initially contained the salt of the metal ions of interest. The second compartment contained a receiving solution of equal volume. The rate of diffusion of the metal ions from the feed to the receiving solution was measured as a function of time. The driving force for moving the ions across the membrane was the chemical potential gradient. The transport of uranium was measured between a feed solution of uranium(VI) in 1 M potassium nitrate at pH 4 and a receiving phase of sodium acetate/acetic acid at pH 5. Initial flux rates of up to  $5 \times 10^{-9}$  moles U/cm<sup>2</sup>-sec were observed. These flux rates are higher than flux rates for uranium(VI) reported for various SLM systems in the literature. Similar studies are in progress with plutonium and other metal ions. Further work will compare transport in related fixed-site carrier membranes where a phosphoryl donor group is incorporated into the thiol compound forming the self-assembled monolayer. Increased understanding of the mechanisms of metal ion transport will allow further development of these promising membrane separation systems.

## New Nuclear Safe Plutonium Ceramic Compositions with Neutron Poisons for Plutonium Storage

A complex of works is conducted to study the possibility of reprocessing surplus weapon-grade plutonium to a critical-mass-free composition with neutron poison. Nuclear safe ceramic compositions of  $\text{PuO}_2$  with four most efficient neutron poisons, Hf, Gd, Li, and B, are fabricated in the laboratory. Various methods for fabrication of the compositions with  $\text{PuO}_2$  depending on neutron poison element are used and studied: a - by sintering initial component powders; b - by impregnation of a porous skeleton made of neutron poison oxide with plutonium sol-gel; c - by sintering microspheres made of plutonium oxide with neutron poison ( $\text{B}_4\text{C}$ ), with the microspheres having a coating completely absorbing alpha particles.

Compositions of  $\text{PuO}_2$  with  $\text{HfO}_2$ ,  $(\text{Hf}, \text{Y})\text{O}_2$  produced by sintering of powders (homogeneous type ceramics) or by impregnation of a porous skeleton made of  $\text{HfO}_2$  with plutonium oxide sol-gel (homogeneous-heterogeneous type ceramics) are studied most comprehensively. The method for producing plutonium oxide, carbonating or burning responsible for oxide purity degree is shown not to influence the ceramics sinterability at a given ratio of plutonium and neutron poison, which is 1/7-8. At this atom ratio the sintering of two oxides,  $\text{HfO}_2$  and  $\text{PuO}_2$ , results in a two-phase structure, the sintering of three oxides,  $\text{HfO}_2$ ,  $\text{Y}_2\text{O}_3$ , and  $\text{PuO}_2$ , leads to triple solid solution of the cubic structure, which is usually considered as most stable in regard to radiation.

The minimum content of  $\text{Y}_2\text{O}_3$  for obtaining the cubic structure is estimated. Quite high-quality samples of various density and porosity were obtained depending on sintering conditions (medium: oxidizing-reducing, oxidizing, vacuum; temperature, time), powder fraction composition, etc. Studying the role of porosity may be of interest to assess the radiation behavior during the composition storage. Coprecipitated powders of Pu, Hf, and Y oxides are shown to provide faster sintering at temperatures lower by 200-300°C, than mechanically mixed powders. The produced samples were of a high quality in homogeneity and component distribution uniformity.

The method for composition production by impregnation of a porous skeleton fabricated from hafnium oxide of monoclinic or cubic structure with plutonium oxide sol-gel is studied. Activated sintering of certain fraction composition hafnium oxide powders was used to produce porous material of certain sizes and quantity of pores to introduce a given quantity of plutonium oxide sol-gel. The technique for porous sample impregnation with sol of various plutonium oxide content is verified.

A method for fabrication of a skeleton from hafnium oxycarbide of porosity suitable for impregnation with a given quantity of plutonium sol-gel is developed and the skeleton is produced. The method is environmentally safest in view of separate skeleton manufacture and plutonium sol production.

Fairly strong samples are produced by sintering of  $\text{PuO}_2$  microspheres, coated with a titanium oxide layer to absorb a particles, with  $\text{B}_4\text{C}$ . Compositions of protective coatings (of enamel types) are verified for the samples fabricated. The method is suitable for using inexpensive efficient boron carbide neutron poison

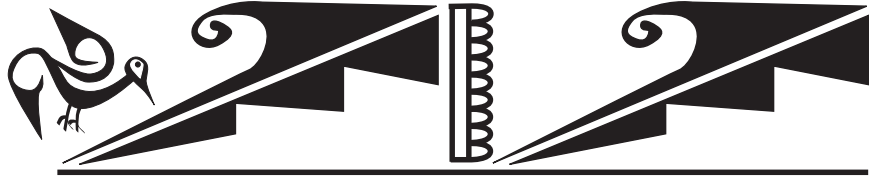
**B. A. Nadykto**  
RFNC-VNIIEF,  
Arzamas-16 (Sarov),  
Nizhni Novgorod  
region, 607190

**L. F. Timofeeva**  
GSCRF-VNIINM,  
Moscow, 123060

within a heterogeneous composition with  $\text{PuO}_2$ . A demerit is the need to apply coating on the microspheres to avoid reaction  $\alpha \rightarrow n$  and the complexity of boron carbide sintering.

The study resulted in the determination of the phase and element composition, structure and physical and mechanical characteristics of the fabricated compositions. The study of composition behavior during storage using the X-ray-structural analysis methods and the positron annihilation method detected changes in oxide lattice parameters and annihilation characteristics due to radiation defect accumulation.

Sintering of compounds  $\text{Li}_2\text{HfO}_3$ ,  $\text{Li}_4\text{SiO}_4$ , and  ${}^6\text{Li}_4\text{SiO}_4$ , produced in the laboratory as well as  $\text{Gd}_2\text{O}_3$  and their compositions with  $\text{PuO}_2$ , where the ratio of plutonium and neutron poisons secures critical-mass-free status of the system, is studied. Good quality samples are produced, and their structure and phase composition are studied. Some of their properties are determined. Some features in structure and phase formation are detected. The sintering of  $\text{Li}_2\text{HfO}_3$  and  $\text{PuO}_2$  results in monoclinic  $\text{HfO}_2$  and cubic  $(\text{Hf}, \text{Pu})\text{O}_2$ ; no lithium containing phase is detected. The sintering of  $\text{Gd}_2\text{O}_3$  and  $\text{PuO}_2$  leads to formation of two solid solutions based on  $\text{Gd}_2\text{O}_3$  and  $\text{PuO}_2$ .



## **Actinides/TRU Wastes**





## Theoretical Predictions of Hydrolysis and Complex Formation of the Heaviest Elements

Studying hydrolysis is one of the most important tasks in solution chemistry of actinides and transactinides since hydrolysis is known to influence such important aspects of chemical behavior as adsorption of the dissolved metals on surfaces of mineral particles, the solubility of oxides and hydroxides or the extent to which the metal can be complexed in solution or extracted from solutions by various agents. It is also a challenge to find an adequate theoretical description of a real process taking place in a complex aqueous media. In the presentation, investigations of hydrolysis and complex formation of group 4, 5 and 6 elements, including the transactinide elements 104, 105 and 106 are described. They were carried out on the basis of results of relativistic calculations of the electronic structure of various hydrated, hydrolyzed and complex compounds of these elements using the fully relativistic *ab initio* density functional method with the GGA approximation for the exchange-correlation potential.<sup>1</sup> Predictions of equilibria of hydrolysis or complex formation reactions have been made using a model which enables determination of free energy changes of the reactions as changes in the ionic and covalent contributions to the binding molecular energy separately. Those contributions were calculated using the Mulliken analysis of the electronic density distribution. Changes in the entropy were also taken into account.

Results of these investigations have shown the changes in the free energy of a hydrolysis reaction to be defined by predominant changes in the ionic (Coulomb) part of the binding molecular energy. Thus, in going over from the 5d transition elements to the 6d elements (transactinides), electrostatics still define the hydrolysis process. Nevertheless, the application of the simple ionic model using formal ionic charges is limited to the 5d elements as the heaviest, and for the more heavy elements, real effective charges must be used calculated via relativistic molecular codes.

The investigations have shown the hydrolysis of the transactinides with the final formation of neutral complexes to follow trends found within lighter homologs in the chemical groups. However, the formation of complexes with electronegative ligands (also with O meaning a further hydrolysis) results in reversed trends in the chemical groups. Thus, hydrolysis of group 6 cations with the formation of the  $\text{MO}_2(\text{OH})_2(\text{H}_2\text{O})_2$  species has the following order:  $\text{Mo} > \text{W} > 106$ . Further hydrolysis with the formation of the negative complexes  $\text{MO}_4^{2-}$  results in a reversal of the trend from W to Sg:  $\text{Mo} > 106 > \text{W}$ . The former sequence was confirmed experimentally by elution of W and Sg from the cationic chromatography column.<sup>3</sup>

A similar reversed trend,  $\text{Pa} > \text{Nb} > 105 > \text{Ta}$ , was predicted for the formation of oxochloro complexes of group 5 elements, Nb, Ta, element 105, and Pa in aqueous HCl solutions.<sup>2</sup> This trend was obtained by calculating the free energy changes of complex formation reactions versus hydrolysis of the complexes. The same trend was predicted for the complex formation of these elements in HF and HBr solutions. This sequence was later confirmed experimentally by extraction of the complexes of group 5 elements and Pa into an aliphatic amine.<sup>4,5</sup>

V. Pershina  
Institut für  
Kernchemie,  
Universität Mainz,  
D-55099 Mainz,  
Germany

Present theoretical investigations being in agreement with the experimental findings have given strong evidence that in the area of very heavy elements with strong relativistic effects any straightforward extrapolations of the properties could result in erroneous conclusions. Therefore, fully relativistic schemes with the best correlation are highly desirable for an adequate description of the systems in the area with high  $Z$  numbers.

### References

1. S. Varga, *et al.*, *J. Chem. Phys.*, in press.
2. V. Pershina, *Radiochim. Acta*, 80, 65 (1998).
3. M. Schädel, *et al.*, *Radiochim. Acta*, 83, 163 (1998).
4. W. Paulus, *et al.* *Radiochim. Acta*, 84, 69 (1999).
5. V. Pershina and B. Fricke, in *"Heavy Elements and Related New Phenomena"*, Ed. W. Greiner and R. J. Gupta, Singapore Scientific, 1999, p. 194.

## New Field of Actinides Solution Chemistry: Electrochemical Study on Phase Transfer of Actinide Ions across Aqueous/Organic Solutions Interface

The main research field of actinides solution chemistry has been related to the development of separation and analytical methods of actinide ions. There are recent studies on a novel electrolytic separation method<sup>1)</sup> and an electrochemical ion-sensor technique,<sup>2)</sup> both of which are based on ion transfer reaction at the interface of two immiscible solution phases. Fundamental electrochemistry of the phase transfer for actinide ions, however, has not been studied extensively. In this presentation, the author will describe (i) the ion transfer reaction of actinide(An) ions such as  $An^{3+}$ ,  $An^{4+}$ ,  $AnO_2^+$  or  $AnO_2^{2+}$ , where An = U, Np, Pu, across the aqueous(*w*)/organic(*org*) solutions interface and (ii) the development of an electrolytic ion separation method as well as actinide-ion selective electrode( $An^{n+}$ -ISE) on the basis of the ion transfer reaction.

The ion transfer of  $An^{n+}$  at the *w*/nitrobenzene(*NB*) interface was investigated by voltammetry using a stationary interface electrode or polarography with an aqueous electrolyte dropping electrode<sup>3)</sup>, by which the relation between the interfacial potential( $\Delta V$ ) corresponding to the transfer energy and current(*I*) corresponding to the amount of transferring ion( $\Delta V$ -*I* curve) were recorded. Crystalviolet-tetraphenylborate( $CV^+TPhB^-$ ) and  $NH_4Cl$  or  $(NH_4)_2SO_4$  was used as a supporting electrolyte of *NB* and *w*, respectively.

In order to facilitate the transfer of  $An^{n+}$  from *w* to *NB*, multidentate phosphine oxide derivative was used as an ionophore in the present work. For the measurement of ion transfer reaction of such radioactive elements as actinides, a new method, i.e., radio-voltammetry for ion transfer at the interface of immiscible electrolyte solutions (RVITIES), was developed and applied to the measurement of the relation between  $\Delta V$  and the amount of ions transferred(*A*) ( $\Delta V$ -*A* curve). The  $\Delta V$ -*A* curve was obtained by performing controlled-potential electrolysis using a stationary *w*/*NB* interface electrode system with mixing the interface by turbine and then determining *A* from the measurement of the radioactivity of each phase.

Actinide ions are highly hydrophilic, and the ion transfer of  $An^{n+}$  from *w* to *org* hardly occurs. For the voltammetric study of ion transfer of such hydrophilic ions, a neutral carrier-type ligand that forms a stable complex with  $An^{n+}$  is added to *org* as an ionophore to facilitate the ion transfer. Anodic waves due to the facilitated transfer of  $UO_2^{2+}$  or  $Pu^{3+}$  were clearly observed in the voltamograms and polarograms recorded with *NB* containing bis(diphenylphosphoryl)methane (BDPPM). From the comparison of the ion transfer potentials of  $An^{n+}$  with and without BDPPM, it was concluded that the transfer of  $UO_2^{2+}$  or  $Pu^{3+}$  from *w* to *NB* was largely facilitated by BDPPM. The  $UO_2^{2+}$  or  $Pu^{3+}$  transfer reaction is of irreversible characteristics, which is attributable to slow processes involved in the ion transfer reaction such as adsorption/desorption of BDPPM or metal-BDPPM complex at the *w*/*NB* interface. The polarographic half wave potentials( $\Delta V_{1/2}$ ) for the transfer of  $UO_2^{2+}$ ,  $NpO_2^+$  and  $Pu^{4+}$  with *w* of 0.1 M  $(NH_4)_2SO_4$  + 0.1 mM  $An^{n+}$  and *NB* of 0.05 M  $CV^+TPhB^-$  + 5 mM BDPPM were -60,  $\geq +106$  and  $\geq +86$  mV (vs.  $TPhE^3$ ), respectively.  $UO_2^{2+}$  transfers efficiently from *w* to *NB* by the electrolysis at more positive potential than  $DV_{1/2}$  of  $UO_2^{2+}$ , e.g. +30 mV. The controlled-potential electrolysis with stationary *w*/*NB*

Yoshihiro Kitatsuji,  
Hisao Aoyagi,  
Zenko Yoshida  
Advanced Science  
Research Center,  
Japan Atomic Energy  
Research Institute  
Tokai, Ibaraki  
319-1195, Japan

Sorin Kihara  
Kyoto Institute of  
Technology  
Matsugasaki, Sakyou-  
ku, Kyoto 606-8585,  
Japan

interface electrode at +30 mV was performed using 0.2 M H<sub>2</sub>SO<sub>4</sub> solution containing 1 mM UO<sub>2</sub><sup>2+</sup> and NB containing 5 mM BDPPM, and it was found that ≥99% of UO<sub>2</sub><sup>2+</sup> transferred into NB by the electrolysis for 15 min. The electrolytic ion separation method has advantages: an addition of a relatively high concentration of hydrophobic counter anion, indispensable for a conventional ion-pair solvent extraction, is not necessary, and the selectivity can be enhanced by precise control of the electrolysis potential.

The fundamental data of An<sup>n+</sup> transfer reaction also led to the development of an ion sensor which is sensitive to An<sup>n+</sup>. In principle, a potential generating at the ion selective electrode(ISE) of a liquid-membrane type corresponds to the *w/org* interfacial potential when the interface is fully depolarized by the ion-transfer. According to this concept of the ISE potential and based on the Pu<sup>3+</sup> facilitated transfer data, Pu<sup>3+</sup>-ISE employing BDPPM ionophore was developed. The ISE cell configuration is

SSE1	1 mM Pu <sup>3+</sup> (HCl solution inner solution	1 mM Pu(BDPPM)3•3TPhB + 10 mM BDPPM (liquid membrane)	10 <sup>-9</sup> 10 <sup>-1</sup> M Pu <sup>3+</sup> test solution	SSE2
------	--	--	---	------

SSE: silver/silver chloride electrode.

The Pu<sup>3+</sup>-ISE exhibited Nernstian response to 1×10<sup>-7</sup> - 1×10<sup>-2</sup> M Pu<sup>3+</sup> in 1 mM HCl medium as the most optimum condition. It was confirmed that 10 times the concentration of UO<sub>2</sub><sup>2+</sup> did not disturb the potential for 1×10<sup>-6</sup> M Pu<sup>3+</sup>. Though the selectivity of the Pu<sup>3+</sup>-ISE developed is still insufficient for its application to the direct speciation of Pu ion, an employment of a new ionophore is expected to enhance the selectivity as well as the sensitivity of the ISE. Sensitivity and a wide dynamic operating range of ISE are usually sufficient for most analytical applications.

The facilitated ion transfer of An<sup>n+</sup> was observed in the presence of ionophore as described above. On the other hand, the studies of the ion transfer without ionophore, i.e., single ion transfer, are also important. These studies clarify the facilitated ion transfer phenomena and give fundamental information on hydration, solvation or coordination of An<sup>n+</sup> in solutions.

In ΔV-I curves observed by conventional voltammetry of polarography, a wave corresponding to the ion transfer of An<sup>n+</sup>, which is highly hydrophilic, is not observed clearly due to residual current corresponding to the transfer of ion(s) of supporting electrolyte(s). In this study the novel method RVITIES was proposed. This method provides several advantages: (i) even at the potential where a large residual current flows the DV-A curve can be obtained, (ii) ion transfer of such low concentration as tracer level can be measured, and (iii) this method can be applied to fully irreversible ion transfer reaction. The relation between DV and A is expressed as

$$\Delta V = -\Delta G_{tr}^0 / zF + (RT/zF)\ln[A/(A_o - A)] + (RT/zF)\ln(v_w/v_{org}) ,$$

where  $\Delta G_{tr}^{0'}$  and  $v$  are the ion transfer free energy and the volume of the individual phase for controlled-potential electrolysis, respectively.  $A$  and  $A_0$  are radioactivities in *org* after the electrolysis and in *w* before the electrolysis. This RVITIES was applied to the measurement of  $\Delta G_{tr}^{0'}$  of  $An^{n+}$ .

### References

1. Y. Kitatsuji, H. Aoyagi, Z. Yoshida and S. Kihara, *Anal. Sci.*, 14, 67 (1998).
2. Y. Kitatsuji, H. Aoyagi, Z. Yoshida and S. Kihara, *Anal. Chim. Acta*, 387, 181 (1999).
3. S. Kihara, M. Suzuki, K. Maeda, K. Ogura, S. Umetani, M. Matsui and Z. Yoshida, *Anal. Chem.*, 58, 2954(1984).

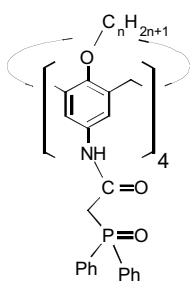
## Extraction of Lanthanides and Actinides from H. A. Waste by Calix[4]arenes Bearing CMPO Units

J. F. Dozol,  
A. Garcia Carrera,  
H. Rouquette  
DCC / DESD / SEP /  
LPT E CEA  
Cadarache 13108  
Saint Paul Lez  
Durance (France)

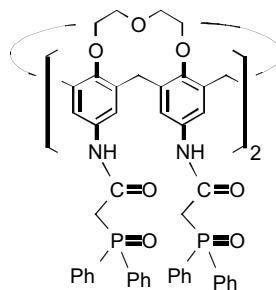
The decategorisation of radioactive liquid waste by removal of  $^{90}\text{Sr}$ ,  $^{137}\text{Cs}$  and actinides (allowing the waste to be sent to a surface disposal after conditioning) or the separation of these long lived nuclides from solutions arising from the PUREX process (in order to destroy them by transmutation or to isolate them in high integrity matrixes) need very specific extractants.

Carbamoylmethyl phosphine oxides are excellent extractants for actinides, especially the (N,N-di-isobutylcarbamoylmethyl) octyl phenyl phosphine oxide used in the TRUEX process. The species extracted contains three CMPO molecules per actinide cation. Thus, it seemed interesting to attach, in a suitable way and on an appropriate platform, three (or more) functional groups of the CMPO type, to better complex the trivalent cations.

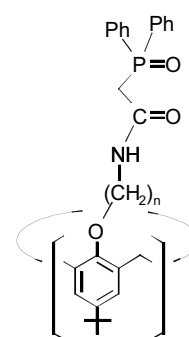
Calixarenes represent a class of cyclic oligomers which are easily available in larger quantities and offer also nearly unlimited possibilities of chemical modification. Especially calix[4]arenes have been used in numerous ways as such a basic platform on which ligating functions can be assembled. Calixarenes bearing CMPO moieties on the wide rim and different alkyl chains (length of alkyl chain ranges from  $\text{CH}_3$  to  $\text{C}_{18}\text{H}_{37}$ ) on the narrow rim were prepared. Compound (R =  $\text{C}_5\text{H}_{11}$ ) was chosen to study the extraction efficiencies of wide rim CMPOs towards nine lanthanides and two actinides (Am, Cm). CMPO, in a concentration 250 fold higher, displays comparable distribution coefficients with cyclic calixarene or acyclic tetramer. Moreover, a strong decrease of the distribution coefficients along the lanthanide series, from 140 for lanthanum to 0.19 for ytterbium was found, which corresponds to a separation factor of nearly three orders of magnitude. CMPO and tetramer displayed a much less pronounced selectivity. This efficiency and selectivity enhancement evidences the role of the preorganisation induced by the calixarene structure.



Calixarenes bearing CMPO units on the wide rim.



Stiff calixarenes.



Calixarenes bearing CMPO units on the narrow rim.



Stiffening of the previously described calixarenes was obtained from calix[4]arene bis crown ether in which adjacent oxygen atoms are bridged at the narrow rim by two diethylene glycol linkers. This stiffening increases the extraction of cations (distribution coefficients higher than 100 are obtained with this rigid calixarene used at a concentration  $10^{-4}\text{M}$ ); however, the more pronounced preorganisation of CMPO ligands in this compound does not change significantly the discrimination of lanthanides.

Another class of calixarenes was synthesised by including CMPO units on the narrow rim of calixarene. Several calixarenes were synthesised with arms bearing CMPO moieties of different length ( $n = \text{C}_2\text{H}_5$  to  $\text{C}_5\text{H}_{11}$ ). For this class of calixarenes, the extracting ability is lower than that displayed by the previous class. One has to point out that a marked maximum of extraction is achieved for calixarene with a spacer including three carbon atoms and that the selectivity order changes with the spacer length. Several other compounds with phosphoryl units (phosphinate or phosphonate) were synthesised. Although their efficiency is lower than that displayed by phosphine oxide moieties, they extract lanthanides and actinides more efficiently than CMPO.

Currently, the selective extraction of actinides from liquid waste arising from the PUREX process and containing almost all of the totality of the fission products, requires two steps: one to separate actinides and lanthanides from most of the other fission products, another for the separation of actinides from lanthanides. With CMPO calixarenes, in only one step, it is possible to separate actinides from the whole of the fission products except for the lightest lanthanides.

## Two New Insoluble Polymer Composites for the Treatment of LLW: 1. Polypyrrole Doped by $\text{UO}_2^{2+}$ Complexing Polyanions 2. $\text{UO}_2^{2+}$ Complexing Sol-gel Based Composites. Stability Constants. Leaching Tests, Alpha and Gamma Irradiation

D. Leroy, L. Martinot,  
P. Mignonsin,  
F. Caprasse,  
C. Jérôme,  
R. Jérôme  
University of Liège,  
4000 Liège, Belgium

In a previous work,<sup>1</sup> we have demonstrated that polyanions like polyacrylamidoglycolic acid (PAAG) and polyacrylamidomethylpropanesulfonic acid (PAMPS) are capable to complex  $\text{UO}_2^{2+}$  ions. Unless they are crosslinked, these polyanions/ $\text{UO}_2^{2+}$  complexes are soluble when submitted to dynamic leaching tests in a Soxhlet extractor. Considering the feasibility of a new process for the storage or for the concentration of low level activity liquid wastes (LLW), we had to strongly enhance the insolubility of these complexes. We have developed two original insolubilization ways, as compared to the crosslinking of the polymer.

### Polypyrrole Doped by $\text{UO}_2^{2+}$ Complexing Polyanions

PAAG and PAMPS polyanions are doping agents of the polycationic polypyrrole (PPy) leading so to an interesting composite structure. Indeed, polypyrrole is completely insoluble in water and, moreover, it is very resistant against leaching in concentrated nitric acid. These properties enhance noticeably the insolubility of the PAMPS/ $\text{UO}_2^{2+}$  and PAAG/ $\text{UO}_2^{2+}$  complexes due to both the electrostatic interactions  $\text{PPy}^+$ /polyanion and to the physical entanglement into the insoluble polycationic chains of PPy.

Moreover, since PPy is an electrically conducting polymer, the electrochemical preparation of the PPy based composites allows the achievement of either thin layers strongly adhering onto the electrode or bulky materials, only by controlling the electrolysis time. This electrochemical process would allow the covering of grids or other supports used in actinide solutions to be treated.

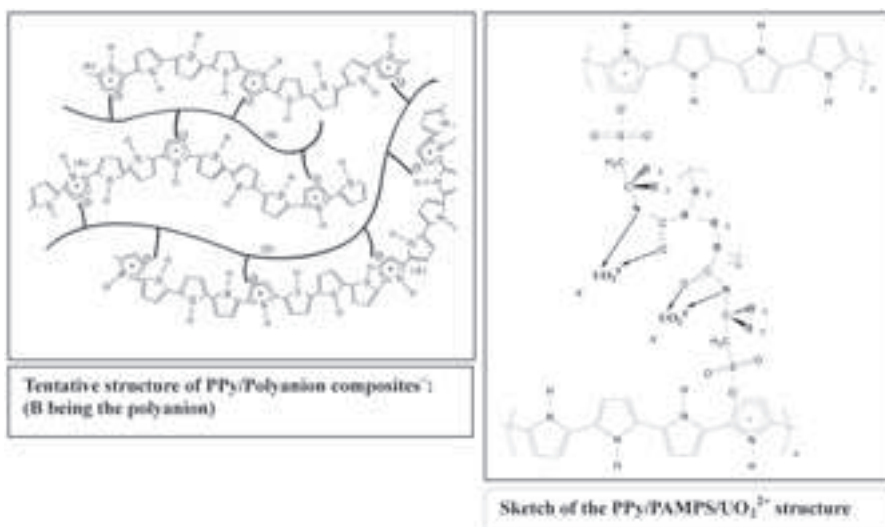
We have determined the level of doping agent and uranyl incorporation into the composites by Rutherford backscattering analysis (RBS), by alpha-counting analysis and also by calcination of the complexes (recovery of uranium oxides). A uranyl content as high as 60 weight % was gained for the PPy/PAAG/ $\text{UO}_2^{2+}$  thin layer composite.<sup>2</sup>

The main complexing interaction proceeds through the secondary amide function of the two polyanions as depicted below for the PPy/PAMPS/ $\text{UO}_2^{2+}$  complex.

### $\text{UO}_2^{2+}$ Complexing Sol-gel Based Composites

Acrylamide, a uranyl complexing monomer, was copolymerized with a triethoxy silane acrylate and acrylamide derivatives. These copolymers were, in turn, reacted with tetraethyl orthosilicate. The final product was a sol-gel powder or film. These sol-gel products are known to be of a nanometric scale, making them appropriate candidates for separation processes.<sup>3</sup>

Similarly to the PPy based composites, we studied the complexation capacity, leaching tests resistance and separation properties.



### Stability Constants

Stability constants for the reaction of complexation between  $\text{UO}_2^{2+}$  and the complexing polymers were gained by an electrochemical technique. Measurement of the shift of the totally reversible reduction wave of  $\text{UO}_2^{2+} / \text{UO}_2^+$  towards more cathodic value in presence of the complexing polymer was ascertained by using differential pulse polarography. This shift allows calculation of stability constants.

The results allow us to draw up a theoretical stability scale which corroborate the results obtained from dynamic leaching tests in soxhlet extractor.

### Resistance of the Composites to Gamma and Alpha Irradiations

There is a lack of data concerning the behaviour of the complexing polymers against irradiation. We have submitted the powdery materials to a gamma irradiation ( $^{137}\text{Cs}$ , 4000 Curies). The absorbed dose rose from  $10^6$  to  $2 \cdot 10^6$  Grays. These irradiations and the subsequent analyses showed a very good resistance of the polymers and the persistency of the uranyl complexing capacity, evidencing so their relevance in the treatment or storage of LLW.

In complementary experiments, the complexing materials were used to fix  $^{233}\text{U}$ , in order to achieve an alpha internal irradiation. The evolution of the release of U in function of the leaching time was followed and found different from the release curve of  $^{238}\text{U}$ .

The PPy based composites electrodeposited as thin layers (100 nm to 2  $\mu\text{m}$ ) were also irradiated by an alpha  $^{241}\text{Am}$  source. Electrochemical and spectroscopic investigations on the irradiated films do not reveal structural damaging.

### References

1. D. Leroy, L. Martinot, C. Jérôme, R. Jérôme, J. Radioanal. Nucl. Chem, 240, 3, 867 (1999).
2. D. Leroy, L. Martinot, M. Debecker, D. Strivay, G. Weber, C. Jérôme, R. Jérôme, accepted for publication in Journal of Applied Polymer Science.
3. J. C. Broudic, O. Conocar, J. E. Moreau, D. Meyer, M. Wong Chi Man, J. Mater. Chem, 1999, 9, 2283.

# Waste Forms from the Electrometallurgical Treatment of DOE Spent Fuel: Production and General Characteristics

**R. W. Benedict,  
S. G. Johnson,  
D. D. Keiser,  
T. P. O'Holleran,  
K. M. Goff**  
*Argonne National  
Laboratory-West  
Idaho Falls, ID 83403,  
USA*

**S. McDeavitt,  
W. Ebert**  
*Argonne National  
Laboratory-East  
Argonne, IL 60439,  
USA*

## Introduction

The Department of Energy (DOE) is proposing to use electrometallurgical technology to treat sodium-bonded spent nuclear fuel that has accumulated from decades of advanced reactor research and development. During a three-year testing program that was completed in August 1999, the technology was demonstrated on a small fraction, 3 metric tons, of the Experimental Breeder Reactor-II (EBR-II) sodium-bonded spent nuclear fuel at Argonne National Laboratory-West (ANL-West).<sup>[1, 2]</sup>

Two types of EBR-II fuel were used in the demonstration, driver and blanket. The driver fuel was uranium-10 wt. % zirconium clad with stainless steel. The spent driver fuel used in the demonstration had an average initial enrichment of approximately 67% and a typical burnup of about 8%. The blanket fuel is comprised of stainless-steel cladding and depleted uranium in metal form and has an average burnup of approximately 0.2%, with a plutonium buildup of several hundred grams per assembly.

## Description of the Electrometallurgical Process

The electrometallurgical fuel treatment uses an electrorefining process that separates the fuel into three products: uranium product, ceramic waste form and metal waste form. This process has been widely discussed and presented thoroughly in the literature.<sup>[1, 2, 3]</sup>

After electrorefining the stainless steel cladding, the noble metal fission products (Zr, Mo, Ru, Tc, Te, Rh, Pd, Nb, others) and some residual actinides that do not react in the electrorefining process, are immobilized in a 15% zirconium 85% stainless steel metal waste form. This alloy was selected based on empirical experience and inspection of the phase diagrams of the primary alloy components (i.e., Fe-Zr, Fe-Cr-Zr, Cr-Zr, Ni-Zr).

As the irradiated fuel is treated, the molten salt accumulates chlorides of the active fission products, sodium and the transuranic elements present in the fuel. To immobilize the salt, it is removed from the EBR and blended with zeolite at 500°C, which sorbs the salt into the zeolite. After cooling, a glass powder is mixed with the salt sorbed zeolite and loaded into steel cans. In a hot isostatic press (HIP), the mixture is converted to a monolithic ceramic waste form with the zeolite being converted entirely to the mineral sodalite.

## Results

### (A) Metal Waste Form

The following metal waste form samples have been produced: (1) 20 cold ingots (1-3 kg) from a tilt pour furnace, (2) 11 cold ingots (15-25 g) from a resistance furnace, (3) 71 spiked ingots (10-20 g) with radioactive constituents, and (4) 3 fully radioactive ingots (4-6 kg). Physical measurements, corrosion tests, immersion

tests, thermophysical tests, and microstructural characterization were conducted on these samples with variations in zirconium content (5-95 wt. %), noble metal content (0-4 wt. %), stainless steel type (304, 316, and HT9), uranium content (0-11 wt. %) and plutonium content (0-10 wt. %). The corrosion and immersion tests indicate that the metal waste form is very durable and does not readily release radionuclides. The normalized release rate for uranium and technetium from alloy samples is less than  $5E-3$  g/m<sup>2</sup>day as obtained in a two year immersion test.<sup>[4]</sup> The microstructural characterization of these alloys and the actual irradiated metal waste ingots produced to date reveal that the alloy, primarily the Fe-Zr phase, exhibits solubility for noble metal fission products and actinides, see Fig. 1A.

### (B) Ceramic Waste Form

The following ceramic waste form samples have been processed and characterized: (1) 45 laboratory scale hot uniaxial press (HUP) samples (<sup>239</sup>Pu and <sup>238</sup>Pu doped, 1-5 g), (2) 104 laboratory scale HIP cans (cold, U doped, Pu/U doped, 50 g), (3) 55 demonstration scale cold HIP cans (1-2 kg), (4) 20 non-radioactive process control samples (10-30 g), (5) 3 scale-up 8 inch diameter HIP products, (6) 2 scale-up 18 inch diameter products, (7) 10 radioactive demonstration-scale HIP cans, and (8) 17 radioactive process control samples.

The waste forms generated were characterized using a variety of methods and techniques, including (1) immersion tests, (2) X-ray diffraction, (3) electron microscopy (see Fig. 2B), (4) neutron diffraction, (5) material properties, (6) vapor hydration tests, (7) drip tests, (8) material interaction tests, and (9) X-ray absorption fine structure. These analyses (over 900 in the completed demonstration phase) encompassed the testing areas of attribute, characterization, accelerated and service condition<sup>[5]</sup> and demonstrated the durability of this waste form.<sup>[6]</sup>

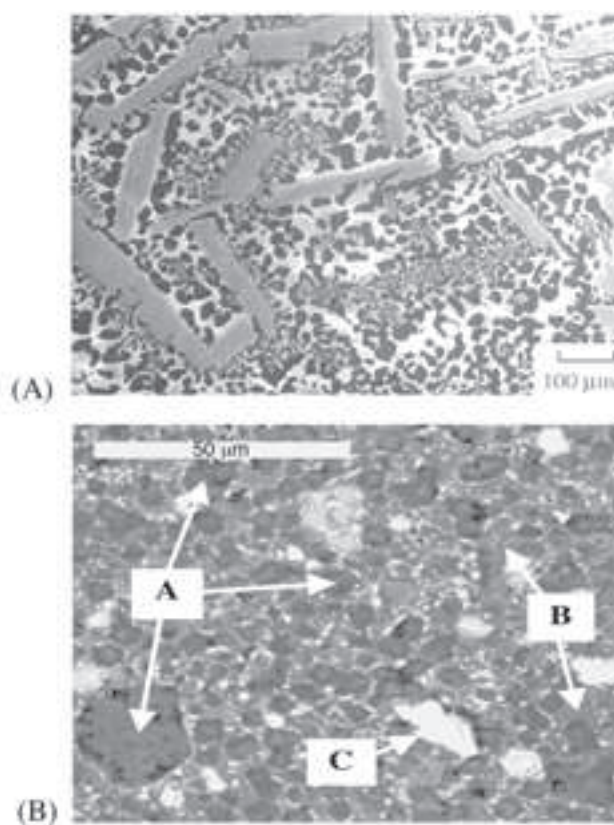


Figure 1.  
Backscattered  
electron images:

(A) SS-15 wt. % Zr-10 wt. % Pu alloy. The darkest regions are an iron solid solution phase; the medium-contrast regions are a  $Zr(Fe,Cr,Ni)_{2+x}$  phase, with the brightest regions in this phase being enriched in Pu.

(B) Ceramic waste form material containing 3.8 wt. % Pu. A. glassy phase, B. sodalite grain, C.  $PuO_2$  inclusion.

Ion irradiation-induced nanocrystal formation can be the result of competition between amorphization and crystal recovery and recrystallization.<sup>[3-5]</sup> Epitaxial growth and nucleation-growth are the primary crystal recovery mechanisms during the process of ion irradiation-induced amorphization. Due to the higher energy barrier for the formation of new crystal nuclei, the probability of nucleation-growth is small as compared with that of epitaxial growth. Thus, the epitaxial recrystallization of the highly damaged materials leads to the formation of nanocrystals at 933 K. As a result, nanocrystals show a preferred orientation similar to that of the original crystalline matrix. At a higher temperature, 973 K, the probability of nucleation increases due to the lower quench rate and longer annealing time. Thus, nanocrystals of random orientation can form around these newly formed nuclei. In this case, ion irradiation-induced nucleation-growth of nanocrystals that occurs in heavily damaged crystalline materials at elevated temperature is similar to thermally activated recrystallization in cold-worked metals.<sup>[6,7]</sup> Epitaxial growth and ion irradiation-induced nucleation-growth both have important effects on the formation and orientation of nanocrystals.

### Acknowledgment

We thank Dr. L. Vance at Australia Nuclear Science and Technology Organization for preparing the samples used in this study.

### References

1. R. C. Ewing, W. J. Weber, W. Lutze, in: E. R. Merz, C.E. Walter (Eds.), *Disposal of Weapon Plutonium*, Kluwer Academic Publishers, Boston, MA, 1996, 65.
2. B. C. Chakoumakos, R. C. Ewing, *Mat. Res. Soc. Symp.* **44** (1985) 641
3. L. M. Wang, et al., submitted to *Mater. Sci. and Engin. A*, 1999.
4. A. Meldrum, et al., *Canadian Mineralogist* **37** (1999) 207.
5. A. Meldrum, S. J. Zinkle, L. A. Boatner, R. C. Ewing, *Nature* **395**, 3 (1998) 56.
6. L. M. Wang, R. C. Birtcher, R.C. Ewing, *Nucl. Instr. and Meth. B* **80/81** (1993) 1109.
7. R. C. Birtcher, L. M. Wang, *Nucl. Instr. and Meth. B* **59** (1991) 966.



# Plutonium and Uranium Disposition in a Sodalite/Glass Composite Waste Form via XAFS

## Introduction

Sodalite/glass composite waste forms are being developed at Argonne National Laboratory for disposal of radioactive fission elements in salt form from the electrometallurgical treatment of spent EBR-II nuclear reactor fuel.<sup>1,2</sup> The salt waste from the electrometallurgical process consists primarily of an LiCl/KCl eutectic salt loaded with various other fission-product chloride salts. In addition, this salt contains up to 2 mol % actinide chlorides, namely, uranium, plutonium and neptunium chlorides. The salt from the treatment process is sorbed by zeolite 4A, which has an aluminosilicate cage structure of nominal composition  $\text{Na}_{12}(\text{AlSiO}_4)_{12}$  and is known for its ability to contain or “occlude” other species within the cage structure. The zeolite 4A, with its occluded fission-element salts, is mixed with glass and heated to high temperatures and pressures to convert the zeolite to a more thermodynamically stable sodalite form and consolidate the waste form. Primary considerations in this process are (1) questions of reactivity of the various salts with the zeolite structure as raised by thermodynamic calculations and (2) the fate of the fission elements in the resulting waste form.

The objective of this work was to determine the fate of plutonium and uranium in this waste form via the XAFS synchrotron technique.<sup>3</sup> Other techniques such as tunneling electron microscopy (TEM) can show crystal structure in great detail but do not have the ability to see the plutonium within the sodalite cage structure other than at the surface of the material being studied. The XAFS technique provides a unique means of determining the local environment of the plutonium and uranium in a true three-dimensional sense and is capable of doing so in situ.

## Description of Work

For the purposes of this experiment, a matrix of four sample types was created. Given the previously stated target actinide loading in the process waste form, the decision was made to utilize 3:1 and 1:3 uranium to plutonium ratios in the salt used where the total actinide loading sums to 2 mol %. Thermodynamic calculations indicate the possible reaction of these actinides with water present in the zeolite at process temperatures in the 500 to 750 degree C. range, so the second axis of the matrix was chosen to consist of zeolite 4A with 0.12 and 3.5 wt % water loadings. Quantities of these zeolites were blended with the actinide-loaded salts at 500 degrees C. They were subsequently mixed with glass powder to a 25 wt % glass loading, packaged in canisters and consolidated at elevated temperature and pressure to form composite sodalite/glass waste forms. These waste forms were sectioned and fragments of them were analyzed via XAFS.

## Results

The results of the waste form patterns were compared against a set of known oxidation-state standards ( $\text{Pu(III)F}_3$ ,  $\text{Pu(IV)O}_2$ ,  $\text{NaPu(V)O}_2\text{CO}_3$ ,  $\text{Ba}_3\text{Pu(VI)O}_6$  and  $\text{UO}_2$ ). These standards were also used to check the efficacy of the FEFF/FEFFIT set of programs as a check of the ability of the programs to generate theoretical output that matched the physical standards. When this was established, compari-

Michael K. Richmann,  
Arthur J. Kropf,  
Donald T. Reed,  
Scot B. Aase,  
Mark C. Hash,  
Larry Putty,  
Dusan Lexa  
*Argonne National  
Laboratory, Argonne,  
IL 60439, USA*



son of the waste forms against known crystallographic  $\text{Pu}_2\text{O}_3$ ,  $\text{PuO}_2$ ,  $\text{PuOCl}$ ,  $\text{PuC}_{13}$ ,  $\text{K}_2\text{PuC}_{15}$  and  $\text{K}_2\text{PuC}_{16}$  data was performed. The plutonium and uranium in the waste forms was found to match the  $\text{PuO}_2$  and  $\text{UO}_2$  cases to significant degree. This would seem to imply formation of the oxides from the actinide chlorides by reaction with the zeolitic water given the absence of water in the salt used to manufacture the waste forms and the low ppm water content environment during processing.

### References

1. C. Pereira, M. C. Hash, M. A. Lewis and M. K. Richmann, "Ceramic-Composite Waste Forms from Electrometallurgical Treatment of Spent Nuclear Fuel," *J. Miner. Met. Mater.*, 49(7), 34 (1997).
2. M. A. Lewis, D. F. Fischer and L. J. Smith, "Salt-Occluded Zeolites as an Immobilization Matrix for Chloride Wastes," *J. Amer. Ceram. Soc.*, 76(11), 2826 (1993).
3. S. D. Conradson, I. Al Mahamid, D. L. Clark, N. J. Hess, E. A. Hudson, M. P. Neu, P. D. Palmer, W. H. Runde and C. D. Tait, "Oxidation-State Determination of Plutonium Aquo Ions Using X-Ray Absorption Spectroscopy," *Polyhedron*, 17(11), 599 (1998).